NACA

RESEARCH MEMORANDUM

AERODYNAMIC LOADS ON AN EXTERNAL STORE ADJACENT TO

A 45° SWEPTBACK WING AT MACH NUMBERS FROM 0.70

TO 1.96, INCLUDING AN EVALUATION

OF TECHNIQUES USED

By Lawrence D. Guy and William M. Hadaway

Langley Aeronautical Laboratory
Langley Field, Va.

NATIONAL ADVISORY COMMITTEE
FOR AERONAUTICS
WASHINGTON
November 15, 1955

NATIONAL ADVISORY COMMITTEE FOR AERONAUTICS

RESEARCH MEMORANDUM

AERODYNAMIC LOADS ON AN EXTERNAL STORE ADJACENT TO

A 45° SWEPTBACK WING AT MACH NUMBERS FROM 0.70

TO 1.96, INCLUDING AN EVALUATION

OF TECHNIQUES USED

By Lawrence D. Guy and William M. Hadaway

SUMMARY

Aerodynamic forces and moments have been obtained in the Langley 9- by 12-inch blowdown tunnel on an external store and on a 45° sweptback wing-body combination measured separately at Mach numbers from 0.70 to 1.96. The wing was cantilevered and had an aspect ratio of 4.0; the store was independently sting-mounted and had a Douglas Aircraft Co. (DAC) store shape. The angle-of-attack range was from -3° to 12° and the Reynolds number (based on wing mean aerodynamic chord) varied from 1.2×10^6 to 1.7×10^6. Wing-body transonic forces and moments have been compared with data of a geometrically similar full-scale model tested in the Langley 16-foot and 8-foot transonic tunnels in order to aid in the evaluation of transonic-tunnel interference.

The principal effect of the store, for the positions tested, was that of delaying the wing-fuselage pitch-up tendency to higher angles of attack at Mach numbers from 0.70 to 0.90 in a manner similar to that of a wing chord extension. The most critical loading condition on the store was that due to side force, not only because the loads were of large magnitude but also because they were in the direction of least structural strength of the supporting pylon. These side loads were greatest at high angles of attack in the supersonic speed range. Removal of the supporting pylon (or increasing the gap between the store and wing) reduced the values of the variation of side-force coefficient with angle of attack by about 50 percent at all test Mach numbers, indicating that important reductions in store side force may be realized by proper design or location of the necessary supporting pylon. A change of the store skew angle (nose inboard) was found to relieve the excessive store side loads throughout the Mach number range. It was also determined that the relative position of the fuselage nose to the store nose can appreciably affect the store side forces at supersonic speeds.

INTRODUCTION

Continued use of external stores on high-speed aircraft has necessitated extensive investigation of their effects on aircraft performance characteristics and also of the effects of the aircraft wing and fuselage interference on the external-store loads. Area rule concepts have been shown to apply to the determination of the drag of aircraft-store configurations at transonic speeds and, to some extent, supersonic speeds (ref. 1). Additional information on the effects of store size, shape, and position on aircraft performance at supersonic speeds is reported in references 2 and 3. Information on external-store loads at transonic and supersonic speeds, however, is relatively meager, although considerable work has been done at high subsonic speeds (refs. 4 and 5, for example) and the effects of store position on the store loads at low angles of attack have been extensively investigated at Mach number 1.6 (ref. 6). There is considerable need for information on external-store loads at transonic and supersonic speeds both from the standpoint of structural support design and as an aid to the estimation of jettisoning characteristics. In order to provide this information, the exploratory investigation conducted in the Langley 9- by 12-inch blowdown tunnel of the effects of stores on the aerodynamic characteristics of a 45° swept wing, an unswept wing, and a 60° delta wing (refs. 2, 7, 8, and 9) has been extended to include the measurement of store loads. The present report presents data for the store in the presence of, but not attached to, the semispan 45° sweptback wing-body combination of reference 7.

The semispan wing had 45° sweepback, an aspect ratio of 4, a taper ratio of 0.6, and NACA 65A006 airfoil sections. The store, which had a Douglas Aircraft Company (DAC) shape, was sting-mounted independently of the semispan-wing—body combination and at no time was it attached or in contact with the wing. Forces and moments on the store and on the wing-body combination were measured simultaneously through an angle-of-attack range of -3° to 12° for a limited number of store positions. Tests were made in the transonic slotted nozzle at Mach numbers between 0.7 and 1.2, and at Reynolds numbers between 1.3×10^6 and 1.7×10^6. Tests were made in three supersonic nozzles at Mach numbers of 1.41, 1.62, and 1.96 and for Reynolds numbers between 1.2×10^6 and 1.5×10^6. Tunnel-boundary interference effects on wing angle-of-attack loading for the transonic nozzle are largely unknown and theoretical corrections are unavailable. Consequently, data were obtained in the transonic nozzle for the 45° sweptback wing in combination with a different test body so that the results might be compared with those of tests of a geometrically similar full-span model in the Langley 16- and 8-foot transonic tunnels. The test results for the model in the Langley 16-foot transonic tunnel are considered to be essentially interference free because of the small size of the model relative to the tunnel test section. In addition to the wing employed

in the store investigation, a second and smaller blowdown tunnel model identical to the first except for size was built and tested to aid in the evaluation of interference effects.

SYMBOLS AND COEFFICIENTS

C_L lift coefficient, $\dfrac{\text{Lift}}{qS_W}$

C_D drag coefficient, $\dfrac{\text{Total drag minus drag at zero lift}}{qS_W}$

C_N normal-force coefficient, $\dfrac{\text{Normal force}}{qS_W}$

C_m pitching-moment coefficient, $\dfrac{\text{Pitching moment about } 0.25\bar{c}}{qS_W\bar{c}}$

C_B bending-moment coefficient, $\dfrac{\text{Bending moment}}{qS_W b/2}$

C_{N_s} store normal-force coefficient, $\dfrac{\text{Store normal force}}{qS_s}$

C_{m_s} store pitching-moment coefficient,
$$\dfrac{\text{Store pitching moment about } 0.4l}{qS_s l}$$

C_{Y_s} store lateral-force coefficient, $\dfrac{\text{Store lateral force}}{qS_s}$

C_{n_s} store yawing-moment coefficient,
$$\dfrac{\text{Store yawing moment about } 0.4l}{qS_s l}$$

B bending moment

q free-stream dynamic pressure

S_W model wing area, semispan or full span

$\bar{c}$ wing mean aerodynamic chord, $\dfrac{\displaystyle\int_0^{b/2} c^2 dy}{\displaystyle\int_0^{b/2} c\, dy}$

c   local wing chord

b   wing span (twice distance from root chord to wing tip)

S_s store maximum cross-sectional frontal area

l closed length of store or fuselage

α angle of attack, deg

z   minimum distance from wing lower surface to store longitudinal axis (positive down)

d   maximum store diameter

x   chordwise distance from line perpendicular to $\bar{c}$ at quarter-chord station to store $0.4l$ point

y   spanwise distance from wing-root chord to store longitudinal axis

V_o free-stream velocity

R   Reynolds number based on $\bar{c}$

M   Mach number

F   original fuselage

F*   long-nose fuselage

β skew angle between store center line and fuselage axis, deg

$\Delta C_{N_{wf}}$, $\Delta C_{m_{wf}}$, $\Delta C_{B_{wf}}$ increment in value of $C_{N_{wf}}$, $C_{m_{wf}}$, $C_{B_{wf}}$ due to presence of store

$\Delta\left(\frac{dC_{N_{wf}}}{d\alpha}\right)$, $\Delta\left(\frac{dC_{m_{wf}}}{d\alpha}\right)$, $\Delta\left(\frac{dC_{B_{wf}}}{d\alpha}\right)$ increment in $\frac{dC_{N_{wf}}}{d\alpha}$, $\frac{dC_{m_{wf}}}{d\alpha}$, and $\frac{dC_{B_{wf}}}{d\alpha}$ due to presence of store

$\frac{d}{d\alpha}$ rate of change of coefficient with angle of attack

$\frac{d}{dC_L}$ rate of change of coefficient with lift coefficient

Subscripts:

wf   wing and fuselage

wi   wing and interference

s   store

p   pylon

f   fuselage

MODELS

The principal dimensions of the semispan-wing—body combinations are shown in figures 1(a) and 1(b). Each wing had 45° sweepback of the quarter-chord line, an aspect ratio of 4.0, a taper ratio of 0.6, and NACA 65A006 airfoil sections parallel to the air stream. The semispan wing, shown in figure 1(a) in combination with a test body consisting of a half body of revolution and a 0.25-inch shim, was used exclusively in connection with the external-store investigation. The same wing is shown in figure 1(b) in combination with a different test body. Also shown in figure 1(b) is a smaller wing-body combination, geometrically similar to the first except for the wing tip. The wings were fabricated from heat-treated steel and the blunt streamwise wing tip of the larger wing was not faired.

The external store had a DAC shape and a fineness ratio of 8.58, based on the closed length. The store was made of steel and cut off at 80 percent of its closed length to permit entry of an internal electrical strain-gage balance. Store ordinates and sting-mounting arrangements are given in figure 2 and a photograph of a typical test condition is shown in figure 3. The $0.4l$ position of the store coincided with the longitudinal position of the wing $0.25\bar{c}$ for all tests.

The struts, or pylons, were made of brass and attached, by pinning and sweating, to the wing surface but not to the external store. The swept and unswept struts had NACA 65A airfoil sections and thickness ratios of 0.03 and 0.10, respectively, parallel to the free-stream direction. The swept strut had a chord length of $0.617\bar{c}$ and the unswept strut, a chord length of $0.470\bar{c}$. In each case the leading edge of the strut was located at the leading edge of the wing. The configurations tested and the relative store positions are presented in figure 4.

TUNNEL

The tests were made in the Langley 9- by 12-inch blowdown tunnel, which is supplied with compressed air at 2 to $2\frac{1}{3}$ atmospheres by the Langley 19-foot pressure tunnel. The air is passed through a drying agent of silica gel and then through finned electrical heaters in the region between the 19-foot tunnel and the blowdown tunnel test section to insure condensation-free flow at supersonic speeds in the test region. The criteria used for the drying and heating necessary to reduce the air dewpoint below critical values are given in reference 10.

Three turbulence damping screens are installed in the settling chamber between the heaters and the test region. Four interchangeable nozzle blocks provide test section Mach numbers of 0.70 to 1.20, 1.41, 1.62, and 1.96.

Supersonic Nozzles

Extensive calibrations of the test-section flow characteristics of the three supersonic fixed nozzles have been made previously and are reported in reference 11. The calibration results indicated the following test section flow conditions:

Average Mach number	1.41	1.62	1.96
Maximum deviation in Mach number . . .	±0.02	±0.01	±0.02
Maximum deviation in stream angle, deg	±0.25	±0.20	±0.20
Average Reynolds number (based on $\bar{c}$ of large model)	1.5×10^6	1.3×10^6	1.2×10^6

Transonic Nozzle

A description of the transonic nozzle, which has a 7- by 10-inch rectangular test section, together with a discussion of the flow characteristics obtained from limited calibration tests is presented in reference 12. Satisfactory flow conditions in the test section are indicated from the minimum Mach number (0.7) to $M = 1.2$. Maximum deviations from the average test section Mach number are given in figure 5(a). Stream-angle deviation probably did not exceed ±0.1° at any Mach number. The average Reynolds numbers of the tests are shown in figure 5(b) as a function of Mach number.

TEST TECHNIQUE

The semispan-wing—fuselage models were cantilevered from a five-component strain-gage balance set flush with the tunnel floor. The balance and model rotated together as the angle of attack was changed. The aerodynamic forces and moments on the model were measured with respect to the balance axes and, in some cases, then rotated to the wind axes. The fuselage was separated from the tunnel floor by a 0.25-inch aluminum shim, which has been shown in references 13 and 14 to minimize the effects of the boundary layer on the flow over the fuselage surface. A clearance gap of about 0.010 inch was maintained between the fuselage shim and the tunnel floor with no wind load.

The external store was attached to the forward end of an internal four-component strain-gage balance. The downstream end of the balance sting was supported by a strut from the tunnel floor, and the store and sting pivoted about a point 12.25 inches ($5.17\bar{c}$) downstream of the wing $\bar{c}/4$. The store angle of attack and position in a direction normal to its own axis were controllable during tests within limits and permitted an angle-of-attack range of about $6°$ per test run. The sting support was repositioned between tests and three runs were required to obtain data throughout the angle-of-attack range from $-3°$ to $12°$.

Two small electrical contacts on the side of the store nearest the wing permitted alinement of the store with the pylon and also gave an indication of fouling between the two. A minimum gap of about 0.02 inch was maintained at all times unless otherwise stated.

ACCURACY OF MEASUREMENTS

An estimate of the probable errors introduced in the present data by instrument-reading errors and measuring-equipment errors are presented in the following table:

C_L . . . . ±0.01

C_{N_W} . . . . ±0.01

C_{m_W} . . . . ±0.002

C_{B_W} . . . . ±0.002

α, deg . . . . ±0.05

C_{N_S}, C_{Y_S} . . . . ±0.01

C_{m_S}, C_{n_S} . . . . ±0.001

α_S, deg . . . . ±0.20

β_s, deg . . . . ± 0.20

x . . . . $\pm 0.015\bar{c}$

y . . . . $\pm 0.01 b/2$

z . . . . $\pm 0.03 d_s$

Chord force on the semispan-wing—body combination in the presence of the external store was measured but not presented because of the unreliability of the results. For this reason measured normal forces for this condition could not be rotated to the wind axes and presented as lift. Chord forces were in error by an unknown amount because of the pressure disturbances originating at the base of the strut supporting the store balance. These disturbances were transmitted forward through the tunnel boundary layer to the base of the test body. Pressure measurements at the base of the test body with and without strut in tunnel indicated that at supersonic speeds these effects were very substantial. There was also some evidence that pressure disturbances originating at the support strut were transmitted forward through the wing wake and thereby affected the wing loading at a Mach number of 1.41 at large angles of attack; consequently, the angle-of-attack range at this Mach number has been arbitrarily limited. The data presented are believed to be free of this interference.

The measurement accuracy given previously for the store angle of attack refers to the angle between the store and the wing and does not include inaccuracies in measurement of the wing-fuselage angle of attack. The minimum gap and the alinement between store and wing in the pitching plane was fixed by setting the heights of the electrical contacts on the store with the wind off. Alinement during tests was determined by simultaneous making or breaking of the two electrical contacts on the store. The vertical position was then determined by means of a calibrated lead screw which moved the store normal to its longitudinal axis. Therefore, the store angle of attack and vertical position relative to the wing were essentially independent of deflection of the store supporting system or of the wing due to air loads. In the lateral plane, the store-position measurement accuracy was determined principally by the deflection of the balance sting due to air loads on the store and sting. These deflections were determined from static load calibrations. The longitudinal location of the store was fixed before each run. The accuracy given previously was essentially the variation in x relative to the wing during each run due to the different points of rotation of the wing and the store.

Tests of the store alone were made both with the electrical contacts raised and with the contacts faired smooth with the store surface. Differences in the measured loads were well within the stated experimental accuracies.

COMPARISON OF TRANSONIC NOZZLE DATA WITH DATA FROM OTHER FACILITIES

The semispan wings and half bodies of revolution (fig. 1(b)) were geometrically similar to the full-span model tested in the transonic tunnels except for the streamwise tip of the larger of the two semispan wings. The full-span model with its three-component internal electrical strain-gage balance and the 18-inch portion of the support sting immediately rearward of the model was tested in both the Langley 16-foot and 8-foot transonic tunnels (refs. 15 and 16). Dimensional details of the wing and fuselage, which were both made of steel, are given in figure 1(b) and are described more fully in reference 16.

The wing of the larger semispan model, which was the same wing as shown in figure 1(a) with a different test body, will be referred to herein as the large wing or model, and the smaller blowdown-tunnel model (fig. 1(b)) will be referred to as the small model. The full-span model used in the tests in the Langley 16- and 8-foot tunnel will be referred to as the sting model. The relative sizes of the various models and of the tunnel test sections are given in table I. The blowdown-tunnel nozzle including the reflected image of the test section nozzle walls and semispan model would correspond to a 10- by 14-inch section slotted on all four sides with the model span occupying the longest dimension.

The variation of the Reynolds number with Mach number is presented in figure 5(b) for the blowdown tunnel, 8-foot, and 16-foot tunnel tests. The accuracy of the presented lift, drag, and pitching-moment coefficients for the 8- and 16-foot tunnel tests were estimated to be within ± 0.02, ± 0.002 and ± 0.004, respectively (ref. 15). Mach number accuracy of the test section for both large tunnels was ± 0.005.

Discussion of Comparisons

The semispan test technique employed in the blowdown tunnel does not permit direct comparison of the basic data with those obtained for full-span sting-mounted models, principally because the test body in the former case was modified by the boundary-layer shim. Consequently, it was necessary to subtract the force and moment coefficients of the fuselage, or test body, from those of the wing-fuselage combinations in all cases and compare only the wing plus interference values thus obtained.

Variations of lift coefficient with angle of attack, pitching-moment coefficient, bending-moment coefficient and drag due to lift coefficient for the wing plus interference are presented in figure 6. Comparisons of the slope parameters $\dfrac{dC_{L_{wi}}}{d\alpha}$ and $\dfrac{dC_{m_{wi}}}{dC_{L_{wi}}}$ are plotted against Mach number in figure 7.

Lift.- At subsonic Mach numbers the lift characteristics of both
the large and small models were in excellent agreement with the sting-
model results up to about an angle of attack of 8°. At higher angles
of attack the agreement was not so good and, for the small wing, the
break in the lift curves appears to have been delayed to higher angles
of attack. Better agreement was shown for the large model except between
Mach numbers 0.98 and 1.06 where the lift curve breaks more sharply than
for the sting model in either 16-foot or 8-foot tunnel. At supersonic
Mach numbers above 1.02, good agreement was shown for both large and small
wings although the lift curves tended to be more linear at moderate angles
of attack. This condition may have been an effect of reflection by the
tunnel walls of the model shock waves back on to the model because, at the
Mach number 1.12 the reflected fuselage-bow shock wave still did not pass
behind the models in the blowdown tunnel. That larger differences were
not shown may, in part, be attributed to the rectangular shape of the
tunnel test section since the reflection of a conical wave from a straight
wall tends to be diffused whereas reflection from a concentric circular
wall, for example, tends to be concentrated, or focused, at the center
line.

Below a Mach number of 0.9, the lift slopes for the semispan models
were somewhat greater than for the 16-foot-tunnel sting-model results
(fig. 7(a)). The differences in the lift slopes for the large and small
wing were small at subsonic Mach number but were somewhat larger at super-
sonic speeds. Maximum values of $\dfrac{dC_{L_{wi}}}{d\alpha}$ were reached at somewhat higher
Mach numbers for the semispan models than for the sting model. The rea-
sons for this result are not clear since blockage corrections, which are
probably very small for this nozzle (ref. 17), of the same sign as for
an open tunnel would be required. It may be that this delay is in some
way connected with the wall-mounting test technique.

Pitching moments.- The wing-plus-interference pitching-moment char-
acteristics are shown for the blowdown tunnel data and the 8- and 16-foot
tunnel results (fig. 6(b)). The curve slopes $\dfrac{dC_{m_{wi}}}{dC_{L_{wi}}}$ agree very well at
zero lift insofar as their variation with Mach number is concerned
(fig. 7(b)). The blowdown tunnel data, however, indicated a slightly
more rearward position of the aerodynamic center at subsonic speeds and
a slightly more forward position at speeds near a Mach number of 1.0 than
did the 16-foot-tunnel results.

Differences in the results of the blowdown tunnel tests and the
16- and 8-foot tunnel tests were shown principally in the speed range
between Mach numbers of 0.94 and 1.04. In this range nonlinear pitching-
moment variations at low lift coefficients occurred for both the large

and small wings. These variations appeared as shifts in the pitching-moment curves, and the slopes of the curves agree well with those of the sting-model data at lift coefficients below 0.2 and above 0.3. This center-of-pressure shift is not reflected in the variations of bending moment with lift coefficient (fig. 6(c)) which appear to be fairly linear. This center of pressure, however, could have shifted laterally as much as is indicated by the pitching-moment shift and would still not be too apparent in the curves for the variation of $C_{B_{wi}}$ with $C_{L_{wi}}$ due to the differences in pitching-moment and bending-moment scales as well as differences in magnitudes of parameters used to nondimensionalize the moments ($\bar{c}$ and $b/2$). Incremental center-of-pressure shifts noted between tests of the wing in the blowdown tunnel and in the 8- and 16-foot tunnels do not appear to be attributable to boundary-induced angle interference or tunnel flow conditions but may in some way result from the wall mounting technique or model size relative to the tunnel. Similar variations in pitching moment at low lift coefficients, in the same Mach number range, were shown in reference 18 for the larger of two wall-mounted, sweptback wings (geometrically similar to the wings in the present report) tested without a fuselage in a slotted tunnel. The smaller wing, however, showed no such variation although the wing area was 12 percent of the tunnel cross-sectional area - a value which lies between the 7- and 16-percent values for the two blowdown-tunnel models.

Differences may also be noted at other Mach numbers at the higher lift coefficients. Above $M = 0.85$, the unstable break at high lift coefficients for the small wing was delayed and reflected the differences in lift noted previously. For the large wing, above $M = 0.98$, the unstable change in pitching moment at high lift coefficients was much more rapid than for the other models. As previously noted, the decrease in lift-coefficient slope at these Mach numbers was much more rapid than was shown by the other tests (fig. 6(a)). No explanation for these differences is presently available. In general, however, the blowdown-tunnel results showed good agreement with the transonic-tunnel results insofar as lift coefficients at which inflections and rapid changes in pitching-moment curves occurred.

Drag.- The drag due to lift (fig. 6(d)) for the large wing was generally in better agreement with the sting-model results than the drag for the small wing. Good agreement is shown for the large wing except at Mach numbers near 1.0 and above 1.08. The drag values reflect the differences in lift behavior previously noted at the higher angles of attack. In particular, the lower drags shown for the small wing at high lift coefficients were largely a result of the lower angle of attack required to sustain the lift coefficients. At high subsonic Mach numbers near 1.0, lower drags were shown for both blowdown-tunnel models at lift coefficients between 0.2 and 0.6. It is interesting to note that these low drag values occurred at the same lift coefficients and Mach numbers at which the largest differences in pitching-moment coefficients

for sting- and wall-mounted models occurred. Caution must be observed in evaluating the drag due to lift characteristics at small supersonic Mach numbers since it is known that the 8-foot-tunnel results are affected by wall-reflected disturbances between $M = 1.04$ and $M = 1.10$. However, since the results from the 8-foot tunnel agree very well with the results from the 16-foot tunnel up to $M = 1.06$, the region of uncertainty is narrowed considerably.

The variation with Mach number of the drag at zero lift for the fuselage alone or the wing-fuselage combination suffered from inadequacies similar to those noted for side wall and bump models in reference 19. In this reference excessively high drag values were noted for the fuselage and were believed to be due largely to the gap between the fuselage and mounting surface. Furthermore, even the wing-fuselage minus fuselage drag at zero lift for such models was found to be inaccurate in the transonic speed range in reference 19. Consequently, drag data for wall-mounted and sting-mounted models are compared in this paper, as in reference 19, on the basis of total drag minus drag at zero lift.

Reliability of Test Technique as Applied to

External-Store Tests

Comparison of wing data obtained in the transonic nozzle of the blowdown tunnel with that obtained for a similar model in other facilities indicated generally satisfactory agreement except in the Mach number range between 0.94 and 1.04. In this range, significant quantitative differences were noted. However, since the flow under the wing lower surface is not as subject to separation or as critical to construction tolerances as the flow over the upper surface, the under-wing flow field should more nearly approach the desired characteristics than is indicated by the force and moment data. It is therefore believed that reasonably reliable results were obtained in the tests of external stores in the under-wing flow field throughout the range of test conditions although some uncertainty exists above $M = 1.02$ because of wall-reflected disturbances from the fuselage and from the store itself. Although the absolute values of the wing loads may in some instances be open to question, it appears from the comparisons of the preceding section, that the incremental changes in wing forces and moments due to the presence of the store should be reliable except at the highest angles of attack at Mach numbers above 0.94. This conclusion is supported by the comparison of both wing and control characteristics of a 60° delta wing with a trailing-edge control tested both in the transonic nozzle and in facilities essentially free from boundary interference (ref. 12).

AERODYNAMIC LOADS ON WING AND ON STORE

An index of the figures presenting the results is as follows:

Wing Loads

The presence of the store, in general, had only small effects on the wing normal-force and bending-moment coefficients at any Mach number for the positions tested (fig. 17). The principal effect of the store was that of eliminating, or at least delaying to a higher angle of attack, the unstable pitching-moment break at moderate angles and subsonic Mach numbers of 0.70 to 0.90 (figs. 10 and 11). For the store position adjacent to the wing lower surface at $0.60b/2$ wing pitch-up was eliminated at least up to an angle of attack of 12°. Moving the store away from the wing to $z/d = 1.0$ (without extension of the pylon) resulted in a return of the pitch-up condition (fig. 10(c)). With extension of the pylon, pitch-up again appeared to have been eliminated at $M = 0.75$ (fig. 11(a)) but was only delayed somewhat at $M = 0.9$ (fig. 11(b)). Even at the lower Mach number the pylon alone had only small effects on the wing pitching moments. Similar effects of external stores on the static longitudinal stability of sweptback wings have been shown in references 20 and 21 and indicate that the store effected an increase in wing section loading just outboard of the store and reduced separation losses near the tips. These effects of the store were very similar to those of wing leading-edge chord-extensions and other auxiliary devices designed to alleviate wing pitch-up (refs. 22 and 23). As in the case of such devices, the store was ineffective in delaying wing pitch-up above $M = 0.9$.

Store Loads

The variations in store normal-force coefficient with α were generally nonlinear for all store positions tested (figs. 14 to 16). Very abrupt small changes in normal-force values are shown at small angles of attack at Mach numbers near 1.0 for store positions adjacent to the wing lower surface (figs. 14 and 16). These effects of wing interference on store normal forces indicate possible local choking of the flow or shock-wave interaction. Moving the store away from the wing decreased the interference, and skewing the store nose 5° inboard apparently slightly increased the Mach number at which these effects occurred (figs. 18 and 19).

No large increases in store normal-force coefficient with increasing angle of attack were shown for any store position in the presence of the wing (figs. 14 to 16). In fact, at the higher angles of attack, the normal-force coefficients were generally considerably smaller in magnitudes than those for the store alone. Furthermore, reference 20, which presents a limited analysis of part of the present data, has indicated that in maneuvering flight at high altitudes the inertia forces due to the weight of a full fuel tank may considerably outweigh the aerodynamic normal forces even at supersonic Mach numbers, at least insofar as the

design of structural supports is concerned. However, the normal forces may be of considerable importance in their effect on the aircraft stability or on wing flutter characteristics.

The most significant results of this investigation are shown by large negative (outwardly directed) side-force coefficients at moderate angles of attack for store positions immediately adjacent to the wing lower surface or to the lower end of a pylon (fig. 15). Data for these store locations indicate outward side forces of very large magnitude at supersonic speeds and present serious problems since the force is in the direction of least structural strength of the pylon. As pointed out in reference 24, large outward side forces at moderate and high angles of attack should not be entirely unexpected since the relieving action of the wing tips on the pressure field of the under side of the wing in a lifting condition is such as to incline the flow in an outward direction, the outward inclination increasing with increasing wing lift. As shown in figures 14 to 16, the side-force-coefficient variations with angle of attack were essentially linear throughout the angle-of-attack range for all Mach numbers, except in a few instances near a Mach number of 1.0.

In references 6 and 24, it has been shown that the store location relative to the wing has a very large effect on the values of C_{Y_α} but that, for a given store location, values of C_{Y_α} are not greatly affected by variation in Mach number. In the present data, values of C_{Y_α} were of the same order of magnitude at supersonic speeds as at subsonic speeds (fig. 19). The effects of position, however, were somewhat obscured since the differences in store position shown in figure 19(c) involve both spanwise and chordwise changes relative to the wing. Also it is not yet clear how the variations of C_{Y_α} with position are affected by the presence of supporting pylons. In the present investigations, values of C_{Y_α} are of about the same order of magnitude for the store at 0.60b/2 and at 0.73b/2 in those cases where the store was adjacent to the wing or the lower end of the pylon and effectively no air gap existed between the store and the forward portion of the wing. Figure 19(a) shows that moving the store vertically from $z = 0.5d_s$ to $z = 1.0d_s$ (without extending the pylon) reduced values of C_{Y_α} by about 50 percent throughout the Mach number range of the tests. Additional displacement to $z = 1.5d_s$ reduced C_{Y_α} only slightly more at supersonic speeds. However, with the store at $z = 1.0d_s$, extending the pylon to a position very near the store (effectively no gap) approximately doubled the values of C_{Y_α}. (Compare figs. 19(a) and 19(c)). It appears, therefore, that at moderate angles of attack there are very powerful effects on store side force of restricting lateral flow between the store and the wing, at least in the vicinity of the wing leading edge. Furthermore, it is probable that very

CONFIDENTIAL   ·

large side-force loads may be carried on the pylon itself. Consideration of these effects indicates that important reductions in store side forces may be achieved by proper design or location of the necessary supporting pylon. Of course, location of the store in regions of lower side loads would reduce the pylon interference effects; however, aircraft perform-ance or wing flutter characteristics could, in some cases, dictate store locations in regions of strong outflow such as apparently exist for the store positions of this report. Further investigation of the pylon interference effects on store side force and of the loads on the pylons is therefore necessary.

In an effort to reduce the large side forces at angle of attack, the store was skewed 5° (nose inboard) relative to the fuselage axis. Figure 19 indicates that the side-force slopes C_{Y_α} were generally unchanged by 5° store sideslip angle. The curves at each vertical store position, however, were displaced by an amount equal to the effect of roughly 4° change in angle of attack (store in the presence of the wing). It may also be pointed out that for the store position adjacent to the wing lower surface, the change in side-force-coefficient values due to sideslip angle was about twice that for the store-alone sideslip values (which equal the store-alone normal-force values of fig. 14). As the store was lowered from the wing one-half the store diameter, however, (no pylon) the shifts in side force due to sideslip angle more nearly approached the store-alone side-force value for 5° sideslip. Even though considerable variation of side-force coefficient with Mach number was evident, it appears that for a given angle of attack (for example, $\alpha = 6^\circ$, fig. 19(b)) store side forces can be held to reasonable values for practical store locations over a large range of Mach numbers by pro-per choice of the store sideslip angle.

The principal effects of Mach number on store side forces are shown in the variation of the coefficients at angles of attack of 0° and 6° in figure 19. In general, maximum positive (inward flow) or minimum negative (outward flow) values of side-force coefficients for a given store loca-tion or angle of sideslip occurred at Mach numbers between 1.1 and 1.2. At Mach numbers above 1.2, the large shifts in side force toward more negative values with increase in Mach number aggravated already critical conditions at high angles of attack. Consideration of the wing flow field at supersonic speeds indicated no reason for such rapid changes in side force with Mach number and it appeared that the position of the fuselage nose relative to the store was involved. Accordingly, the fuse-lage forebody was moved forward $0.5l$ (store length) and limited data were obtained for two store positions in the presence of the wing-fuselage combination and at one store position in the presence of the fuselage alone (fig. 20). For the store in the presence of the fuselage alone, the effects of fuselage-nose positions on store side-force and yawing-moment coefficients at $\alpha = 0^\circ$ were negligible below $M = 1.0$ but were

CONFIDENTIAL

sizable above M = 1.0 (fig. 20(c)). These effects were exaggerated
by the presence of the wing at M = 1.96 and extending the fuselage-
nose position resulted in a large reduction in the side-force change
with Mach number above M = 1.2. At low supersonic speeds, the differ-
ences in side-force coefficients shown were probably due to reflection
by the tunnel walls of the fuselage-bow shock wave since, at M = 1.2,
the reflected shock passes behind the store only in the case of the
original fuselage. At higher Mach numbers, disturbances from the fuse-
lage forebody affect the store side forces directly. For example, at
M = 1.96, the large negative side-force coefficients appear to result from
intersection of the fuselage bow wave with the store. The magnitude of
the coefficients was reduced by 50 percent at $\alpha = 0^{\circ}$ when the fuselage
forebody was extended so that the bow wave passed well ahead of the store
nose. (Note relative position of Mach lines in fig. 20(c).) The effect
of nose position on store side-force and yawing-moment coefficients was
essentially constant with angle of attack and the slopes of their values
against angle of attack were generally unaffected (figs. 20(a) and 20(b)).
The effect of fuselage-nose position on store normal forces and pitching
moments was small and unimportant and these data are not presented.

CONCLUSIONS

An investigation of the aerodynamic forces (except drag) and moments
on both a 45° sweptback wing-fuselage combination and an external Douglas
Aircraft Company (DAC) store in the presence of each other at Mach num-
bers between 0.70 and 1.96 indicated the following:

1. For the positions tested, the presence of the store, in general,
had only small effects on the wing normal-force and bending-moment coef-
ficients at any Mach number tested. The principal effect of the store
was that of delaying the wing-fuselage pitch-up tendency at Mach numbers
between 0.70 and 0.90 to higher angles of attack in a manner similar to
that of a wing chord-extension.

2. The most critical store-loading condition appeared to be caused
by the store side force, both because of its magnitude at high angles of
attack and because its direction was in that of the least structural
strength of the pylon. The variations of side-force coefficient with
angle of attack were essentially linear and the curve slopes were of
about the same order of magnitude at subsonic and supersonic speeds.

3. The side-force coefficients increased very rapidly in a negative
(outboard) direction with increasing angle of attack. The largest slopes
of store side force against angle of attack were obtained with the store
adjacent to the wing or an extended pylon. Removal of the pylon (or
increasing the gap between the store and wing) reduced values of the
slopes by about 50 percent throughout the Mach number range of the tests;

thus, important reductions in store side forces may be realized by proper design or location of the necessary supporting pylon.

4. The effects of Mach number are shown principally as a displacement of the curves of side-force coefficient against angle of attack rather than in slope changes. At supersonic speeds, increasing Mach number displaced the curves negatively and thereby further increased the negative side-force coefficients at the higher angles of attack. The magnitude of this negative displacement, however, was largely influenced by the position of the fuselage nose relative to the store location.

5. Changing the store skew angle caused a displacement of the curves of side-force coefficient against angle of attack and thus permitted reduction in side forces at a given angle of attack. The slopes of the curves, however, were not appreciably affected.

6. No large increases in the store normal-force coefficients were indicated with increase in angle of attack and Mach number for any store position tested. In fact, at the higher angles of attack, the normal-force coefficients were generally considerably lower than the store-alone values.

7. Qualitatively, the aerodynamic characteristics of the wing plus interference obtained by use of a shimmed semispan model in the transonic nozzle were in reasonably good agreement with the results obtained for a geometrically similar full-span model in the Langley 8- and 16-foot transonic tunnels. Quantitatively, significant differences in the results were shown, principally in the Mach number range between 0.94 and 1.04. In this range and above a lift coefficient of 0.2, the pitching-moment curves indicated that the center of pressure was somewhat ahead of that of the full-span model and the drag due to lift was in poor agreement. Evidence of some interference was shown in the slopes of the curves of lift coefficient against angle of attack at both subsonic and supersonic Mach numbers.

Langley Aeronautical Laboratory,
    National Advisory Committee for Aeronautics,
        Langley Field, Va., July 26, 1955.

REFERENCES

1. Smith, Norman F., Bielat, Ralph P., and Guy, Lawrence D.: Drag of External Stores and Nacelles at Transonic and Supersonic Speeds. NACA RM L53I23b, 1953.

2. Jacobsen, Carl R.: Effects of Size of External Stores on the Aerodynamic Characteristics of an Unswept and a 45° Sweptback Wing of Aspect Ratio 4 and a 60° Delta Wing at Mach Numbers of 1.41, 1.62, and 1.96. NACA RM L52K20a, 1953.

3. Smith, Norman F., and Carlson, Harry W.: The Origin and Distribution of Supersonic Store Interference From Measurement of Individual Forces on Several Wing-Fuselage-Store Configurations. I.- Swept-Wing Heavy-Bomber Configuration With Large Store (Nacelle). Lift and Drag; Mach Number, 1.61. NACA RM L55A13a, 1955.

4. O'Bryan, Thomas C.: Flight Measurement of Aerodynamic Loads and Moments on an External Store Mounted Under the Wing of a Swept-Wing Fighter-Type Airplane. NACA RM L53G22, 1953.

5. Silvers, H. Norman, and King, Thomas J., Jr.: Investigation at High Subsonic Speeds of Bodies Mounted From the Wing of an Unswept-Wing—Fuselage Model, Including Measurements of Body Loads. NACA RM L52J08, 1952.

6. Smith, Norman F., and Carlson, Harry W.: The Origin and Distribution of Supersonic Store Interference From Measurement of Individual Forces on Several Wing-Fuselage-Store Configurations. II.- Swept-Wing Heavy-Bomber Configuration With Large Store (Nacelle). Lateral Forces and Pitching Moments; Mach Number, 1.61. NACA RM L55E26a, 1955.

7. Jacobsen, Carl R.: Effects of the Spanwise, Chordwise, and Vertical Location of an External Store on the Aerodynamic Characteristics of a 45° Sweptback Tapered Wing of Aspect Ratio 4 at Mach Numbers of 1.41, 1.62, and 1.96. NACA RM L52J27, 1953.

8. Jacobsen, Carl R.: Effects of Systematically Varying the Spanwise and Vertical Location of an External Store on the Aerodynamic Characteristics of an Unswept Tapered Wing of Aspect Ratio 4 at Mach Numbers of 1.41, 1.62, and 1.96. NACA RM L52F13, 1952.

9. Jacobsen, Carl R.: Effects of the Spanwise, Chordwise, and Vertical Location of an External Store on the Aerodynamic Characteristics of a 60° Delta Wing at Mach Numbers of 1.41, 1.62, and 1.96. NACA RM L52H29, 1952.

10. Burgess, Warren C., Jr., and Seashore, Ferris L.: Criterions for
    Condensation-Free Flow in Supersonic Tunnels. NACA TN 2518, 1951.

11. May, Ellery B., Jr.: Investigation of the Effects of Leading-Edge
    Chord-Extensions on the Aerodynamic and Control Characteristics
    of Two Sweptback Wings at Mach Numbers of 1.41, 1.62, and 1.96.
    NACA RM L50L06a, 1951.

12. Guy, Lawrence D.: Effects of Overhang Balance on the Hinge-Moment
    and Effectiveness Characteristics of an Unswept Trailing-Edge
    Control on a 60° Delta Wing at Transonic and Supersonic Speeds.
    NACA RM L54G12a, 1954.

13. Conner, D. William: Aerodynamic Characteristics of Two All-Movable
    Wings Tested in the Presence of a Fuselage at a Mach Number of 1.9.
    NACA RM L8H04, 1948.

14. Mitchell, Meade H., Jr.: Effects of Varying the Size and Location
    of Trailing-Edge Flap-Type Controls on the Aerodynamic Characteris-
    tics of an Unswept Wing at a Mach Number of 1.9. NACA RM L50F08,
    1950.

15. Whitcomb, Charles F., and Osborne, Robert S.: An Experimental Inves-
    tigation of Boundary Interference on Force and Moment Characteristics
    of Lifting Models in the Langley 16- and 8-Foot Transonic Tunnels.
    NACA RM L52L29, 1953.

16. Osborne, Robert S., and Mugler, John P., Jr.: Aerodynamic Character-
    istics of a 45° Sweptback Wing-Fuselage Combination and the Fuselage
    Alone Obtained in the Langley 8-Foot Transonic Tunnel. NACA
    RM L52E14, 1952.

17. Wright, Ray H., and Ward, Vernon G.: NACA Transonic Wind-Tunnel
    Test Sections. NACA RM L8J06, 1948.

18. Sleeman, William C., Jr., Klevatt, Paul L., and Linsley, Edward L.:
    Comparison of Transonic Characteristics of Lifting Wings From
    Experiments in a Small Slotted Tunnel and the Langley High-Speed
    7- by 10-Foot Tunnel. NACA RM L51F14, 1951.

19. Donlan, Charles J., Myers, Boyd C., II, and Mattson, Axel T.: A
    Comparison of the Aerodynamic Characteristics at Transonic Speeds
    of Four Wing-Fuselage Configurations As Determined From Different
    Test Techniques. NACA RM L50H02, 1950.

20. Silvers, H. Norman, and O'Bryan, Thomas C.: Some Notes on the Aero-
    dynamic Loads Associated With External-Store Installations. NACA
    RM L53E06a, 1953.

21. Silvers, H. Norman, King, Thomas J., Jr., and Alford, William J., Jr.:
    Wind-Tunnel Investigation at High Subsonic Speeds of the Effects
    of Wing-Mounted External Stores on the Loading and Aerodynamic
    Characteristics in Pitch of a 45° Sweptback Wing Combined With a
    Fuselage. NACA RM L54A21, 1954.

22. West, F. E., Jr., and Henderson, James H.: Relationship of Flow
    Over a 45° Sweptback Wing With and Without Leading-Edge Chord-
    Extensions to Longitudinal Stability Characteristics at Mach Num-
    bers From 0.60 to 1.03. NACA RM L53H18b, 1953.

23. Weil, Joseph, and Morrison, William D., Jr.: A Study of the Use of
    Leading-Edge Notches as a Means for Improving the Low-Speed Pitching-
    Moment Characteristics of a Thin 45° Swept Wing of Aspect Ratio 4.
    NACA RM L53J27a, 1953.

24. Guy, Lawrence D.: Loads on External Stores at Transonic and Super-
    sonic Speeds. NACA RM L55E13b, 1955.

TABLE I.- DIMENSIONS OF TUNNEL TEST SECTIONS AND MODELS

(a) Tunnel test sections

Langley tunnels	Effective test section size	Test section cross-sectional area, sq ft
9- by 12-inch blowdown tunnel	7 in. × 10 in.	0.486
16-foot transonic tunnel	15.95 ft diameter	199.9
8-foot transonic tunnel	7.30 ft diameter	42.9

(b) Ratio of model-to-tunnel dimensions

Model	Tunnel	Ratio of wing plan-form area of model to cross-sectional area of tunnel test section
Large	Langley 9- by 12-inch blowdown tunnel	0.16
Small	Langley 9- by 12-inch blowdown tunnel	0.07
Sting	Langley 16-foot transonic tunnel	0.005
Sting	Langley 8-foot transonic tunnel	0.0233
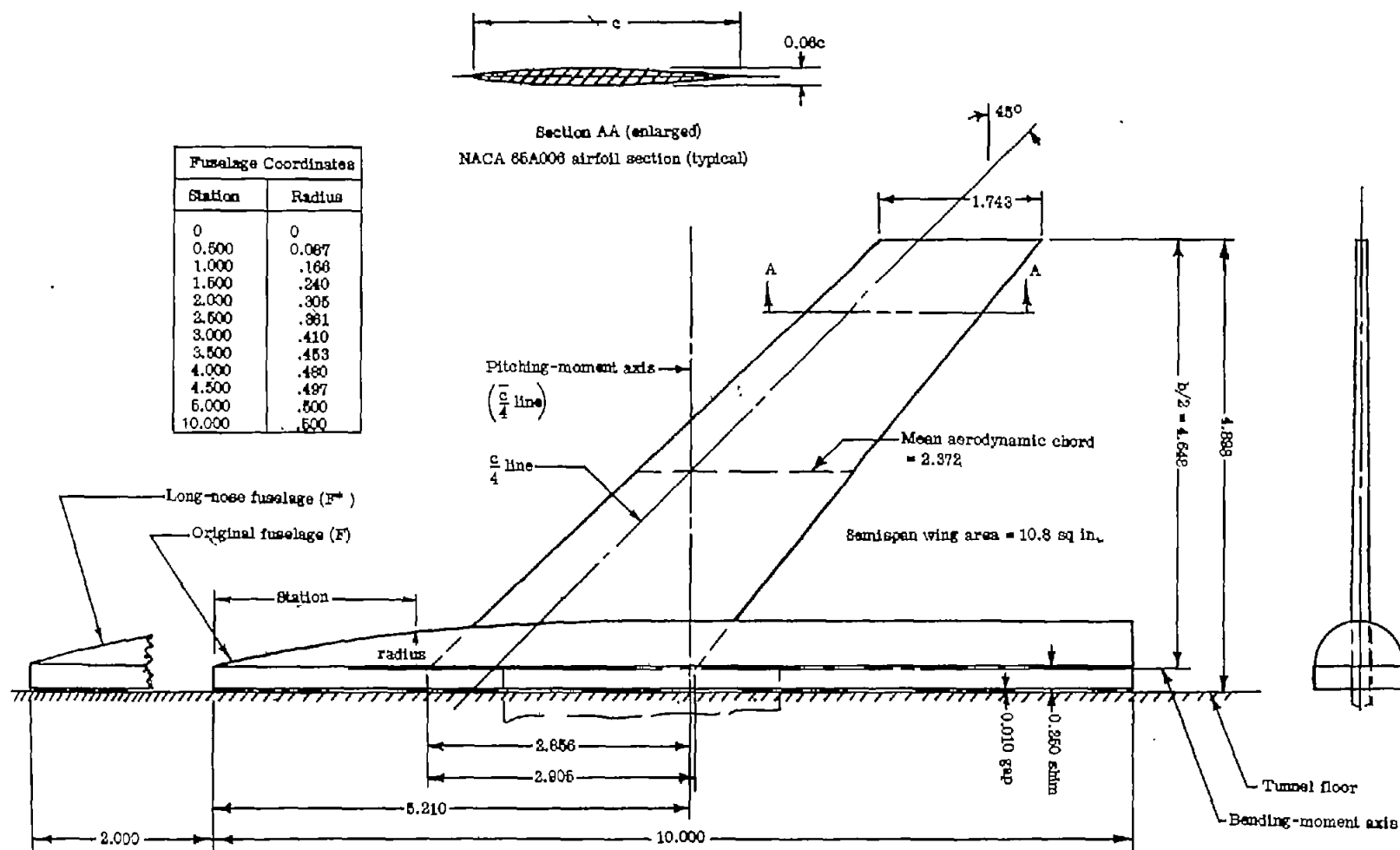
(a) Large model tested in Langley 9- by 12-inch blowdown tunnel.

Figure 1.- Details of 45° sweptback wings of aspect ratio 4.0. All
dimensions are in inches.

TABULATED GEOMETRIC CHARACTERISTICS

FUSELAGE COORDINATES			
x/l	r/l	x/l	r/l
0	0	0.4500	0.04143
.0050	.00231	.5000	.04167
.0075	.00296	.5500	.04130
.0125	.00428	.6000	.04024
.0250	.00722	.6500	.03843
.0500	.01205	.7000	.03562
.0750	.01613	.7500	.03128
.1000	.01971	.8000	.02526
.1500	.02593	.8151	.02326
.2000	.03090	.8333	.02063
.2500	.03465	.8500	.01852
.3000	.03741	.9000	.01135
.3500	.03933	.9500	.00439
.4000	.04063	1.0000	0

L.E. radius = 0.0005 l

Wing

Aspect ratio 4.0
Taper ratio 0.8
Airfoil section parallel .... NACA 65A006
   to free stream

Wing area .... 144 sq in.
Wing semispan .... 12.000 in.
Mean aerodynamic chord .... 6.125 in.
Root chord .... 7.500 in.
Tip chord .... 4.500 in.
Wing incidence .... 0°
Maximum body diameter .... 3.33 in.

.815 l = 32.608
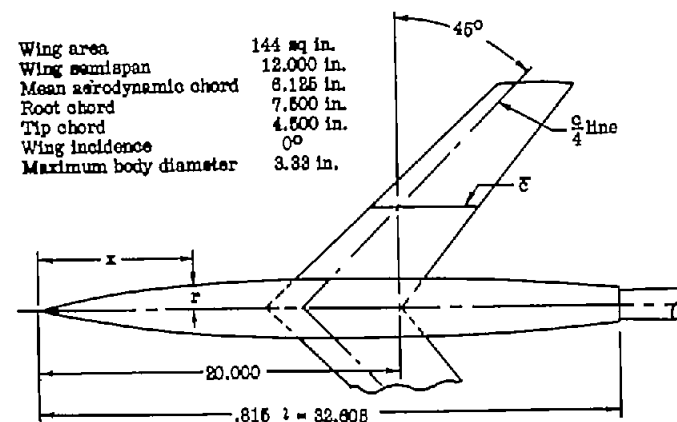
16-FOOT AND 8-FOOT TRANSONIC TUNNEL MODEL

Twice semispan wing area ..... 21.60 sq in.
Wing semispan .... 4.548 in.
Mean aerodynamic chord .... 2.373 in.
Root chord .... 2.905 in.
Tip chord .... 1.743 in.
Wing incidence .... 0°
Maximum body diameter .... 1.292 in.

7.746

$\frac{5}{6}$ l = 12.910
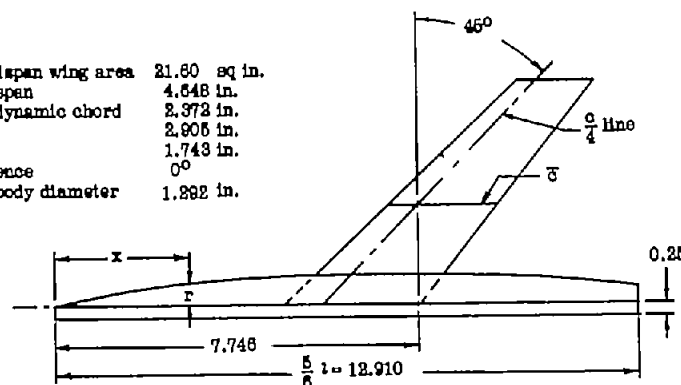
Twice semispan wing area ..... 9.802 sq in.
Wing semispan .... 3.131 in.
Mean aerodynamic chord .... 1.596 in.
Root chord .... 1.967 in.
Tip chord .... 1.174 in.
Wing incidence .... 0°
Maximum body diameter .... 0.870 in.

5.218

$\frac{5}{6}$ l = 8.696
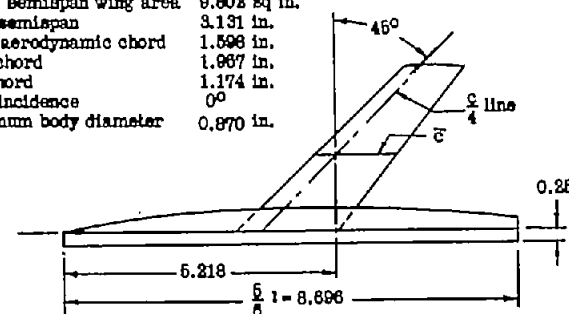
BLOWDOWN TUNNEL MODELS

(b) Details of wing models tested in three different facilities.

Figure 1.- Concluded.

Douglas Store Ordinates	
Station	Radius
0	0
.076	.036
.188	.080
.299	.118
.411	.140
.519	.160
.630	.176
.742	.188
.966	.211
1.185	.227
1.408	.233
1.983	.233
2.206	.229
2.426	.219
2.645	.203
2.873	.184
3.200	.148
3.990	0

Figure 2.- Details of the sting-mounted DAC store. All dimensions are in inches.
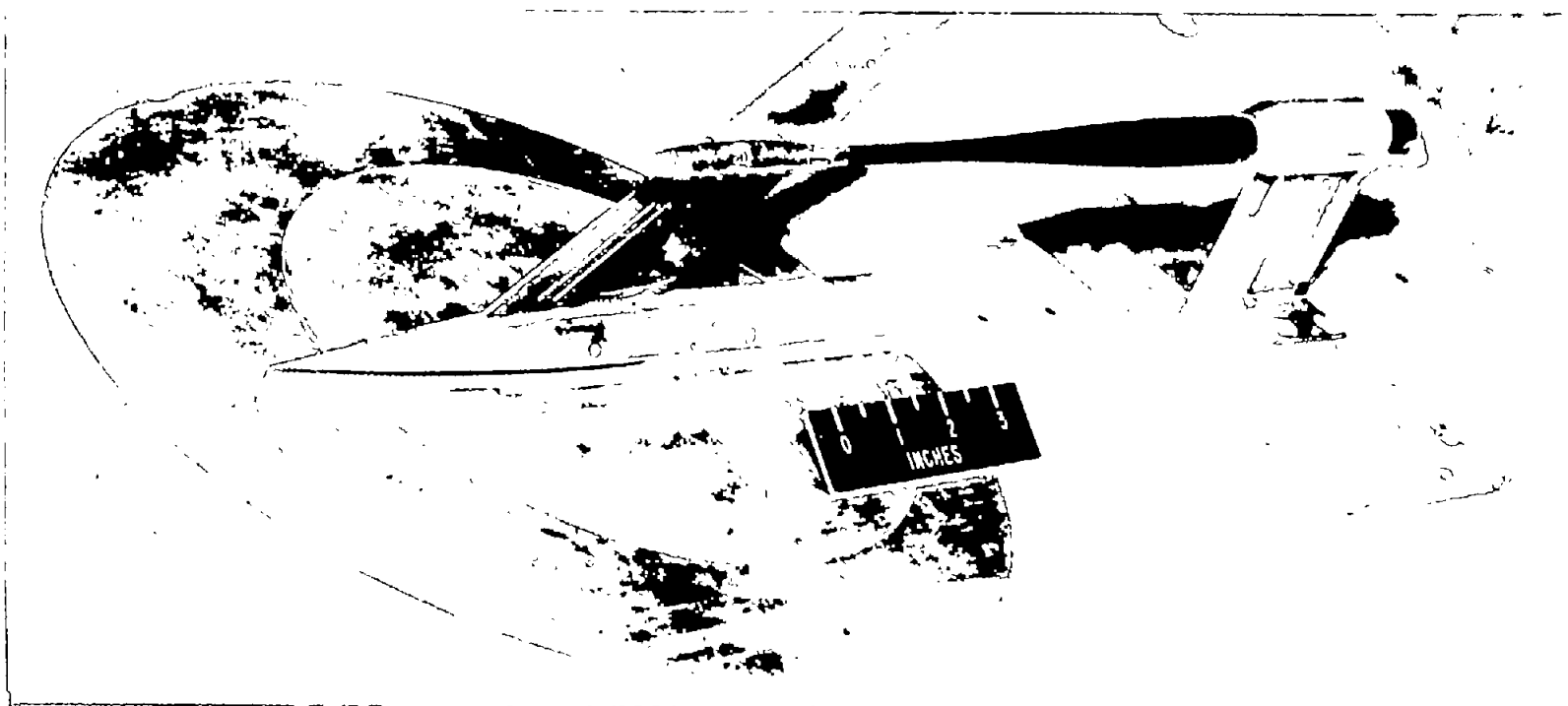
L-85821

Figure 3.- Photograph of a typical test setup. $\left(\text{Store position: } \dfrac{2y}{b} = 0.60; \right.$

$\left. \dfrac{z}{d} = 1.0; \dfrac{x}{c} = 0. \right)$
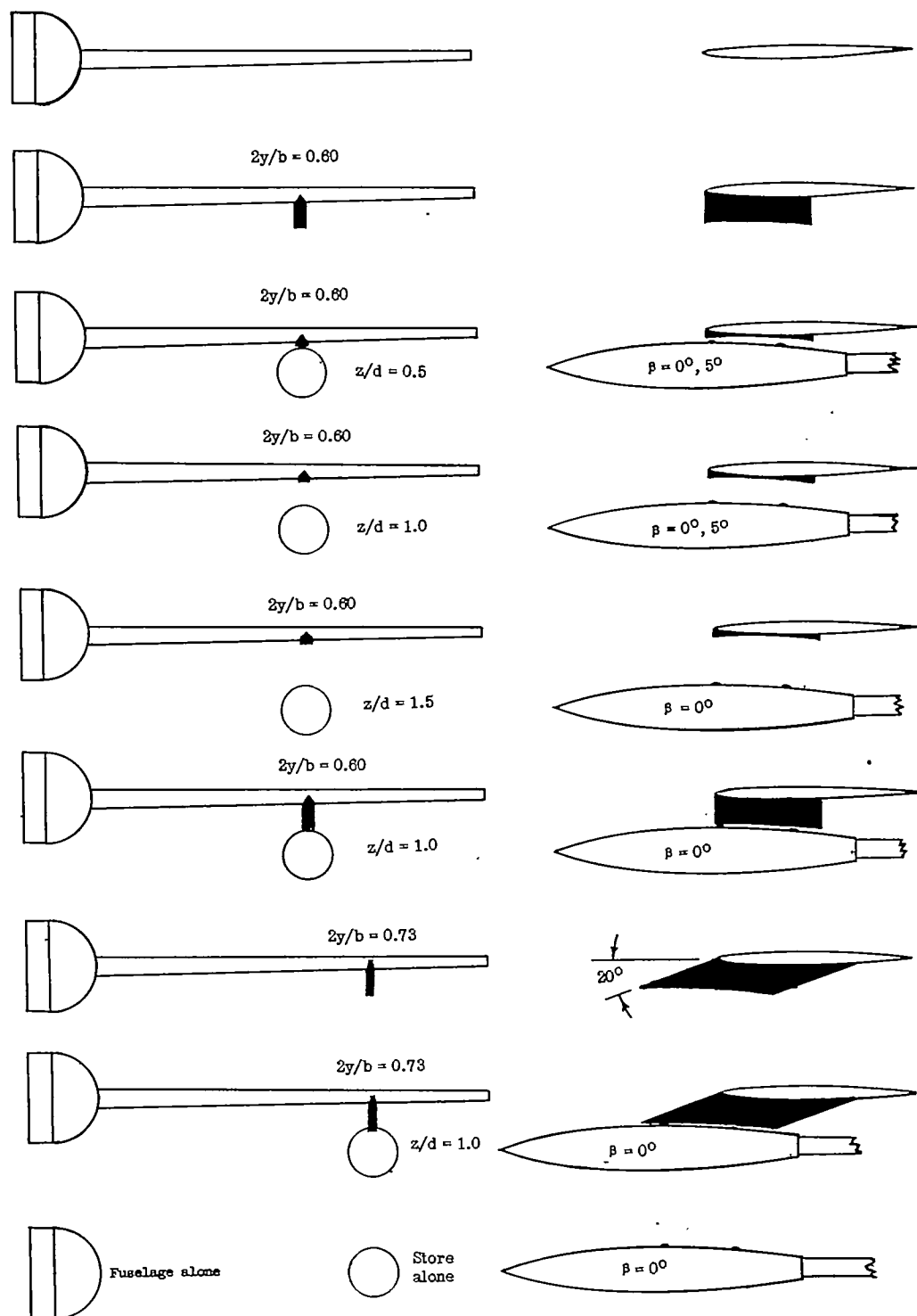
Figure 4.- Configurations tested for Mach numbers between 0.70 and 1.96.
$$\frac{X}{c} = 0.$$

$\pm .1$

ΔM

0

.6   .7   .8   .9   1.0   1.1   1.2

M
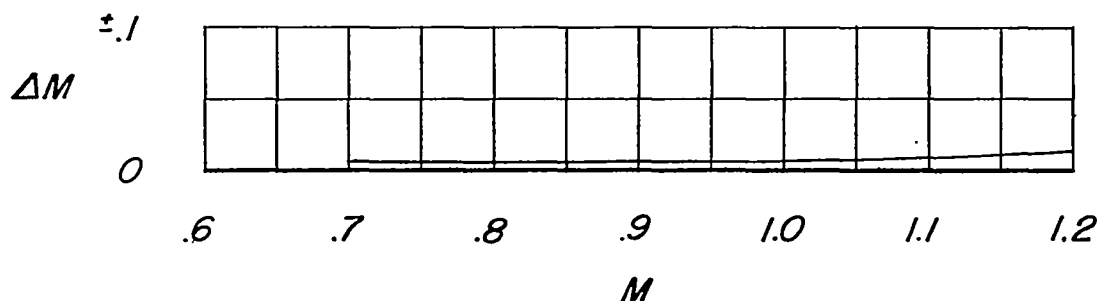
(a) Maximum deviation from average test section Mach number in transonic
blowdown tunnel (tunnel clear).

――――――― 9- by 12-inch blowdown tunnel   Large model
― ― ― ― ― 9- by 12-inch blowdown tunnel   Small model
――― ― ――― 16-foot transonic tunnel   Sting model
――― ― ――― 8-foot transonic tunnel   Sting model

3×10^6

2

R

1

0

.6   .7   .8   .9   1.0   1.1   1.2

M
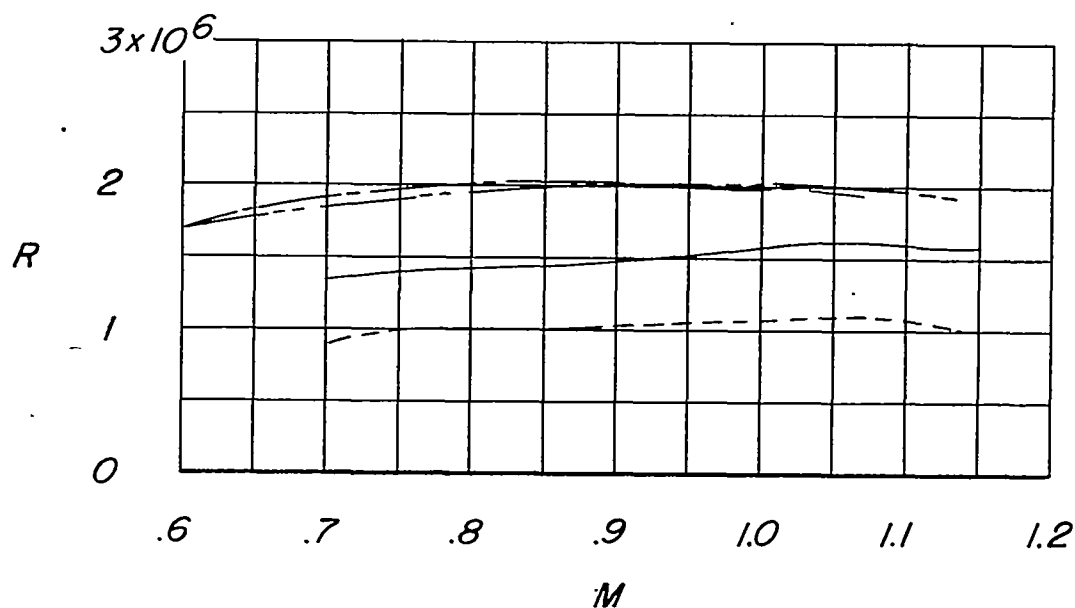
(b) Variation of test Reynolds number based on $\bar{c}$ with Mach number for
$45°$ wing in various facilities.

Figure 5.- Variation of Reynolds number and deviation of test-region Mach
number with Mach number.
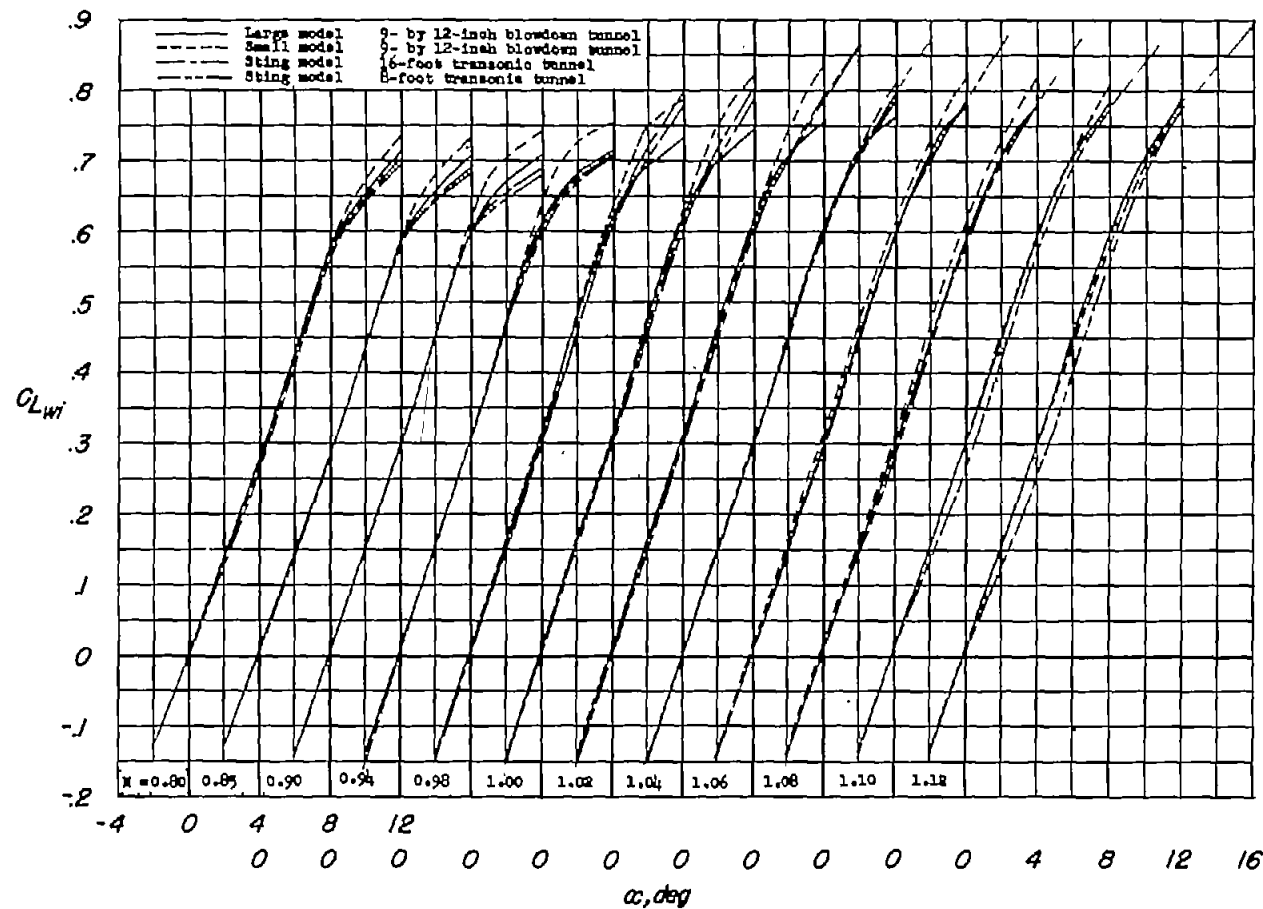
(a) $C_{L_{wi}}$ against α.

Figure 6.- Variation of lift coefficient with angle of attack, pitching-moment coefficient, bending-moment coefficient, and drag due to lift coefficient for wing plus wing-fuselage interference.
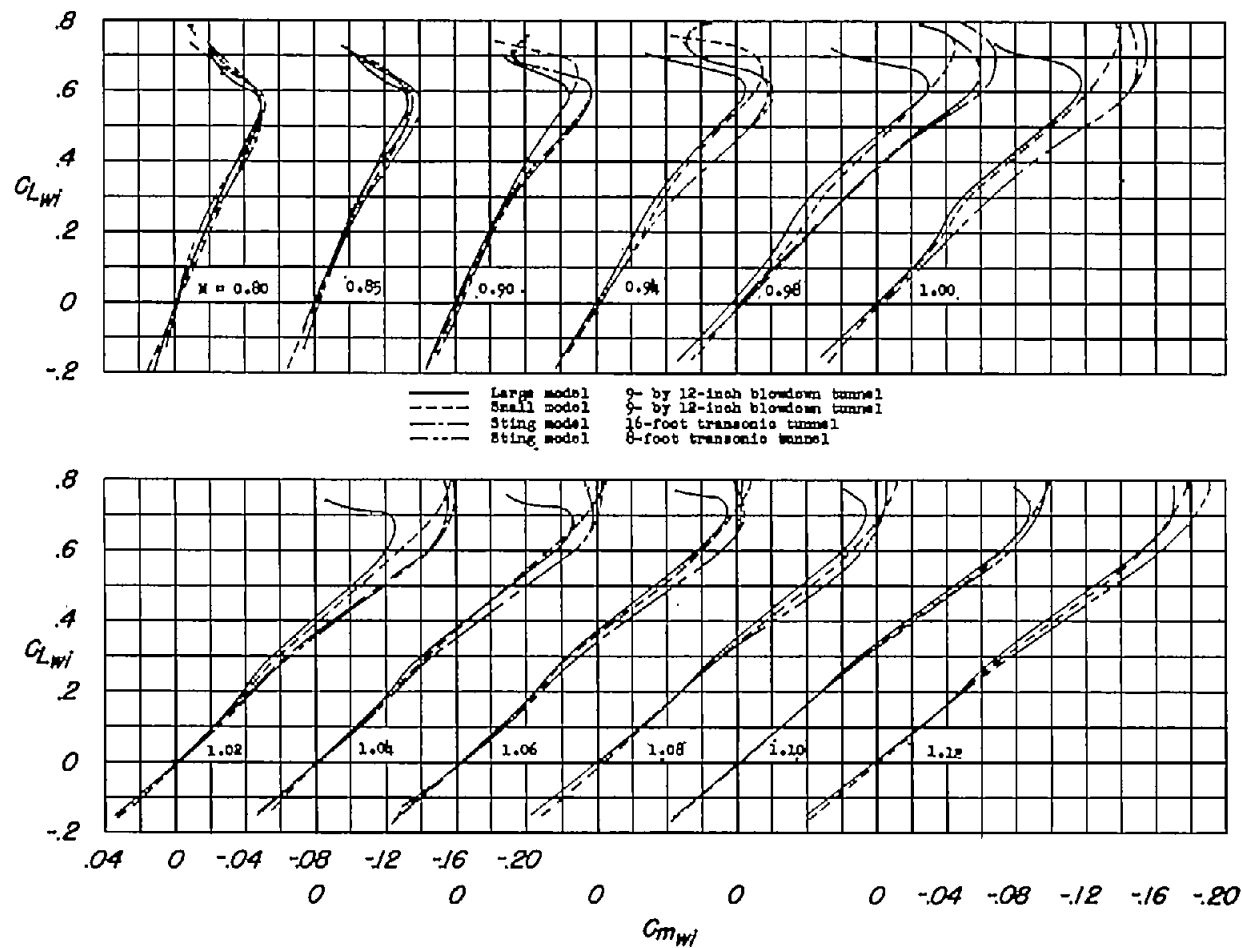
(b) $C_{L_{wi}}$ against $C_{m_{wi}}$.

Figure 6.- Continued.
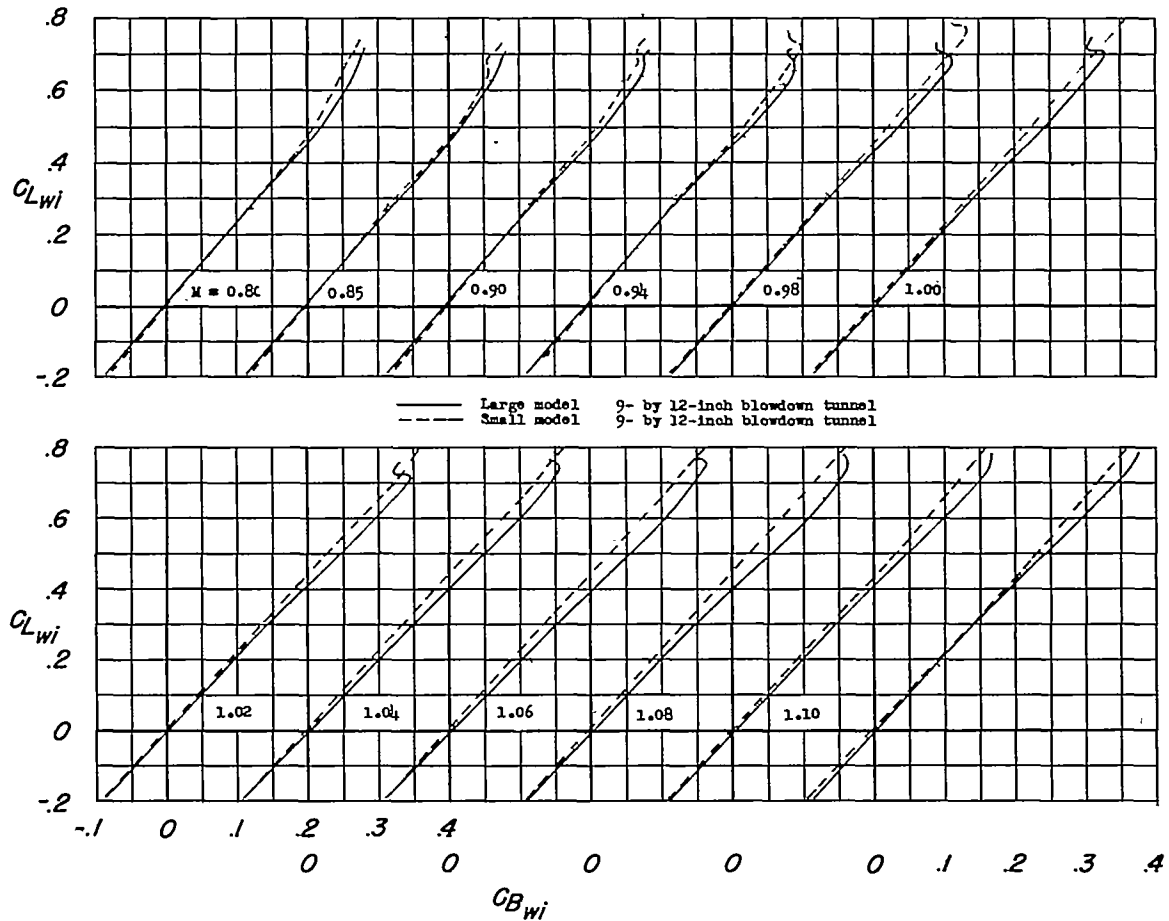
(c) $C_{L_{wi}}$ against $C_{B_{wi}}$.

Figure 6.- Continued.
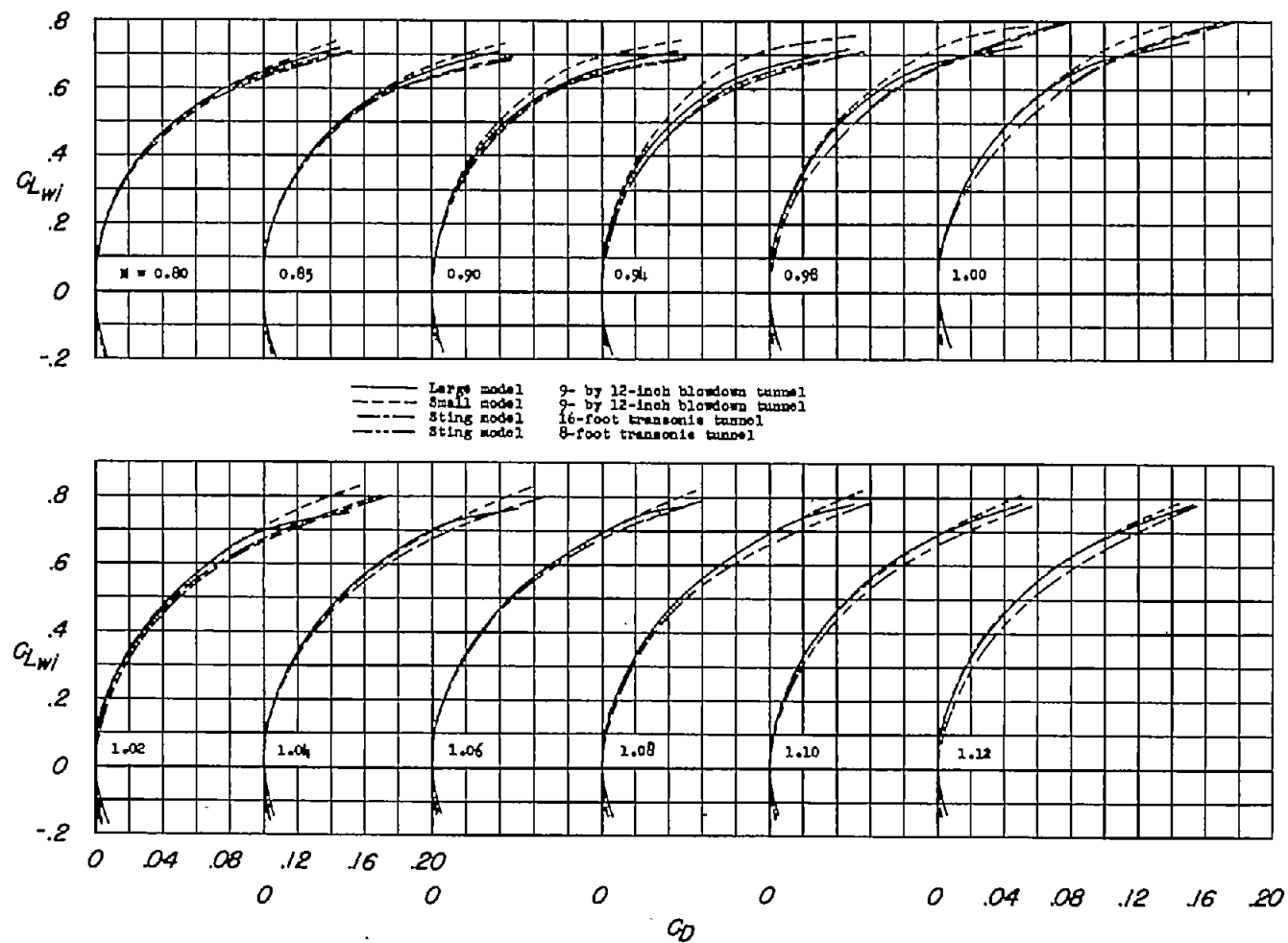
(d) $C_{L_{wi}}$ against C_D.

Figure 6.- Concluded.
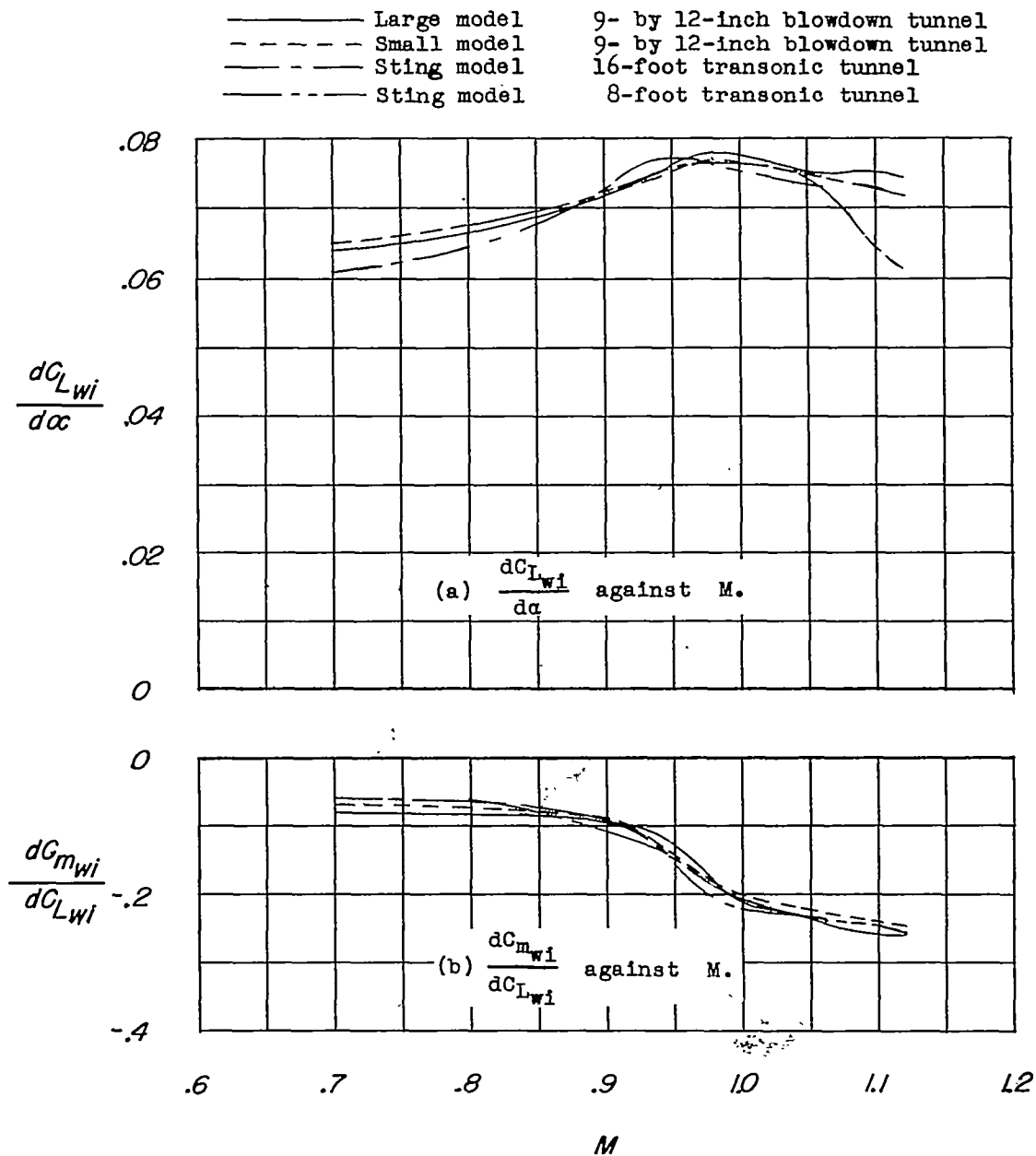
Figure 7.- Variation with Mach number of lift-curve slope and static longitudinal stability parameter for wing with interference. $C_{L_{wi}} = 0$.
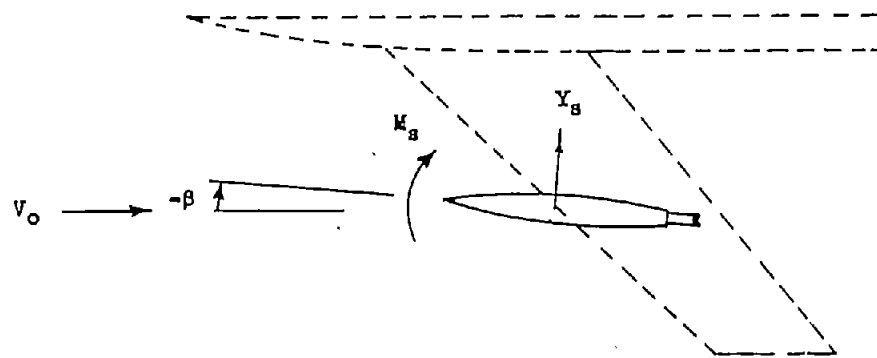
Lateral plane
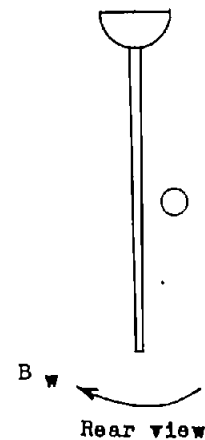
Rear view
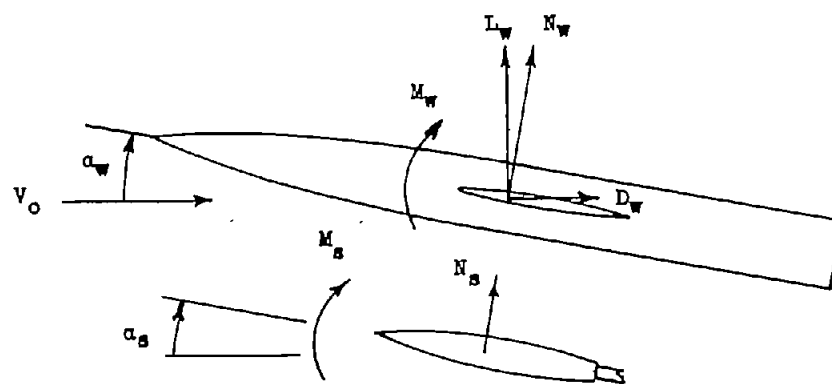
Longitudinal plane

Figure 8.- Positive direction of forces and moments measured on cantilevered
wing-fuselage model and on sting-mounted store model.
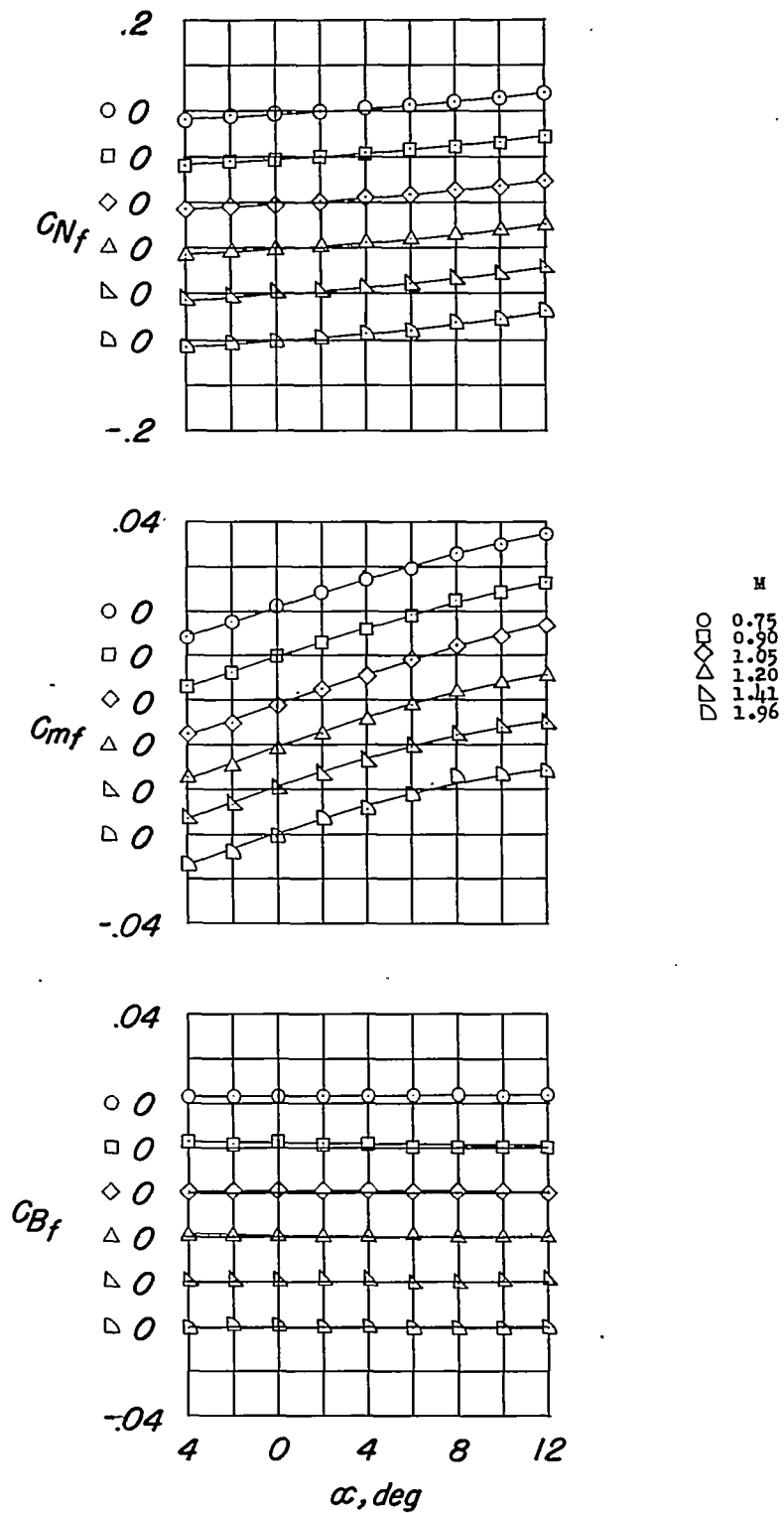
Figure 9.- Aerodynamic characteristics of the original fuselage alone.

	$\frac{2y}{b}$	$\frac{x}{c}$	$\frac{z}{d}$	β
○	—	—	—	—
□	.6	0	.5	0°
◇	.6	0	1.0	0°
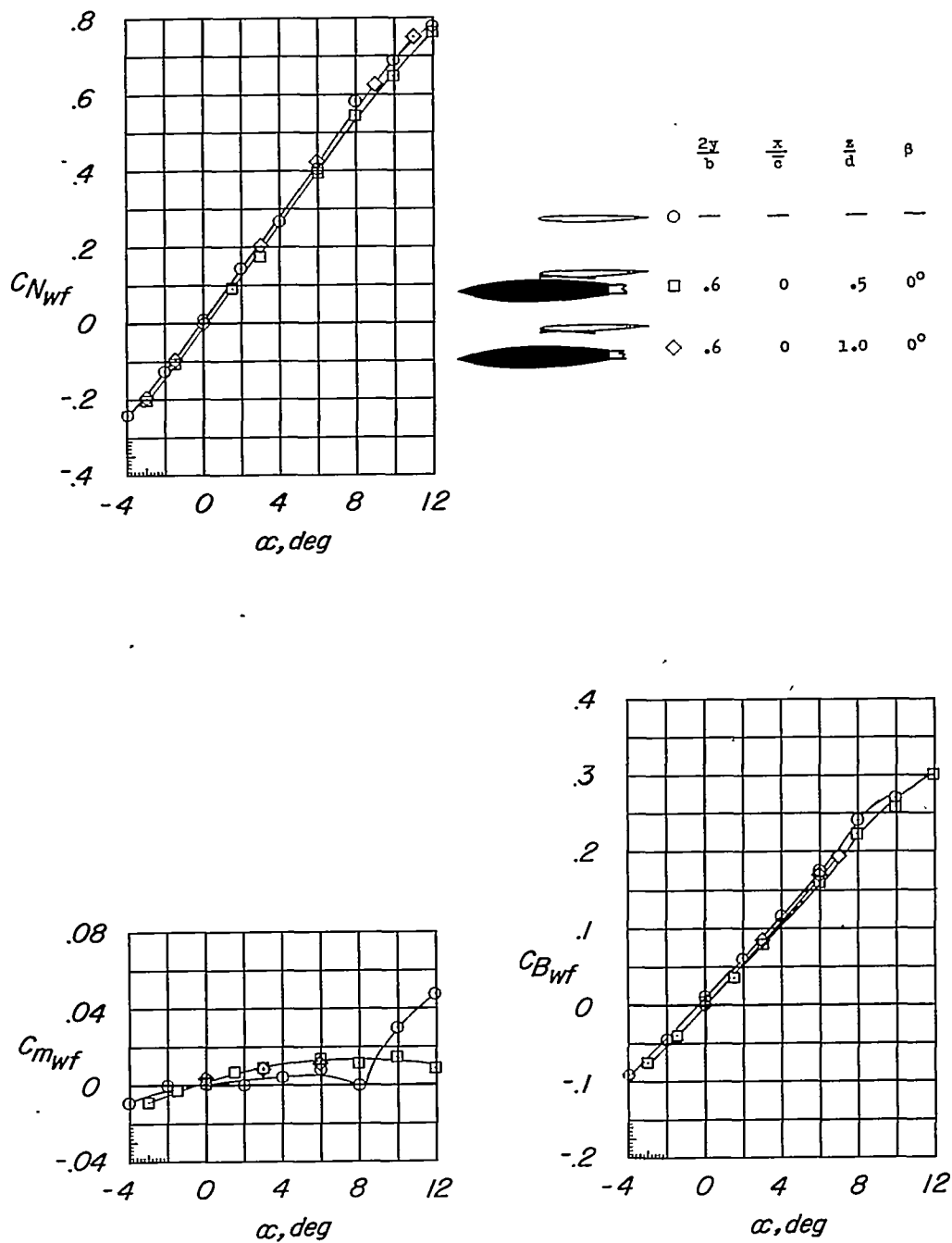
(a)   M = 0.70.

Figure 10.- Influence of the DAC store at various vertical positions on the aerodynamic characteristics of the wing-fuselage. $\frac{2y}{b} = 0.60$; original fuselage.

	$\frac{2y}{b}$	$\frac{x}{c}$	$\frac{z}{d}$	β
○	—	—	—	—
□	.6	0	.5	0°
◇	.6	0	1.0	0°

(b) M = 0.80.

Figure 10.- Continued.

$$\frac{2y}{b} \qquad \frac{x}{c} \qquad \frac{z}{d} \qquad \beta$$

		$\frac{2y}{b}$	$\frac{x}{c}$	$\frac{z}{d}$	β
○	—	—	—	—
□	.6	0	.5	0°
◇	.6	0	1.0	0°
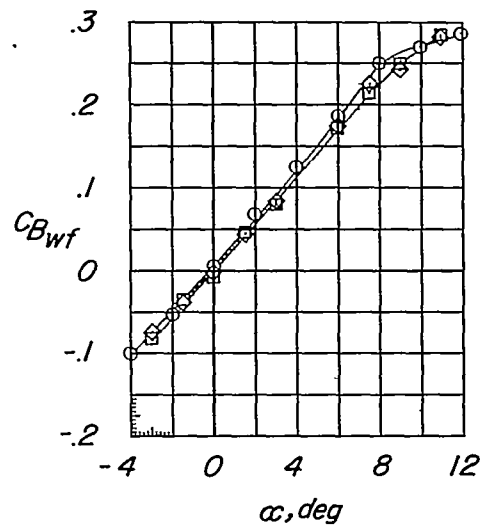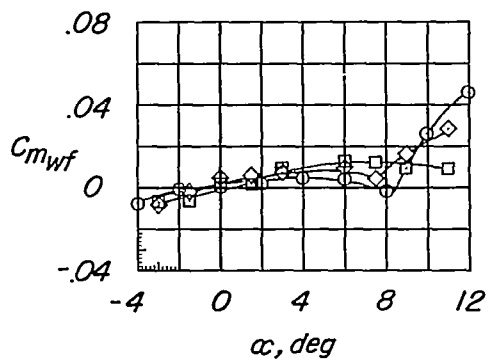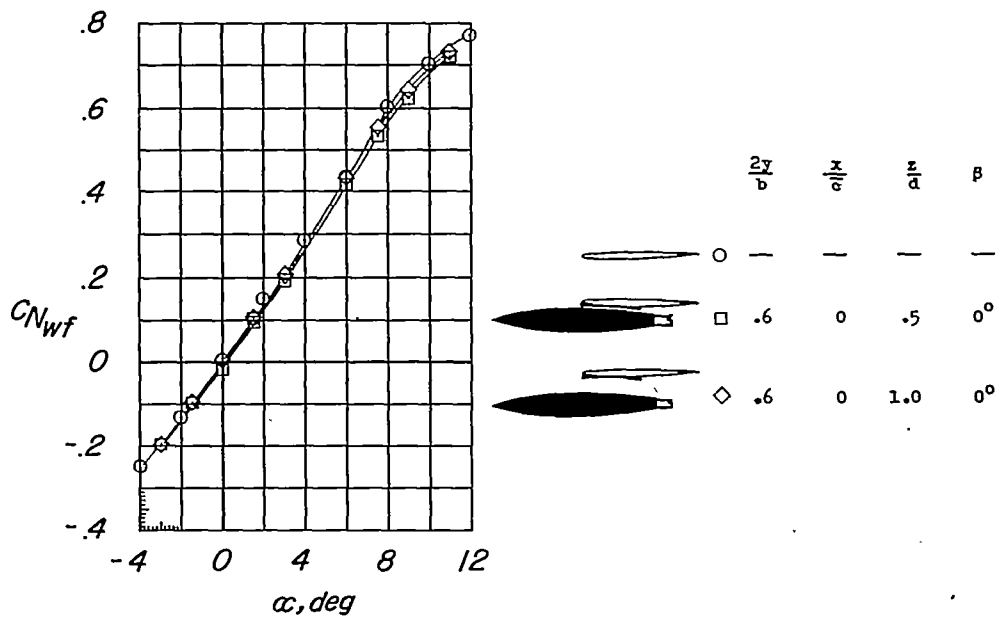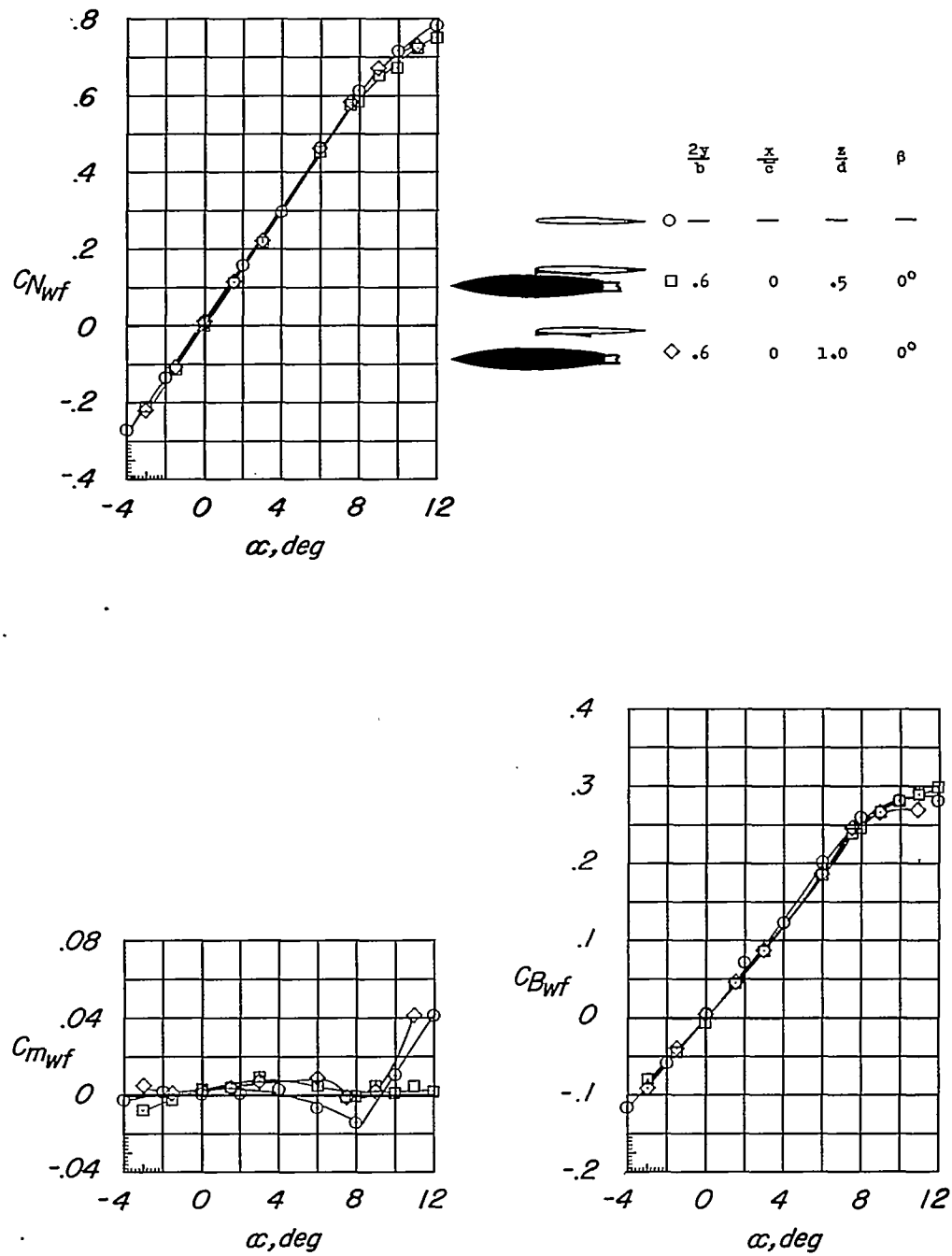
(c)   M = 0.90.

Figure 10.- Continued.

	$\frac{2y}{b}$	$\frac{x}{c}$	$\frac{z}{d}$	β
○	—	—	—	—
□	.6	0	.5	0°
◇	.6	0	1.0	0°
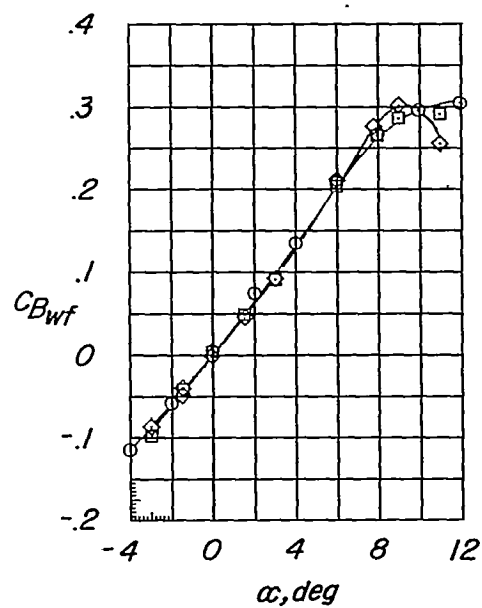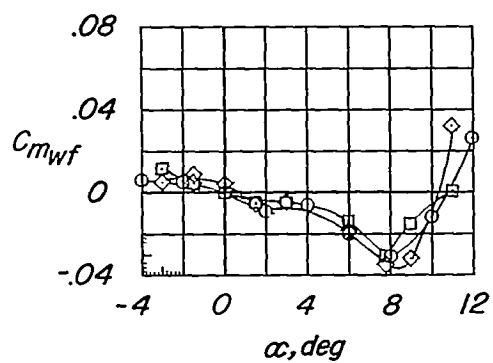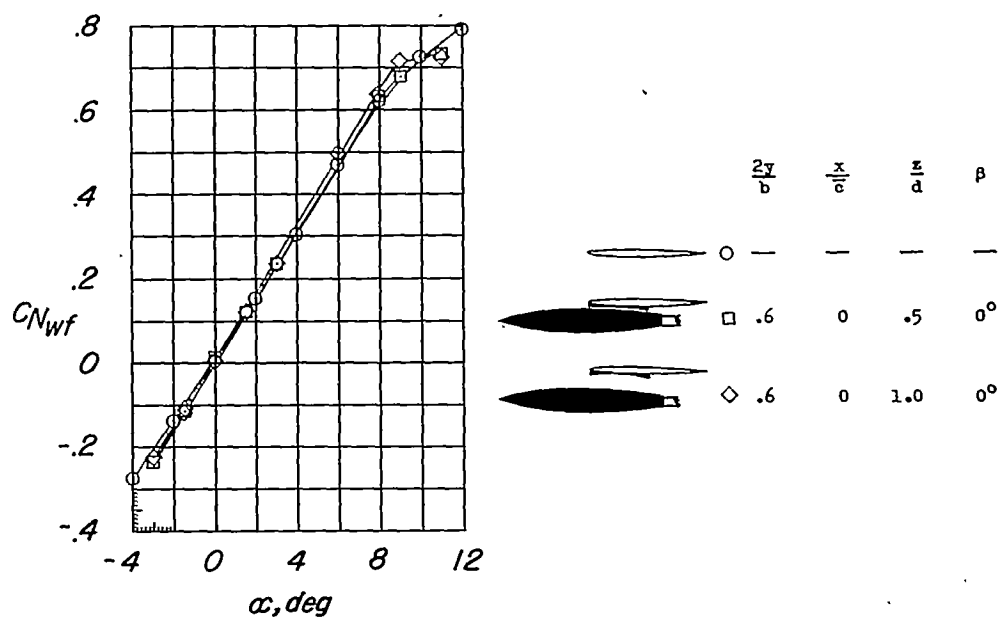
(d)   M = 0.95.

Figure 10.- Continued.
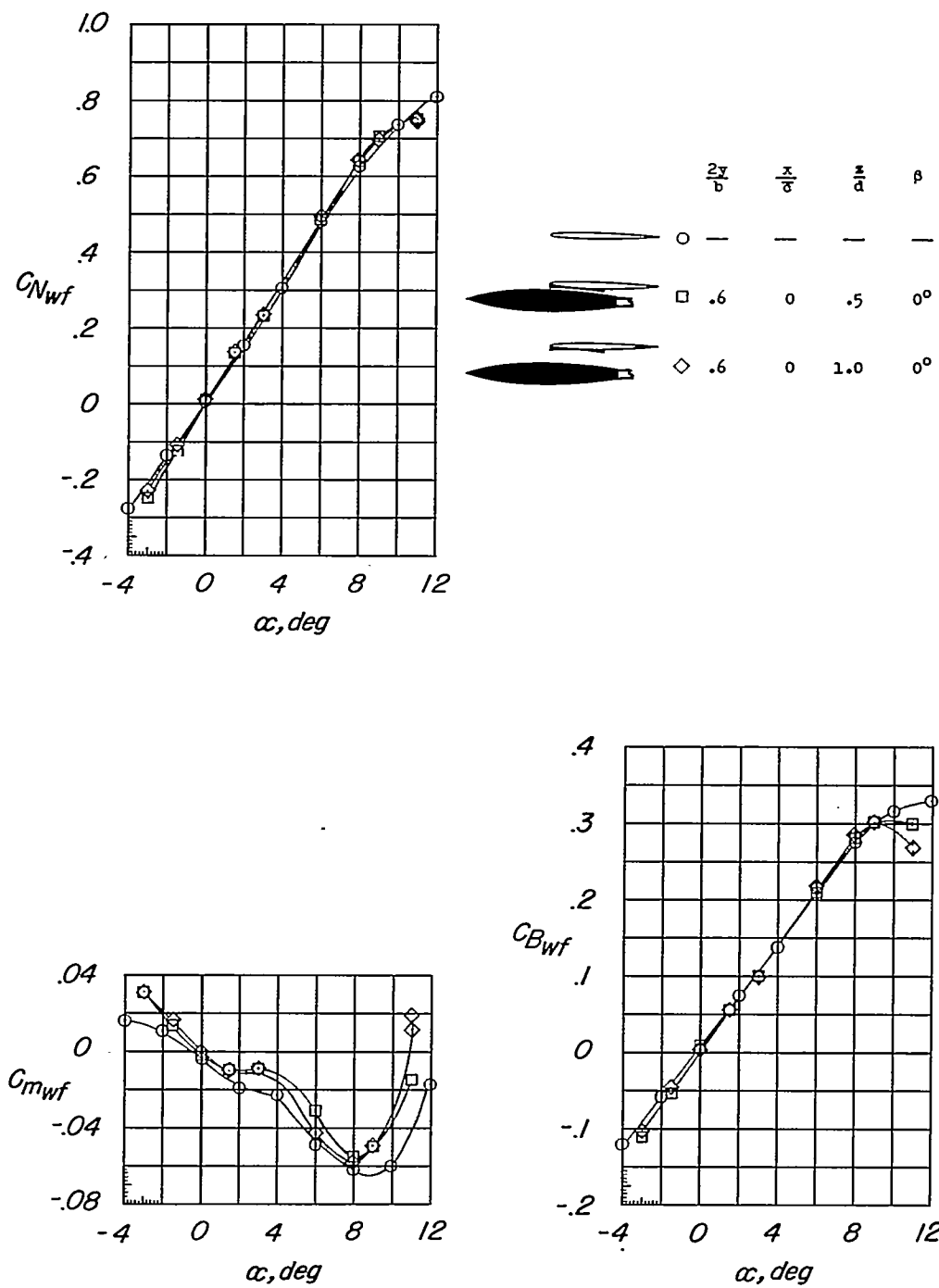
(e) M = 1.00.

Figure 10.- Continued.
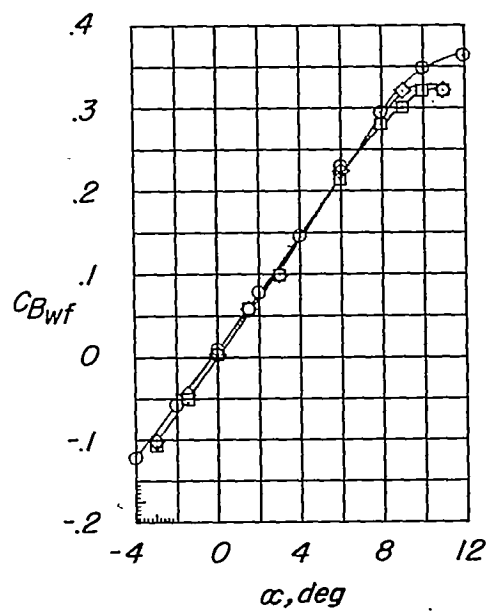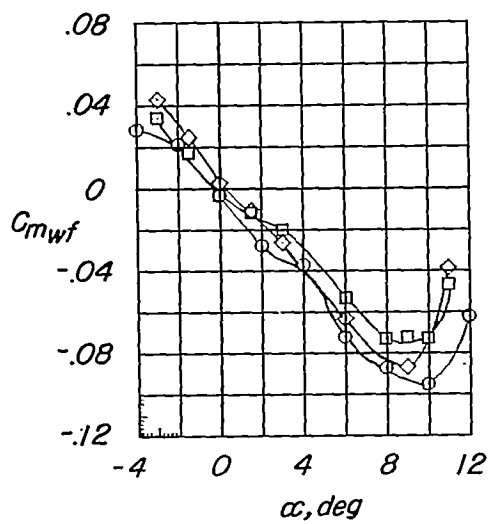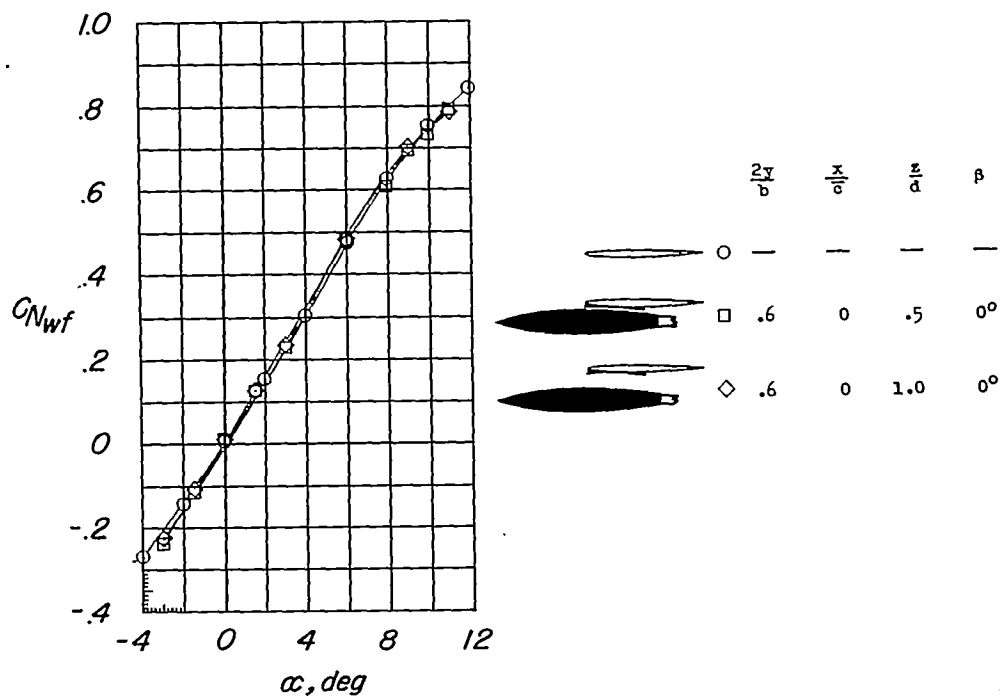
(f) M = 1.05.

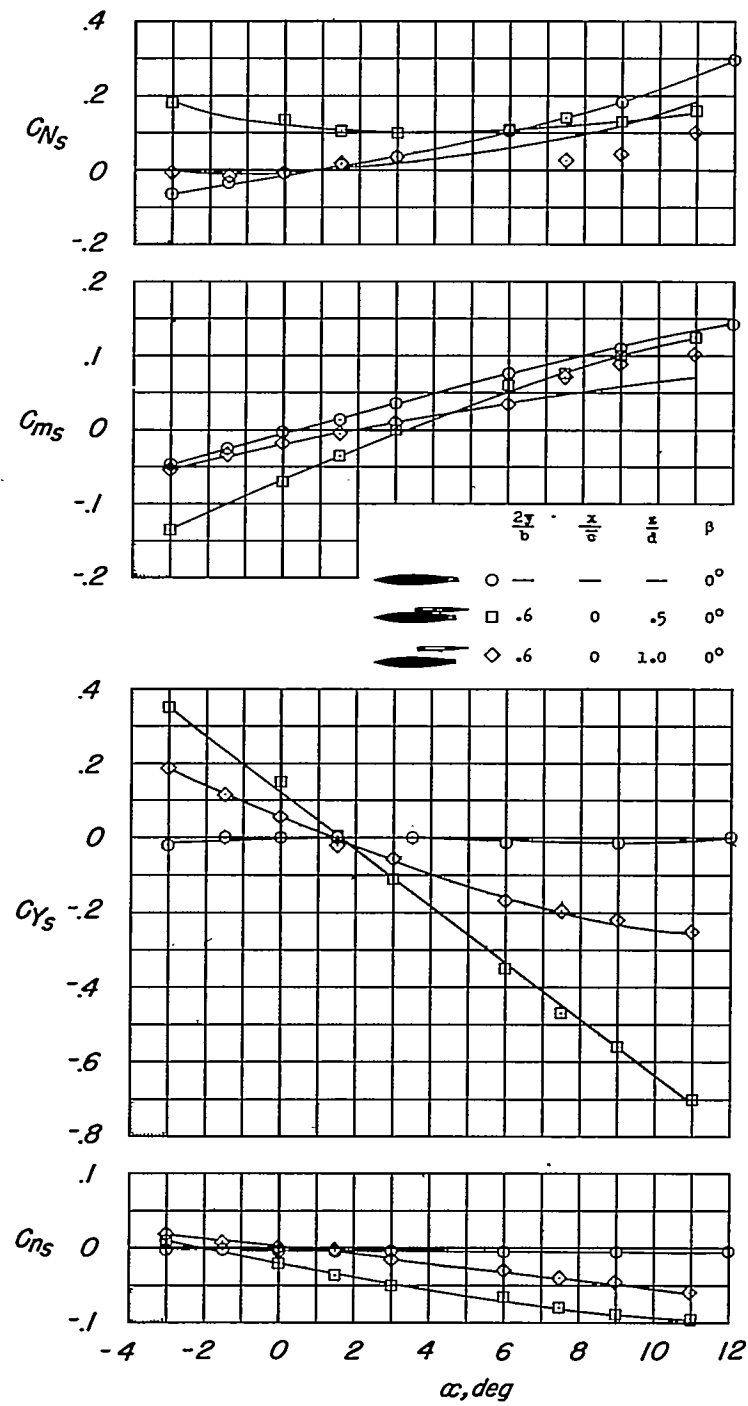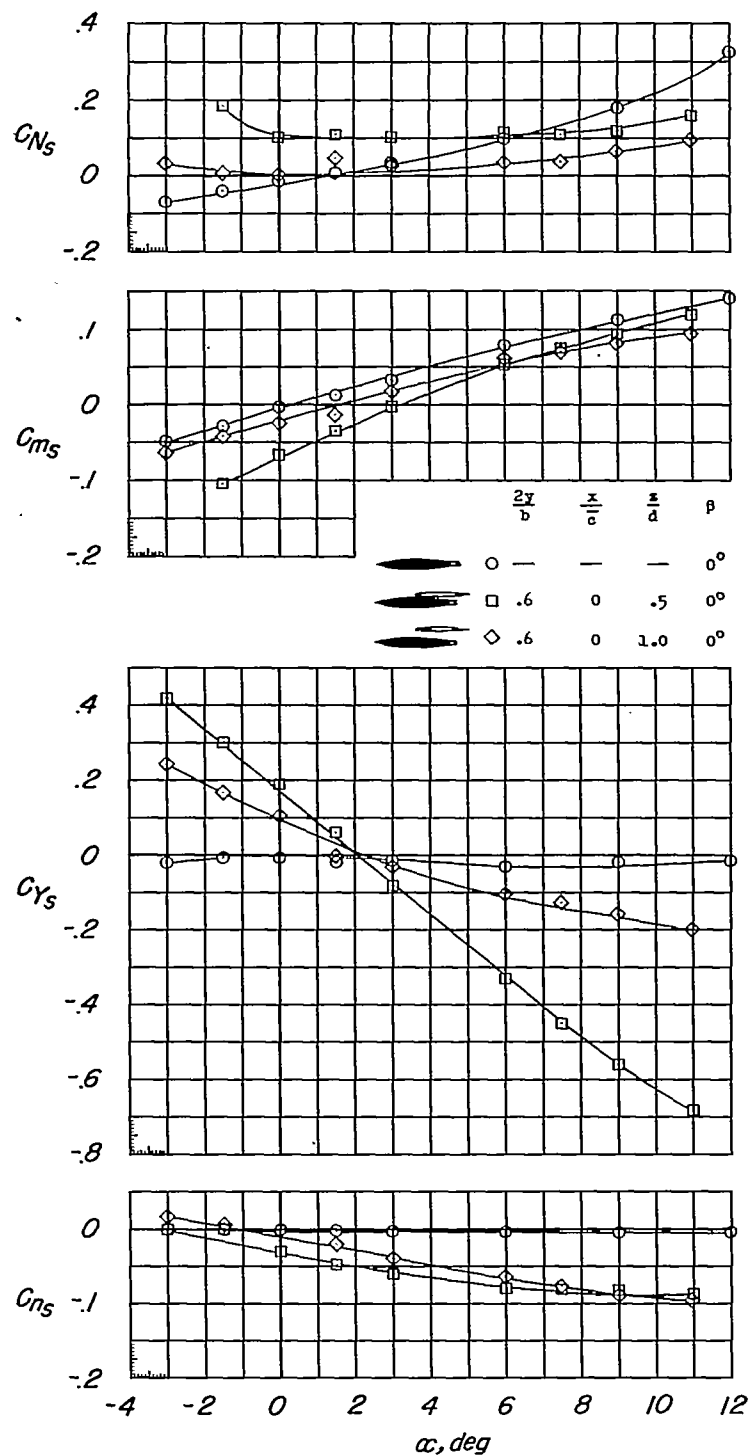Figure 10.- Continued.

(g) M = 1.20.

Figure 10.- Continued.

The chart legend:

	$\frac{2y}{b}$	$\frac{x}{c}$	$\frac{z}{d}$	β
○	—	—	—	—
□	.6	0	.5	0°
◇	.6	0	1.0	0°
△	.6	0	1.5	0°

$C_{N_{wf}}$ α, deg

$C_{m_{wf}}$ α, deg

$C_{B_{wf}}$ α, deg

(h)   M = 1.41.

Figure 10.- Continued.

	$\frac{2y}{b}$	$\frac{x}{c}$	$\frac{z}{d}$	β
○	—	—	—	—
□	.6	0	.5	0°
◇	.6	0	1.0	0°
△	.6	0	1.5	0°
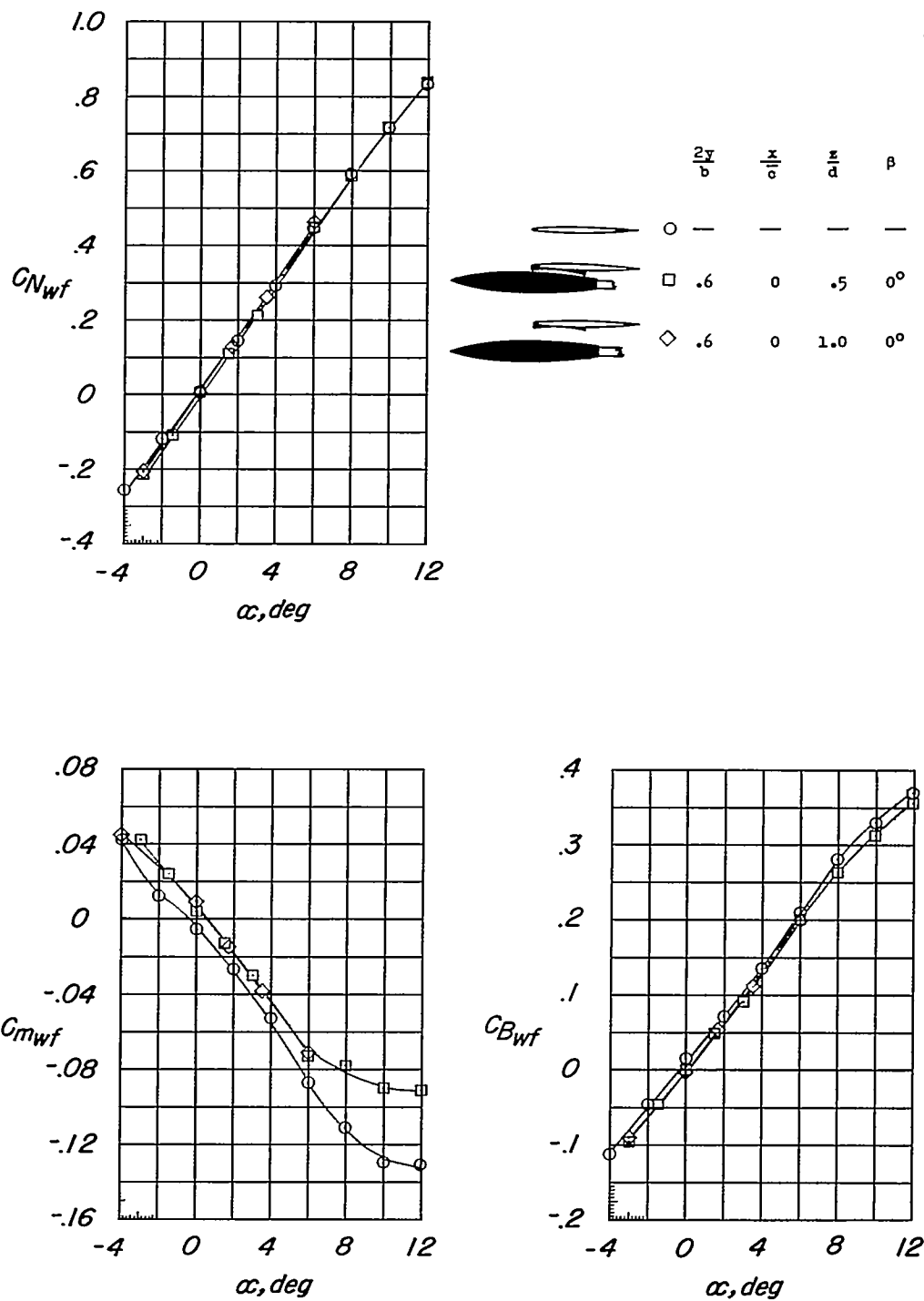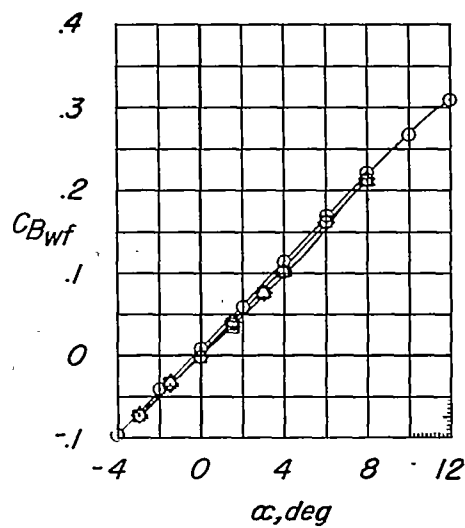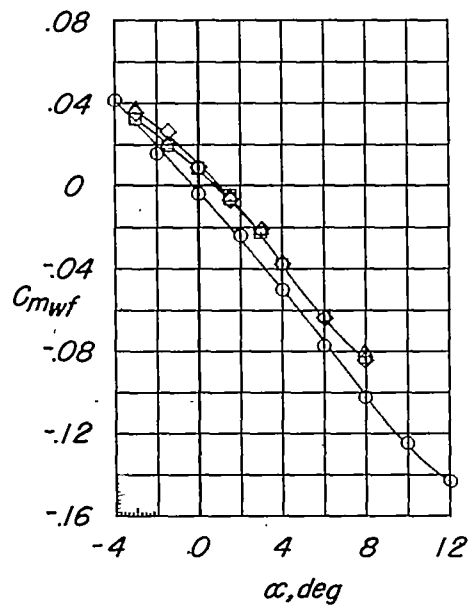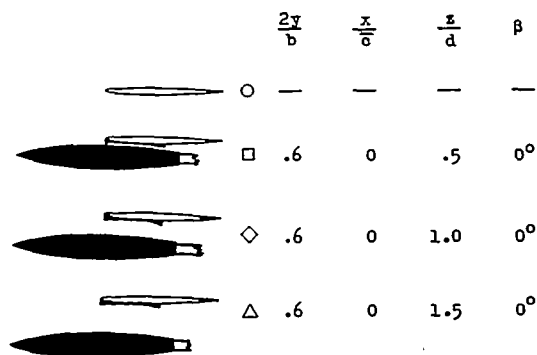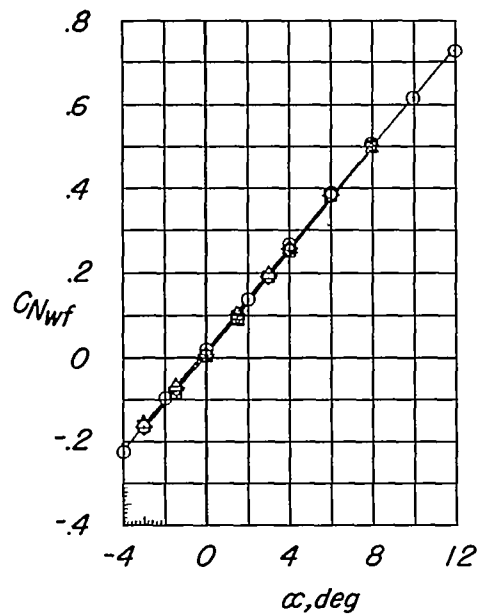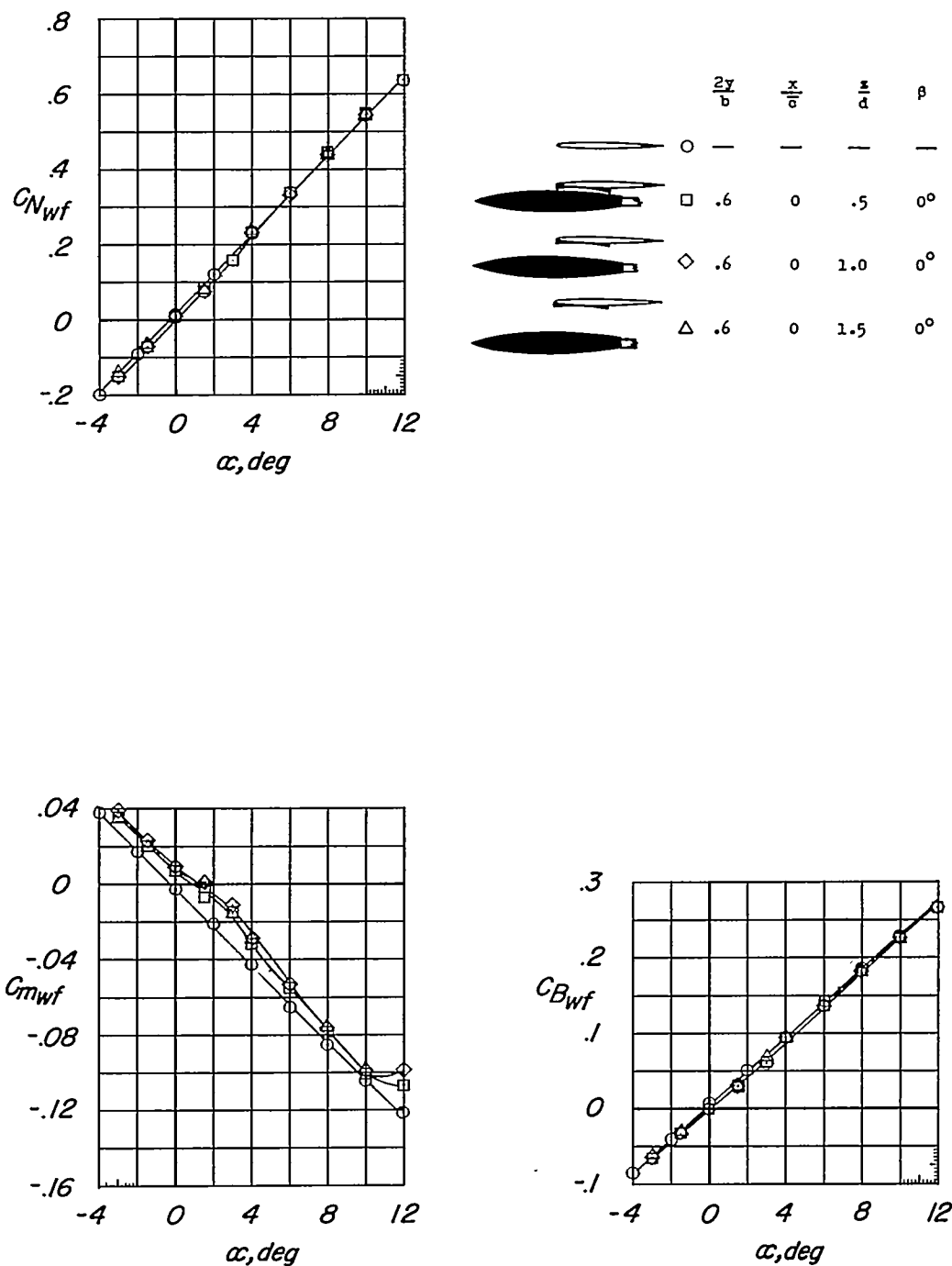
(i) M = 1.62.

Figure 10.- Continued.
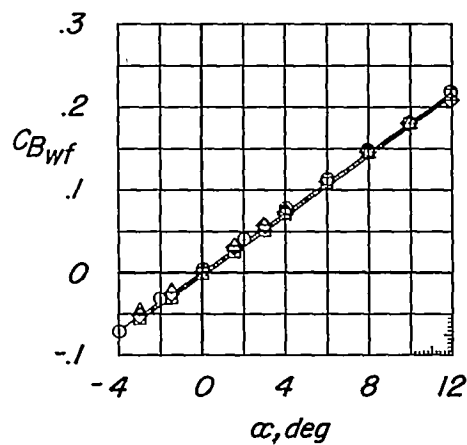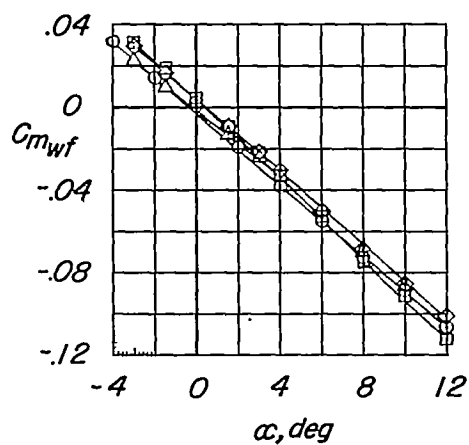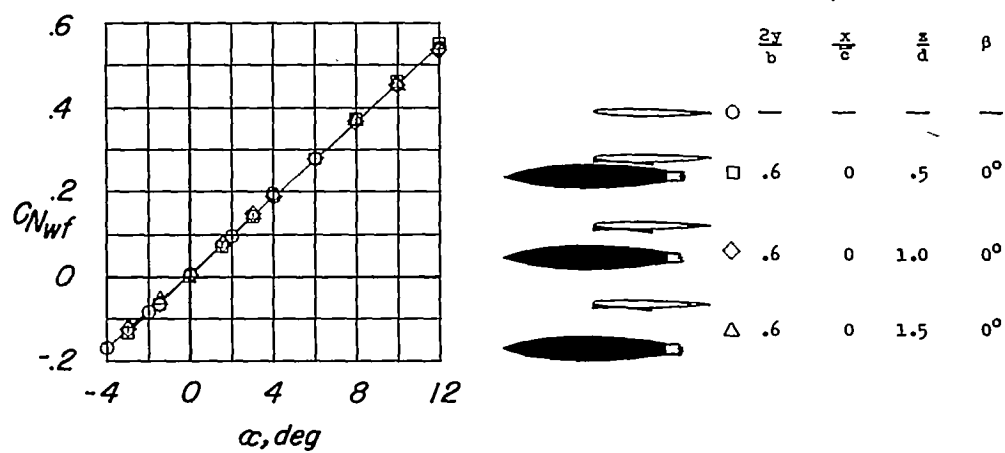
(j) M = 1.96.

Figure 10.- Concluded.
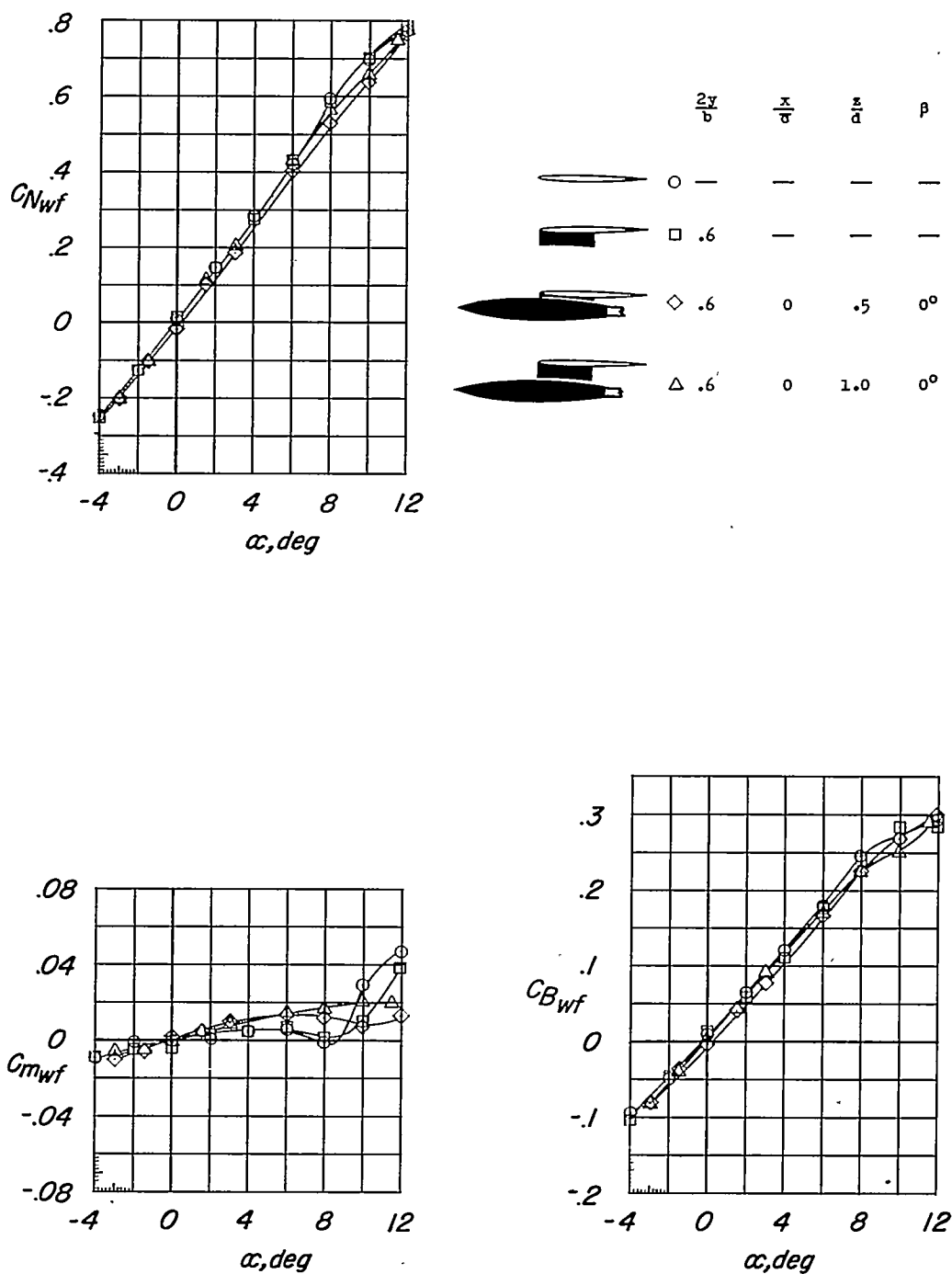
(a) M = 0.75.

Figure 11.- Influence of the DAC store on the aerodynamic characteristics of the wing-fuselage including effects of pylon. $\frac{2y}{b} = 0.60$; original fuselage.

	$\dfrac{2y}{b}$	$\dfrac{x}{c}$	$\dfrac{z}{d}$	β
○	—	—	—	—
□	.6	—	—	—
◇	.6	0	.5	$0°$
△	.6	0	1.0	$0°$
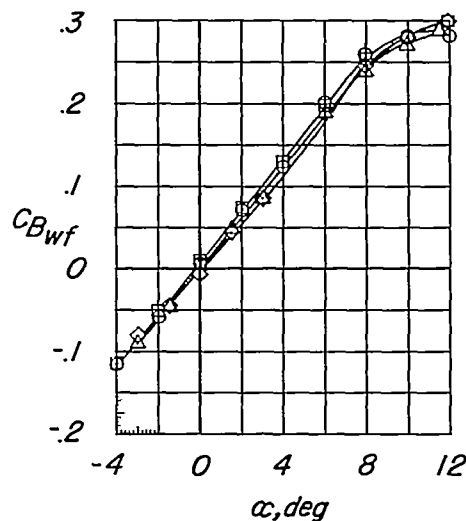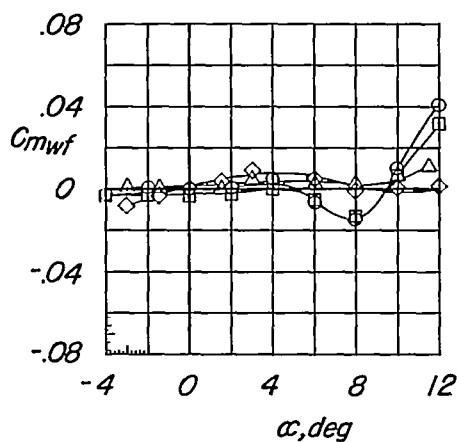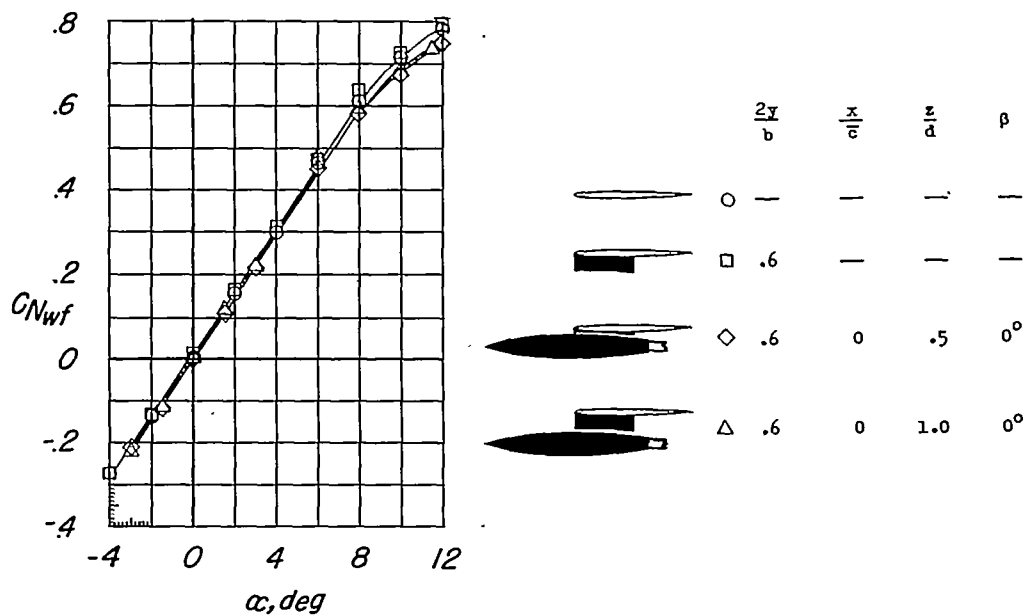
(b) M = 0.90.

Figure 11.- Continued.
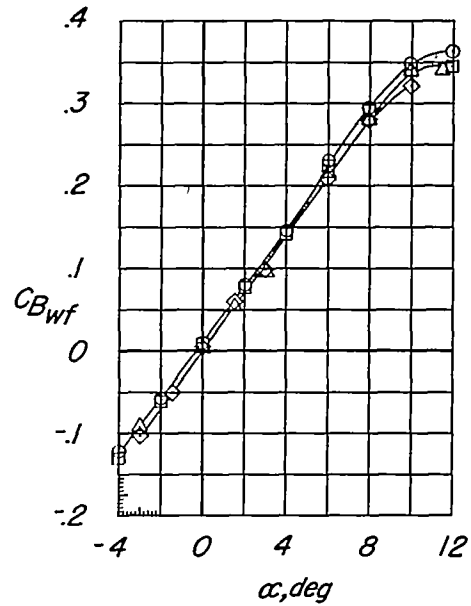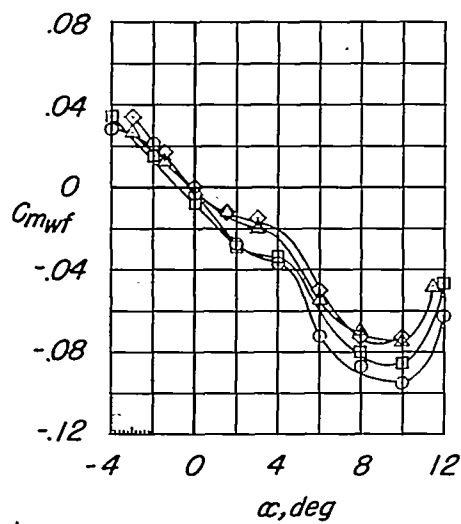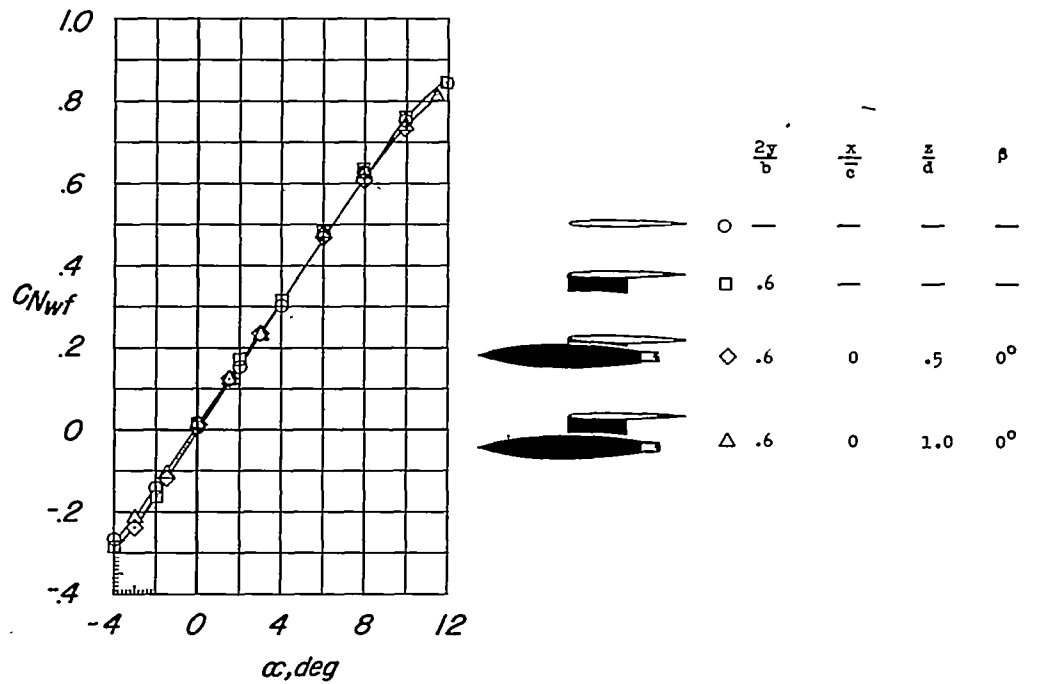
(c)   M = 1.05.

Figure 11.- Continued.

		$\frac{2y}{b}$	$\frac{x}{c}$	$\frac{z}{d}$	β
	O	—	—	—	—
	□	.6	—	—	—
	◇	.6	0	.5	0°
	△	.6	0	1.0	0°
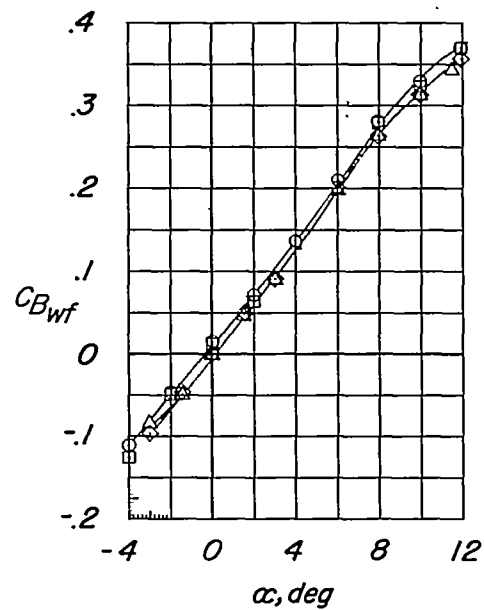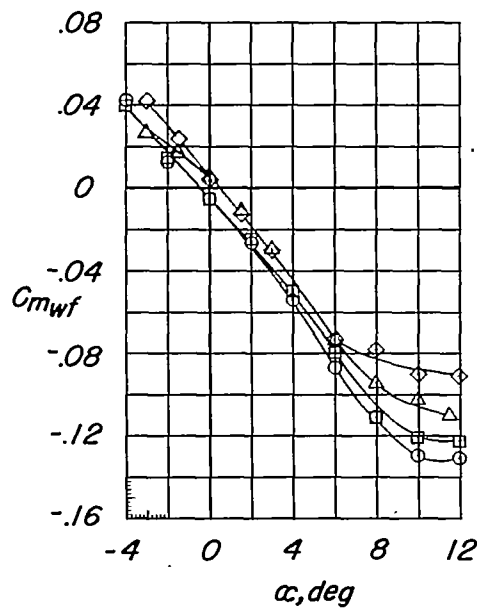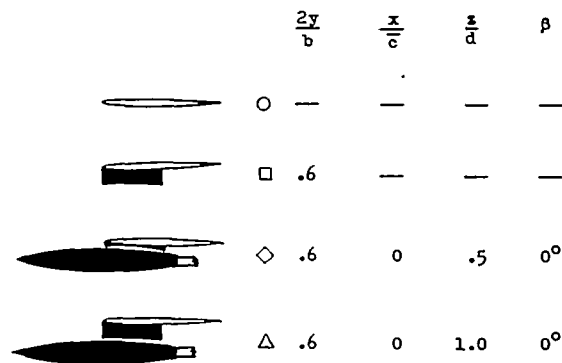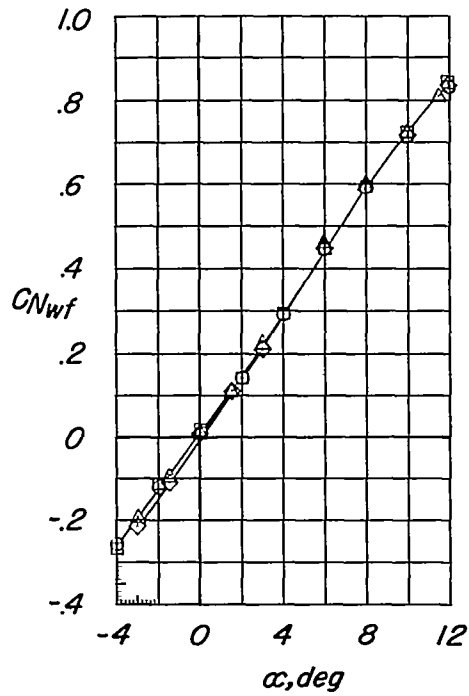
(d) M = 1.20.

Figure 11.- Continued.
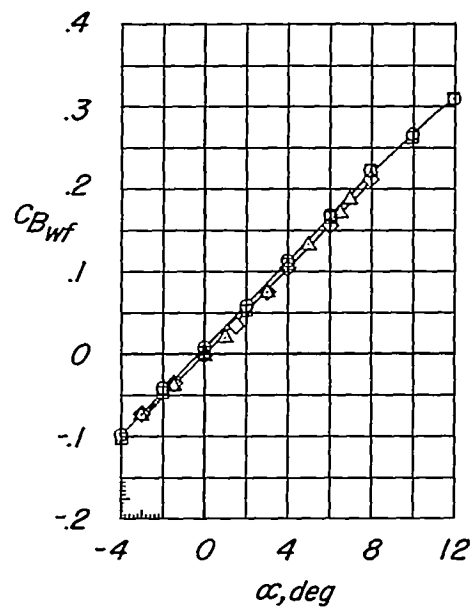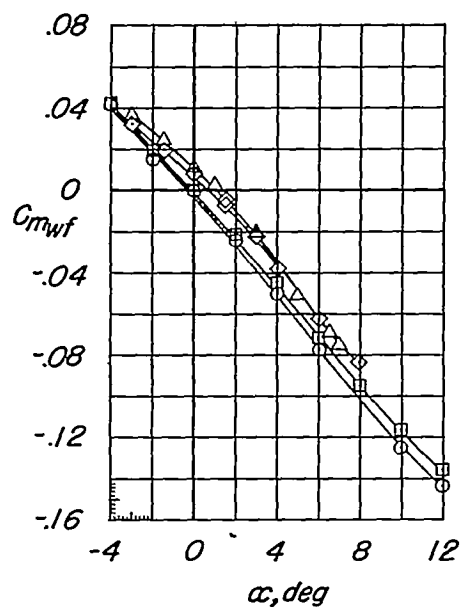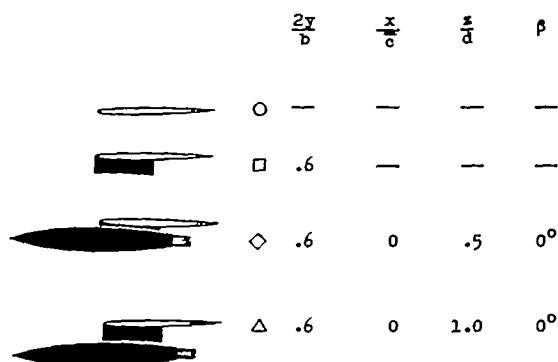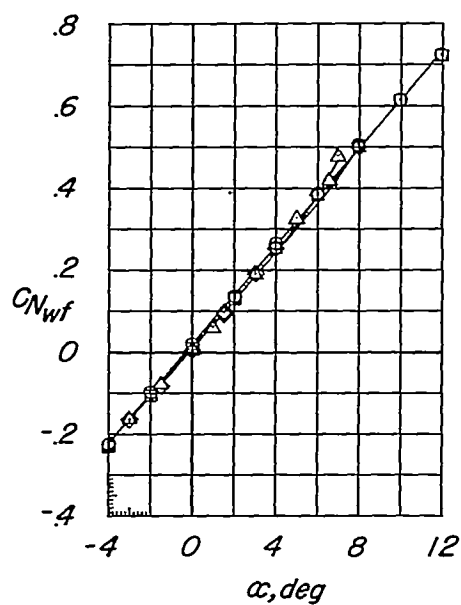
(e) M = 1.41.

Figure 11.- Continued.

	$\frac{2y}{b}$	$\frac{x}{c}$	$\frac{z}{d}$	β
O	—	—	—	—
□	.6	—	—	—
◇	.6	0	.5	0°
△	.6	0	1.0	0°
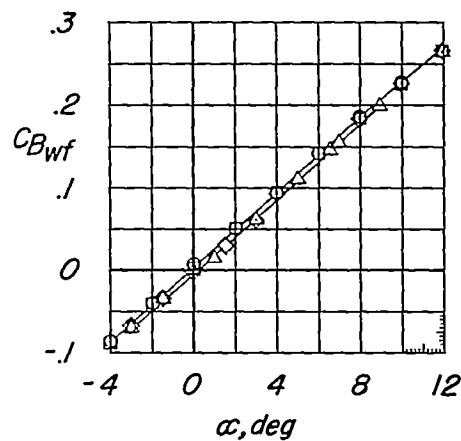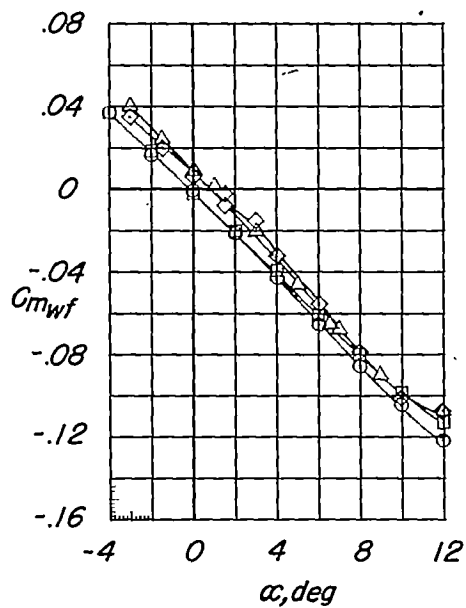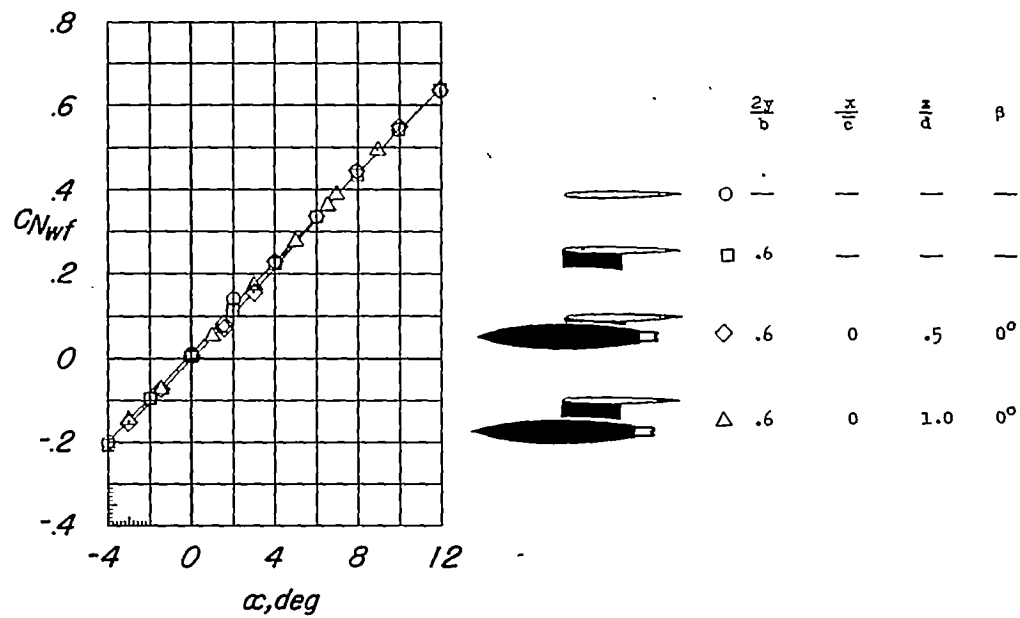
(f) M = 1.62.

Figure 11.- Continued.
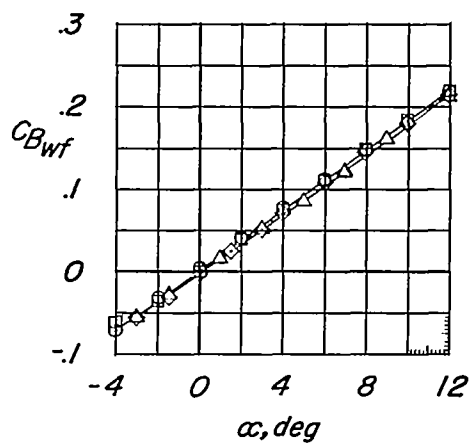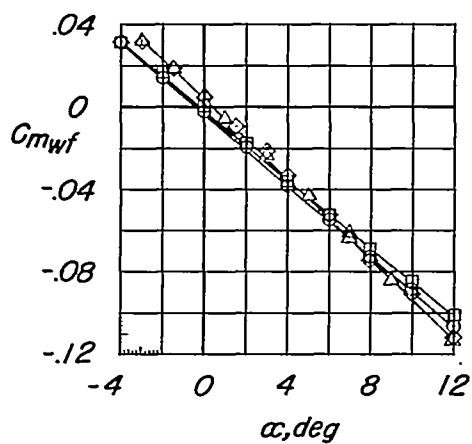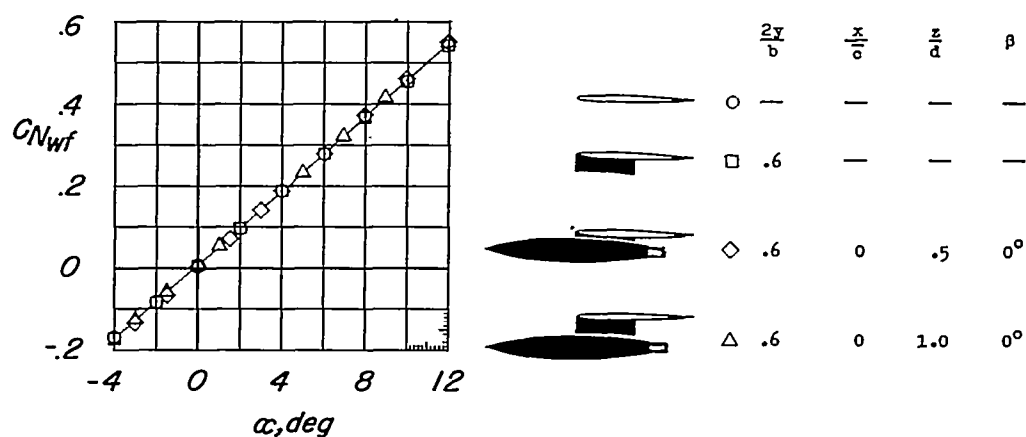
(g) M = 1.96.

Figure 11.- Concluded.
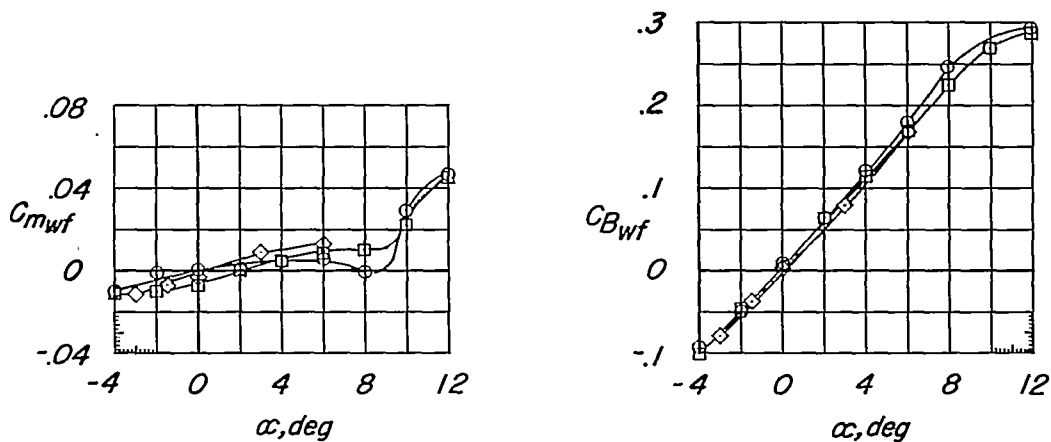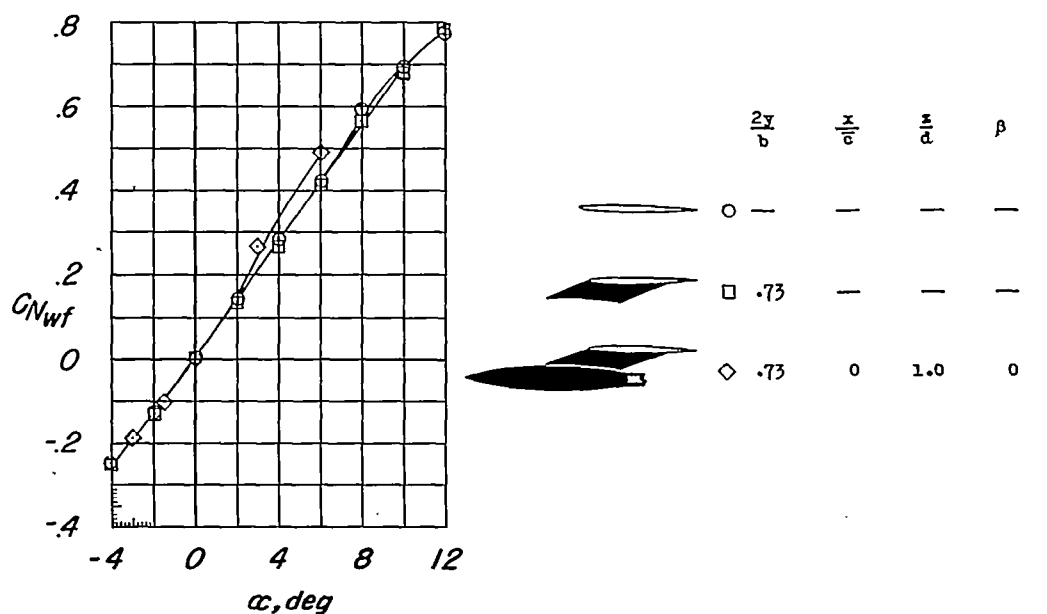
(a)   M = 0.75.

Figure 12.- Influence of the DAC store on the aerodynamic characteristics
of the wing-fuselage including effects of pylon.   2y/b = 0.73; original
fuselage.

.8

.6

.4

.2

C_{Nwf}

0

-.2

-.4

-4   0   4   8   12

α, deg

	$\frac{2y}{b}$	$\frac{x}{a}$	$\frac{z}{d}$	β
○	—	—	—	—
□	.73	—	—	—
◇	.73	0	1.0	0

.08

C_{mwf}

.04

0

-.04

-4   0   4   8   12

α, deg

.3

.2

.1

C_{Bwf}

0

-.1

-.2

-4   0   4   8   12

α, deg
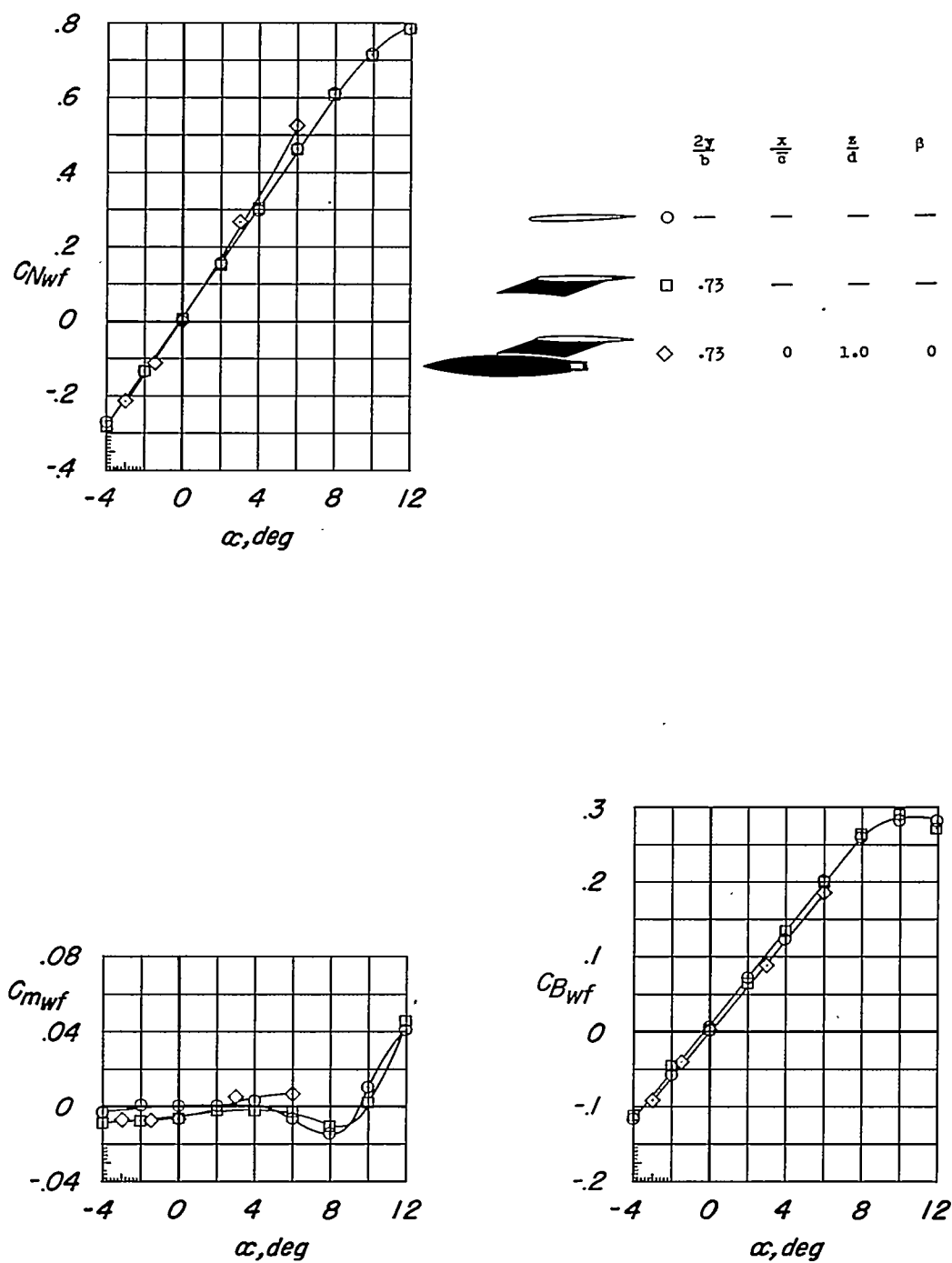
(b)   M = 0.90.
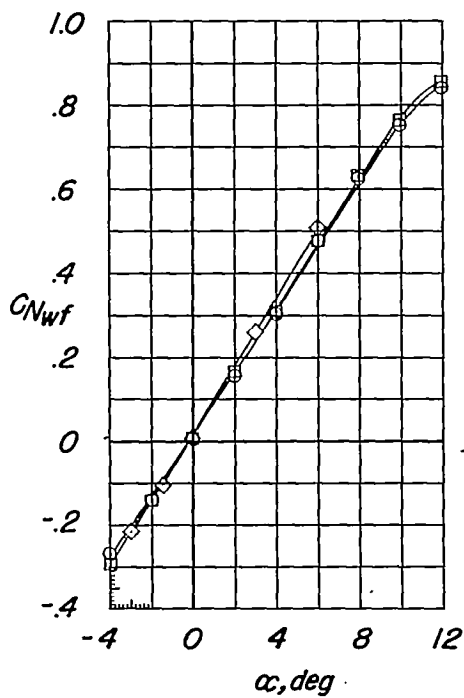
Figure 12.- Continued.
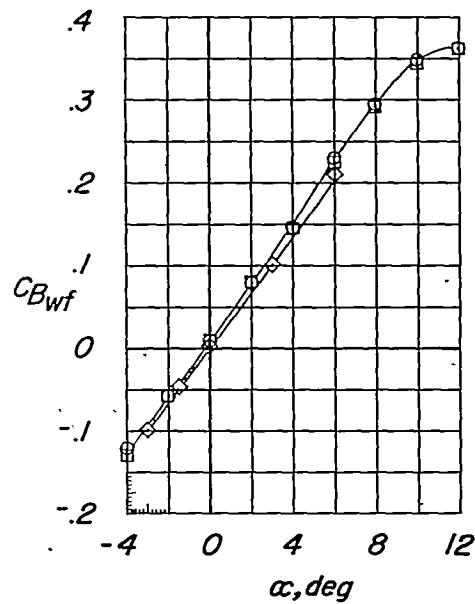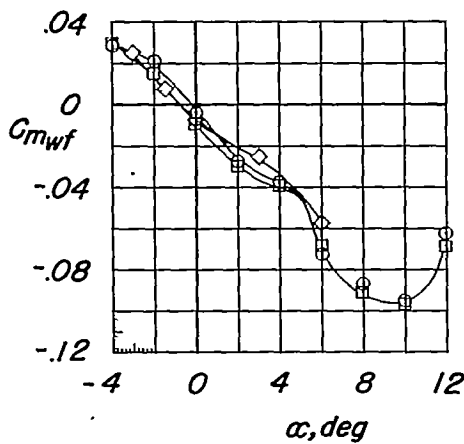
(c) M = 1.05.

Figure 12.- Continued.

56
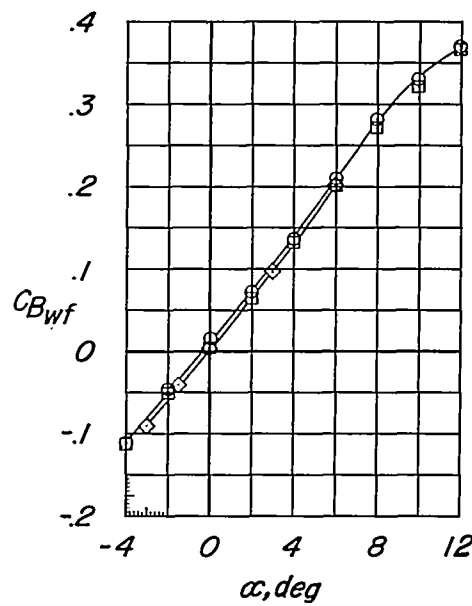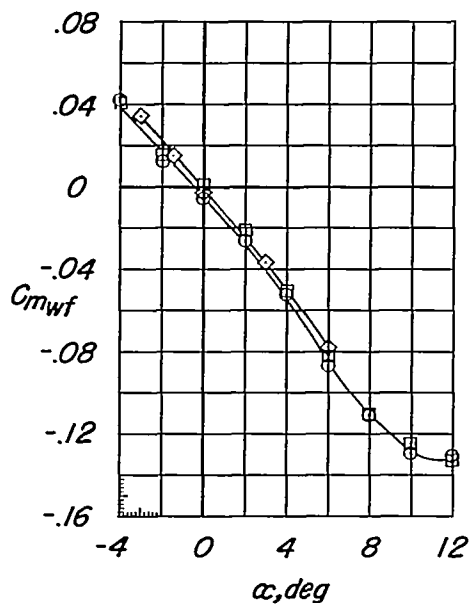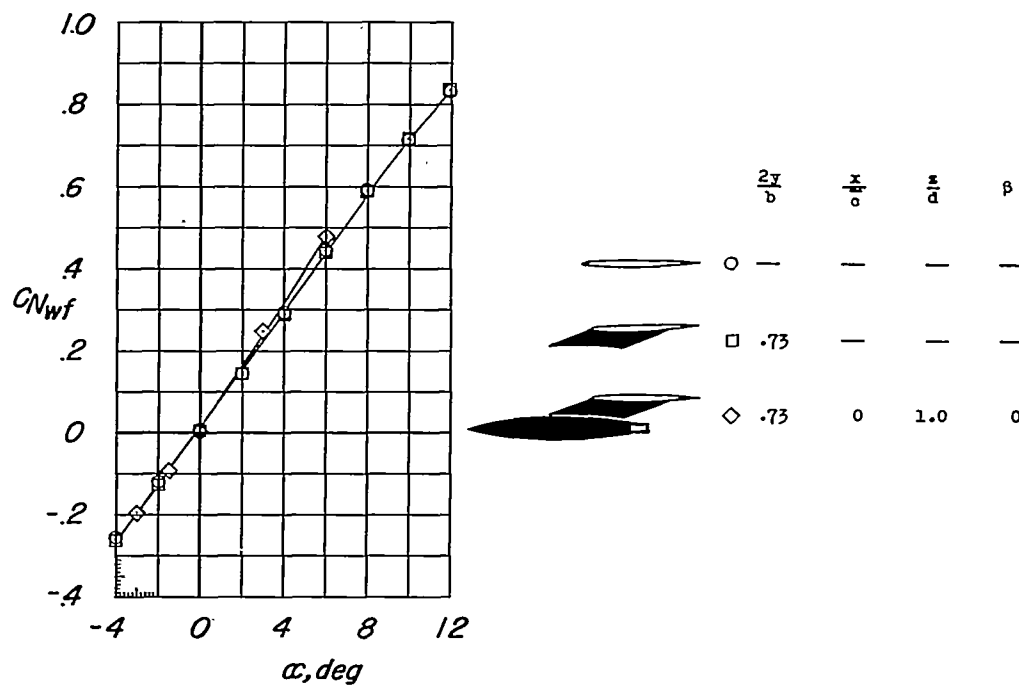
(d) M = 1.20.

Figure 12.- Continued.
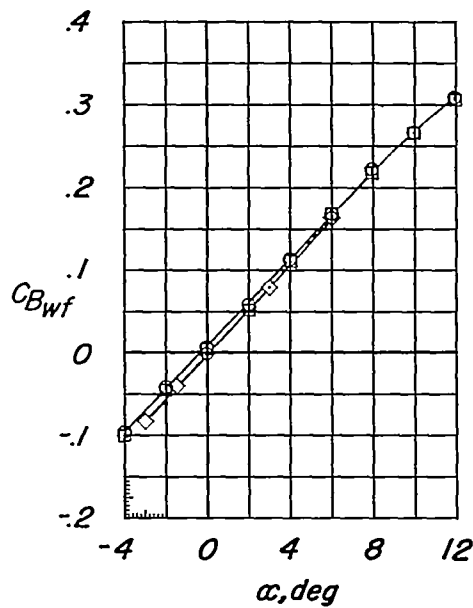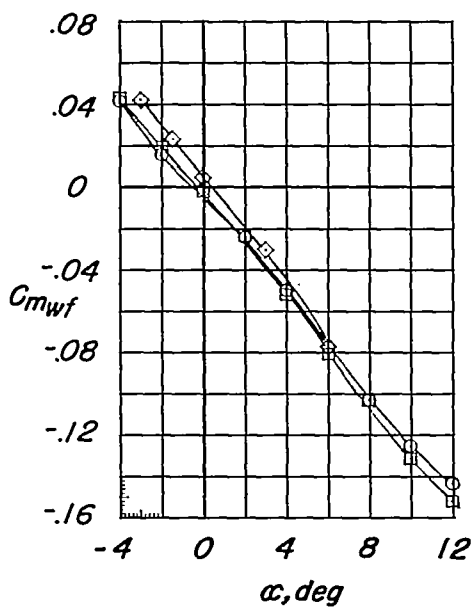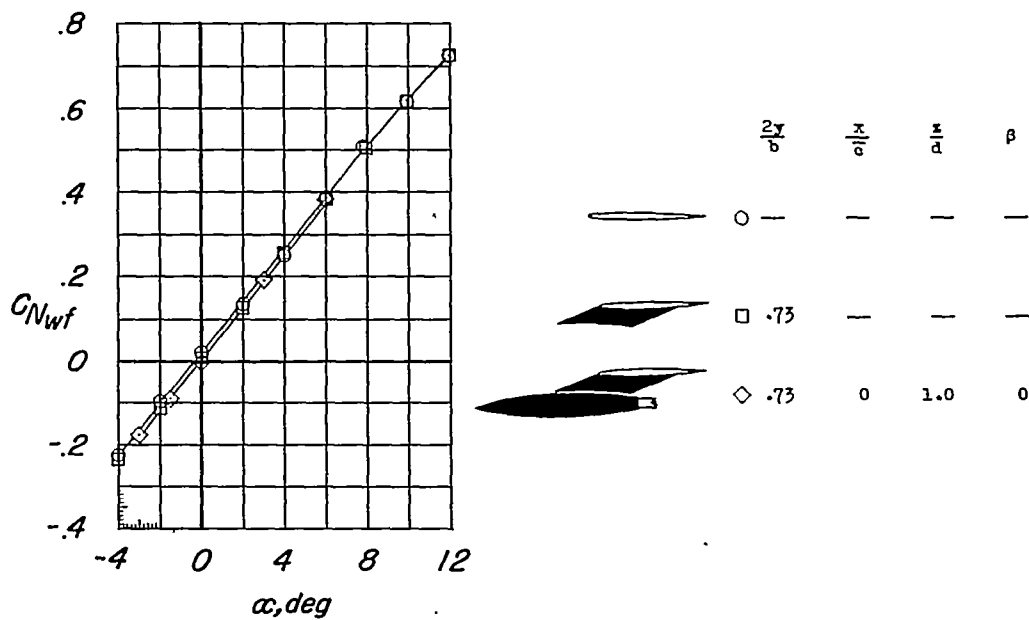
(e)   M = 1.41.

Figure 12.- Continued.
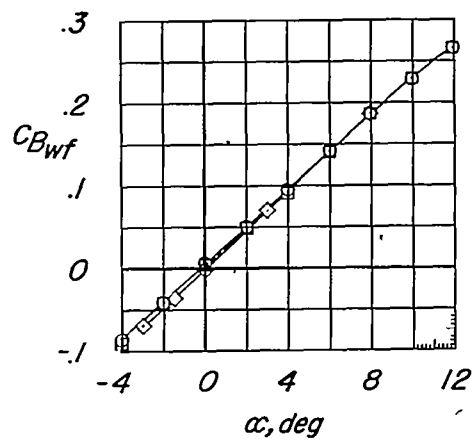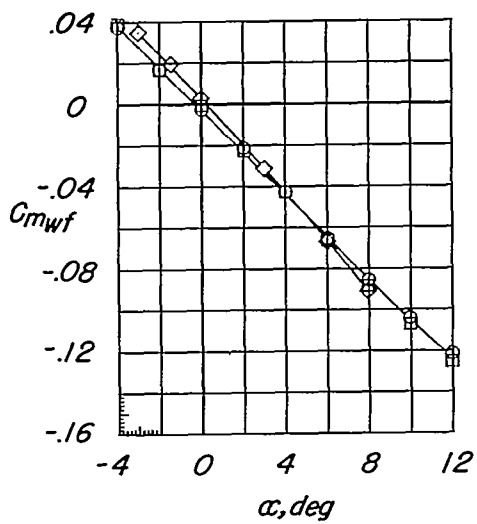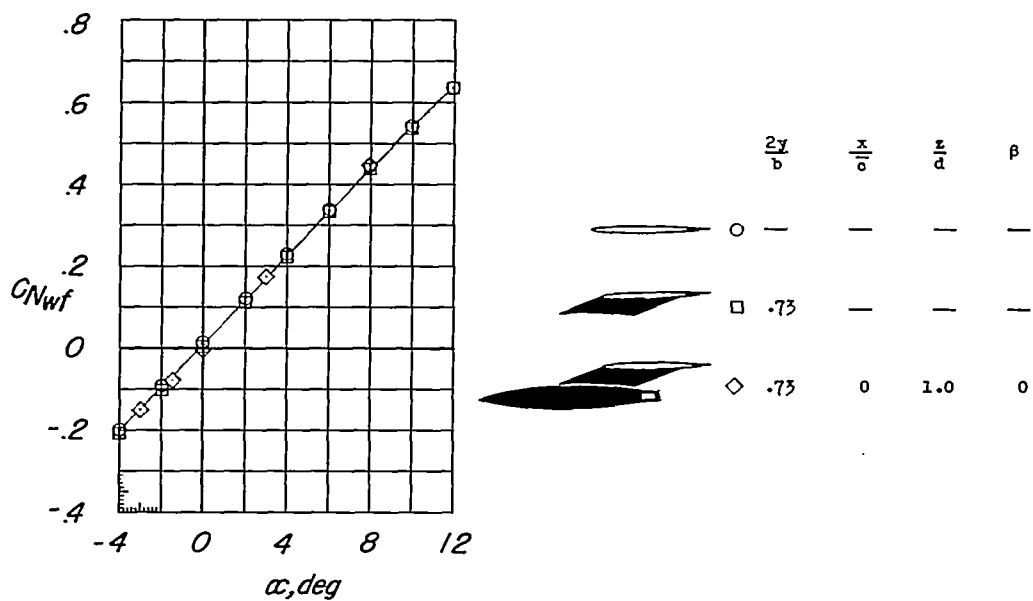
(f)   M = 1.62.

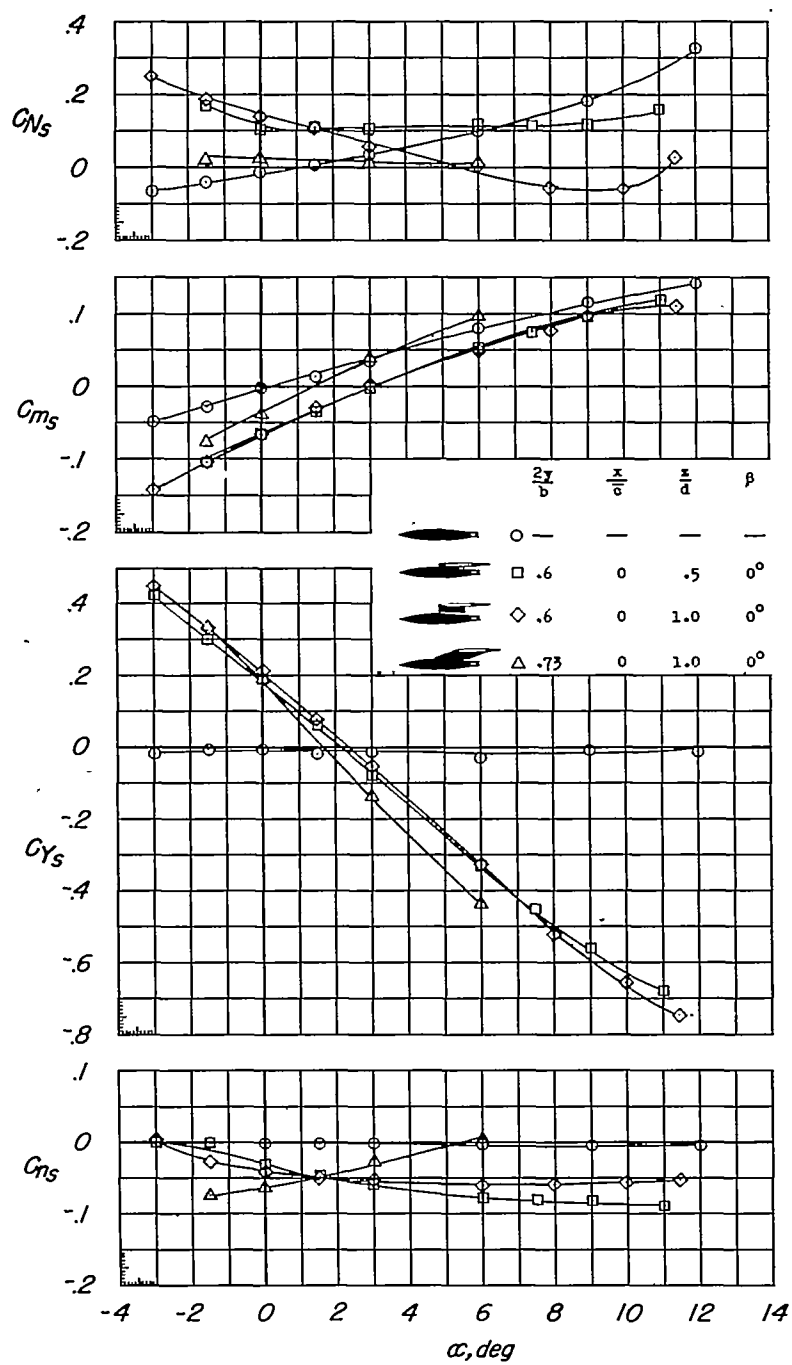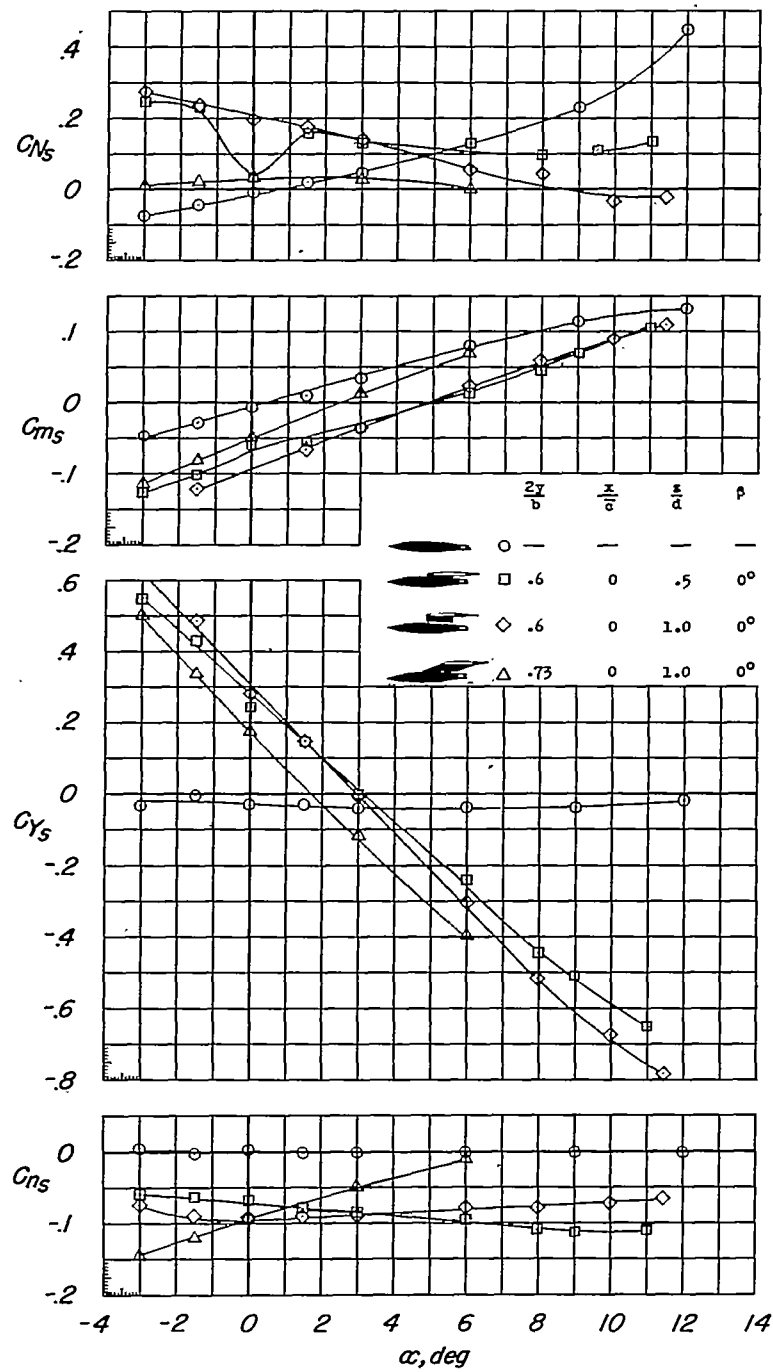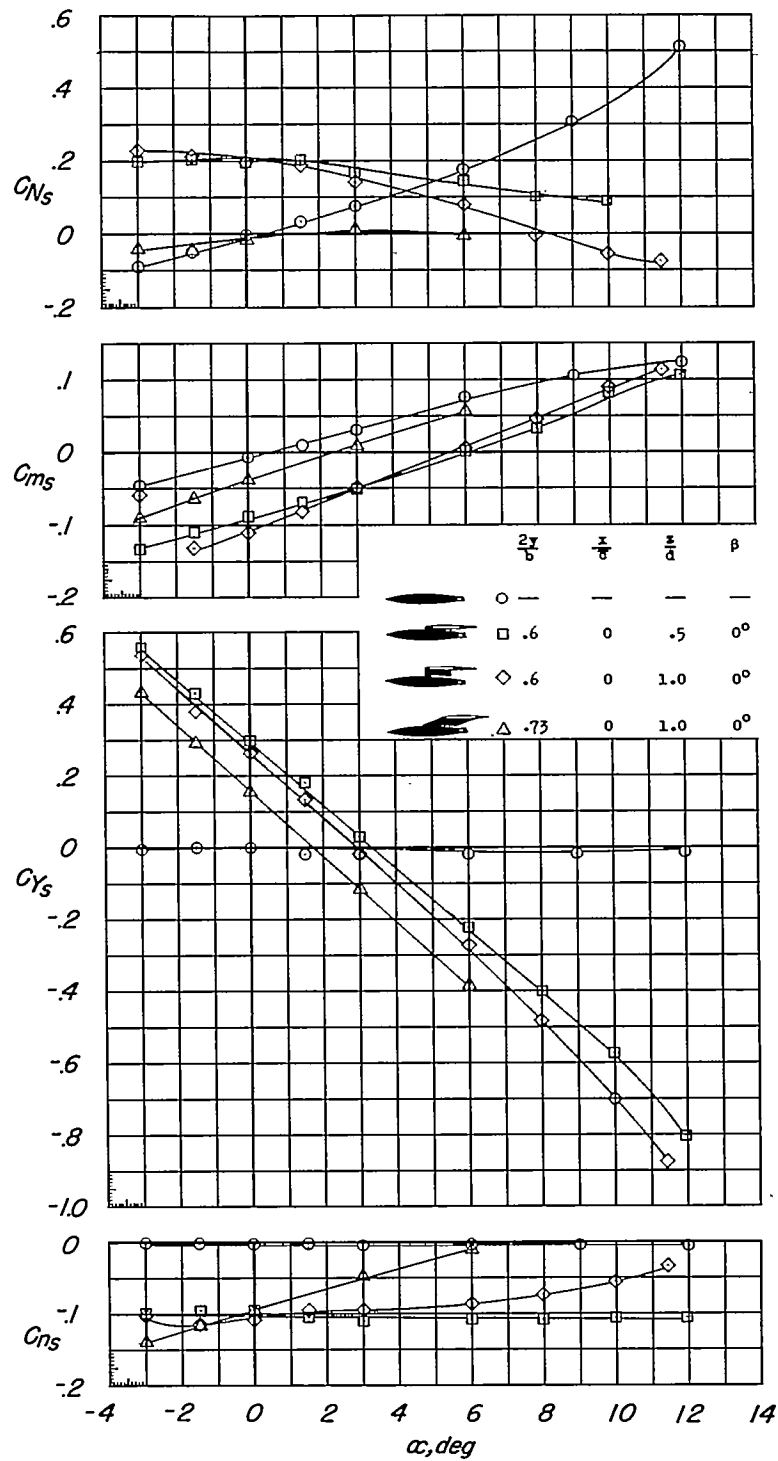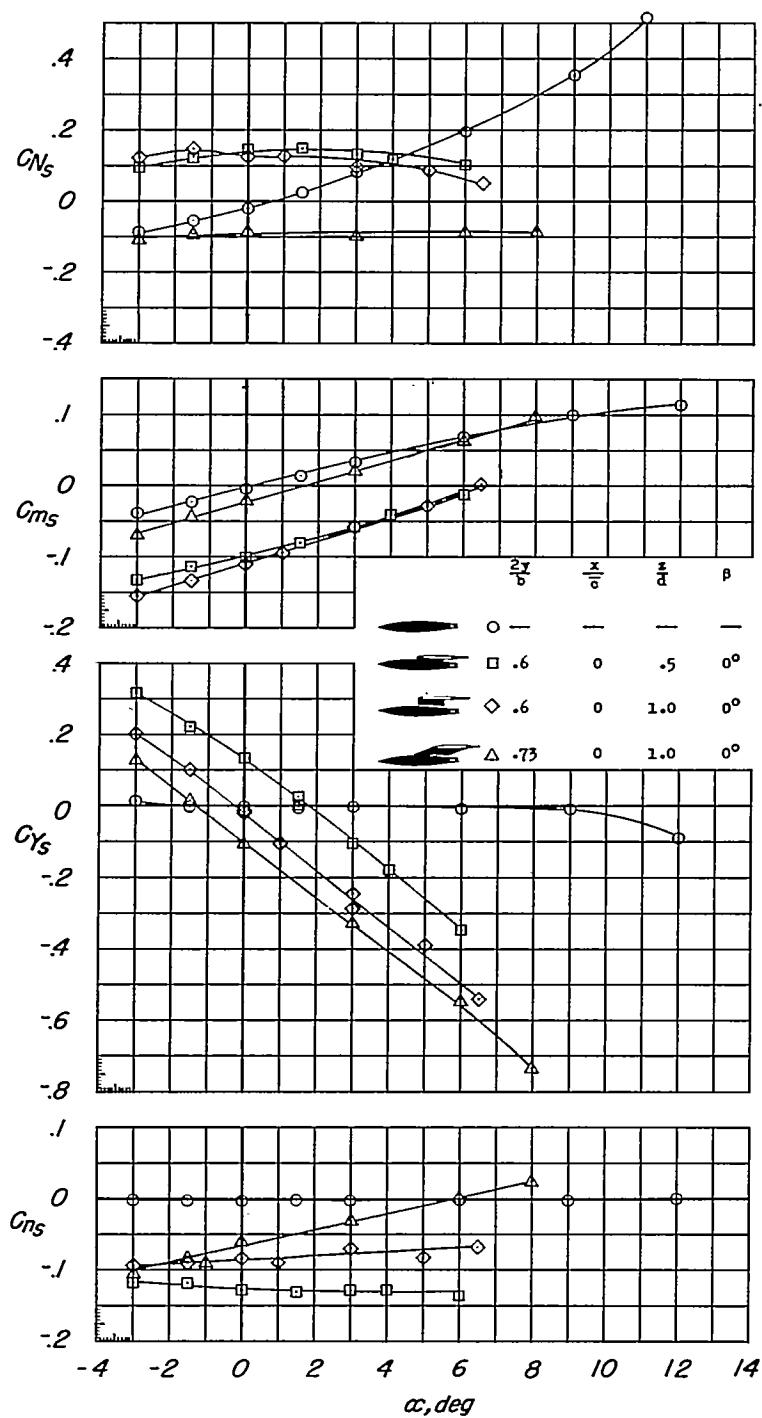Figure 12.- Continued.
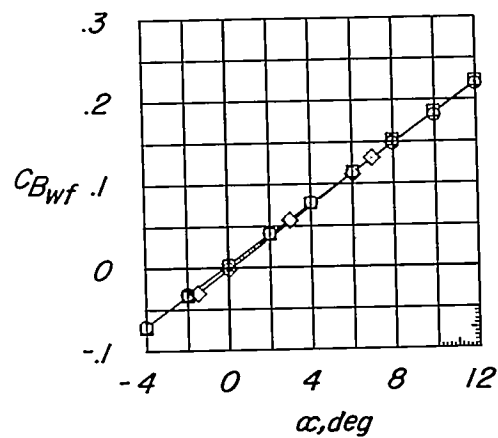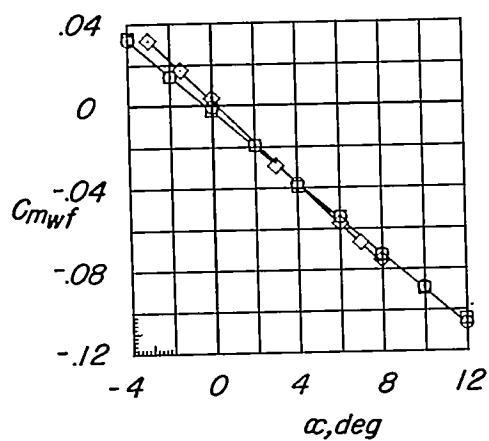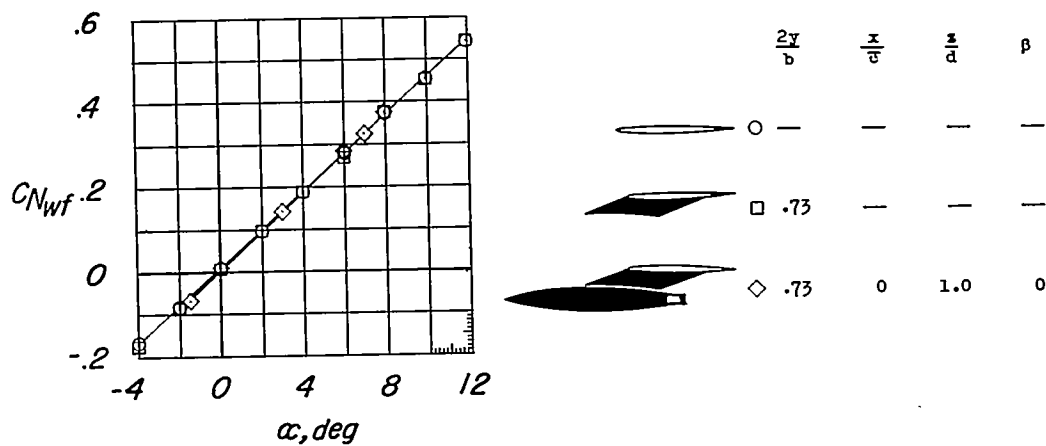
(g)   M = 1.96.

Figure 12.- Concluded.

	$\frac{2y}{b}$	$\frac{x}{c}$	$\frac{z}{d}$	β
○	—	—	—	—
□	.6	0	.5	5°
◇	.6	0	1.0	5°
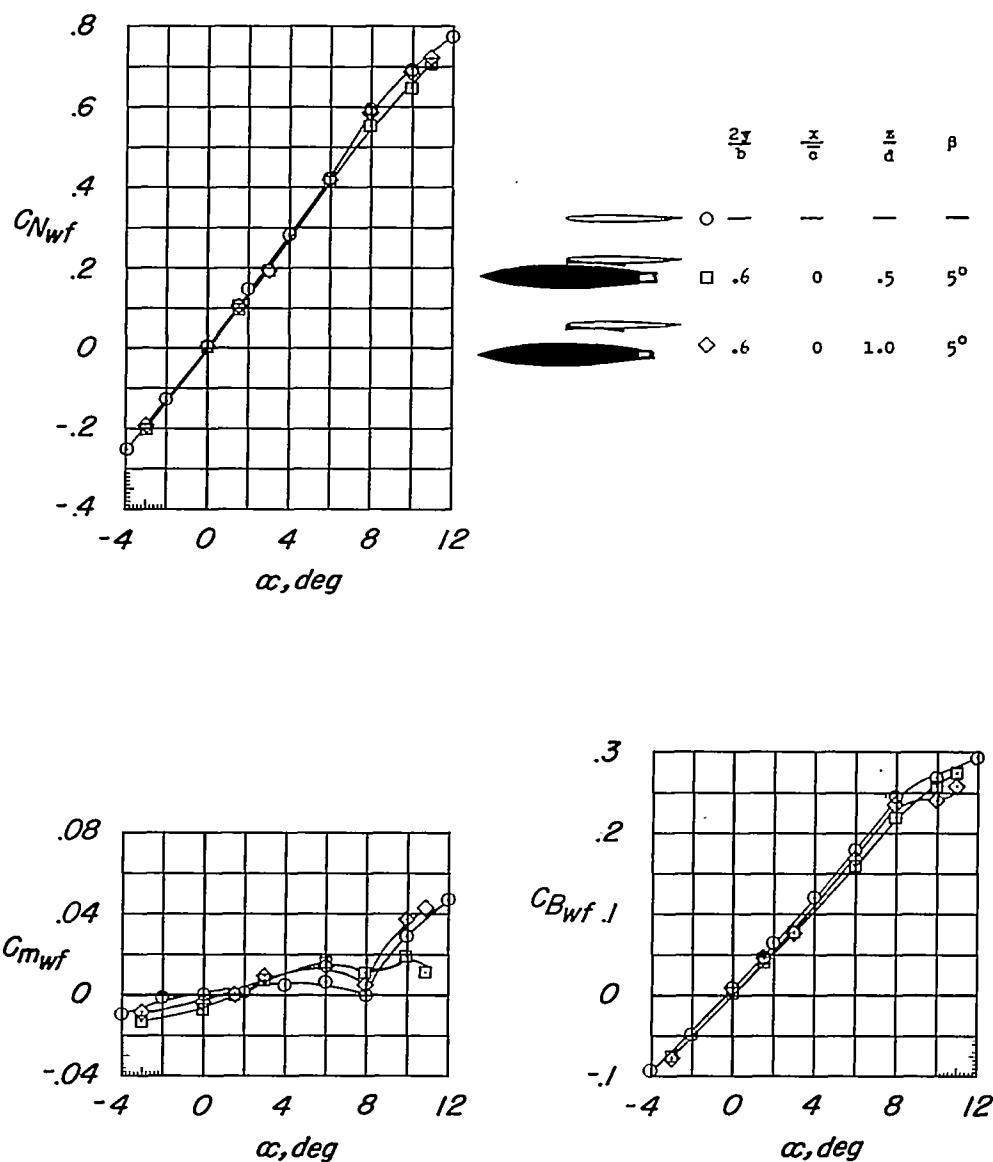
(a) M = 0.75.

Figure 13.- Influence of the DAC store at 5° skew angle on the aerodynamic characteristics of the wing-fuselage. $2y/b = 0.60$; original fuselage.

(b) M = 0.90.

Figure 13.- Continued.

$C_{N_{wf}}$

.8
.6
.4
.2
0
-.2
-.4

-4 0 4 8 12

α, deg

		$\frac{2y}{b}$	$\frac{x}{c}$	$\frac{z}{d}$	β
◯	—	—	—	—	—
□	.6	0	.5	5°
◇	.6	0	1.0	5°

$C_{m_{wf}}$

.04
0
-.04
-.08

-4 0 4 8 12

α, deg

$C_{B_{wf}}$

.4
.3
.2
.1
0
-.1
-.2

-4 0 4 8 12

α, deg
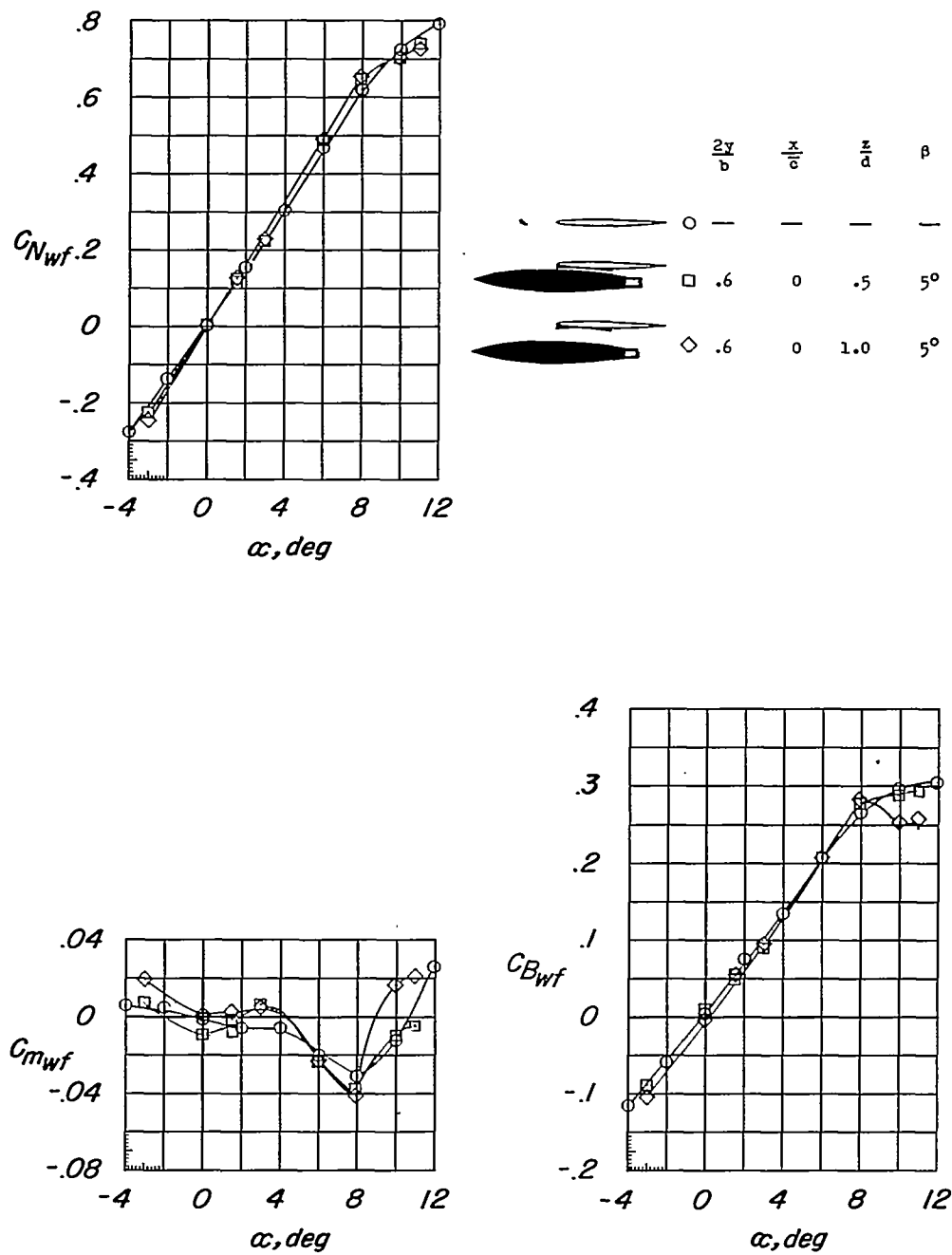
(c) M = 0.95.

Figure 13.- Continued.

(d) M = 1.00.

Figure 13.- Continued.

		$\frac{2y}{b}$	$\frac{x}{c}$	$\frac{x}{d}$	β
	○	—	—	—	—
	□	.6	0	.5	5°
	◇	.6	0	1.0	5°
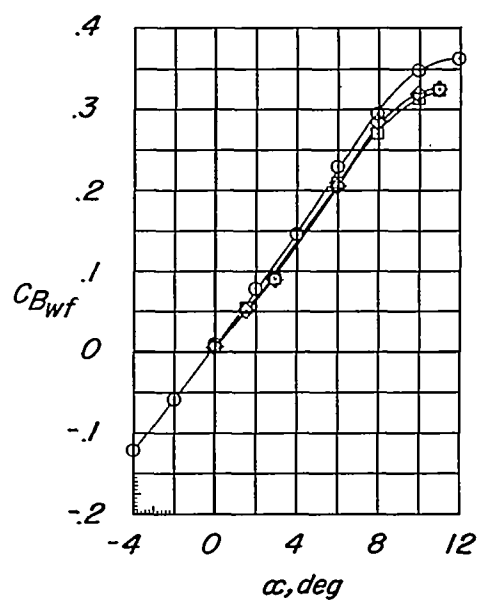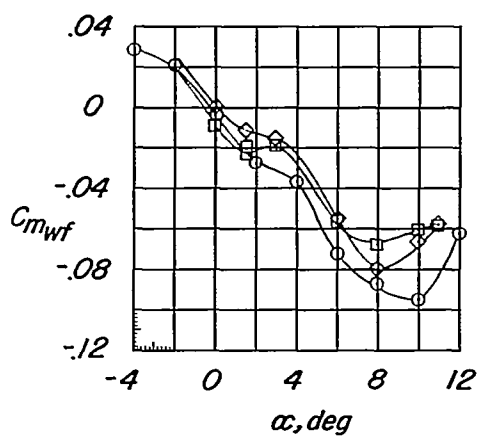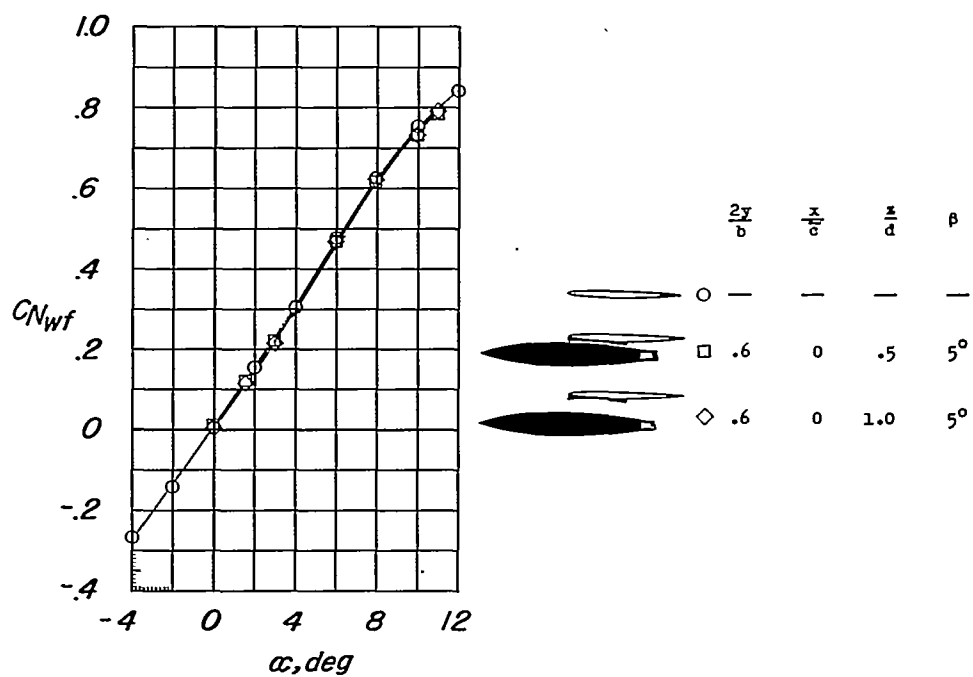
(e) M = 1.05.

Figure 13.- Continued.

(f)   M = 1.20.

Figure 13.- Continued.

$C_{N_{wf}}$

α, deg

	$\frac{2y}{b}$	$\frac{x}{c}$	$\frac{z}{d}$	β
$\circ$	—	—	—	—
$\square$	.6	0	.5	5°
$\diamond$	.6	0	1.0	5°

$C_{m_{wf}}$

α, deg

$C_{B_{wf}}$

α, deg

(g)   M = 1.41.

Figure 13.- Continued.

$C_{N_{wf}}$

α, deg

		$\frac{2y}{b}$	$\frac{x}{c}$	$\frac{z}{d}$	β
○		—	—	—	—
□		.6	0	.5	5°
◇		.6	0	1.0	5°

$C_{m_{wf}}$

α, deg

$C_{B_{wf}}$

α, deg
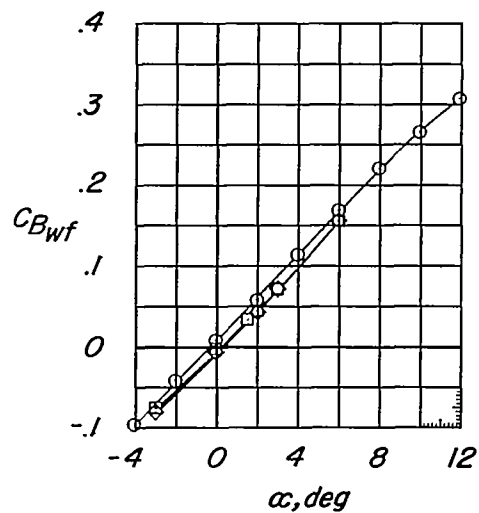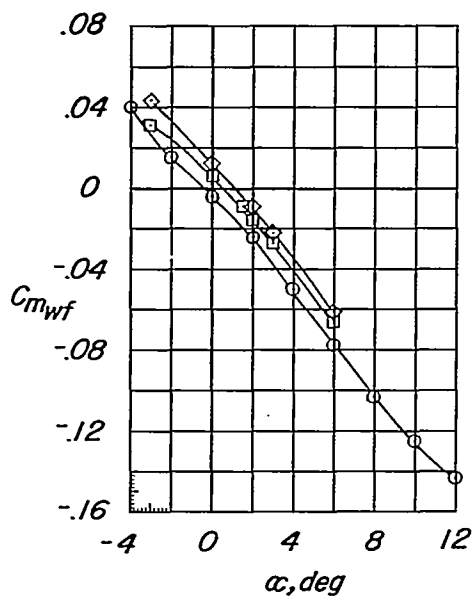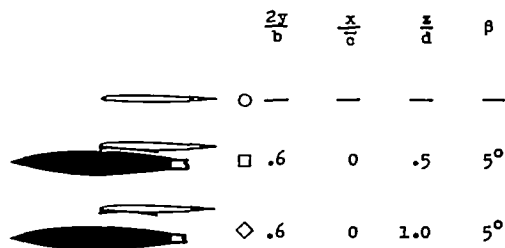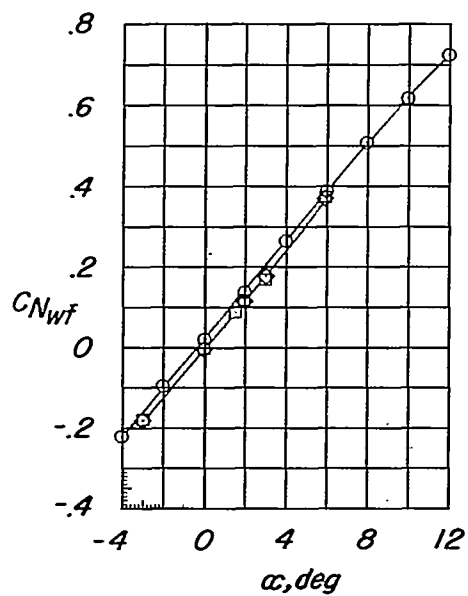
(h)   M = 1.62.

Figure 13.- Continued.

	$\frac{2y}{b}$	$\frac{x}{c}$	$\frac{z}{d}$	β
○	—	—	—	—
□	.6	0	.5	5°
◇	.6	0	1.0	5°

(i)   M = 1.96.

Figure 13.- Concluded.
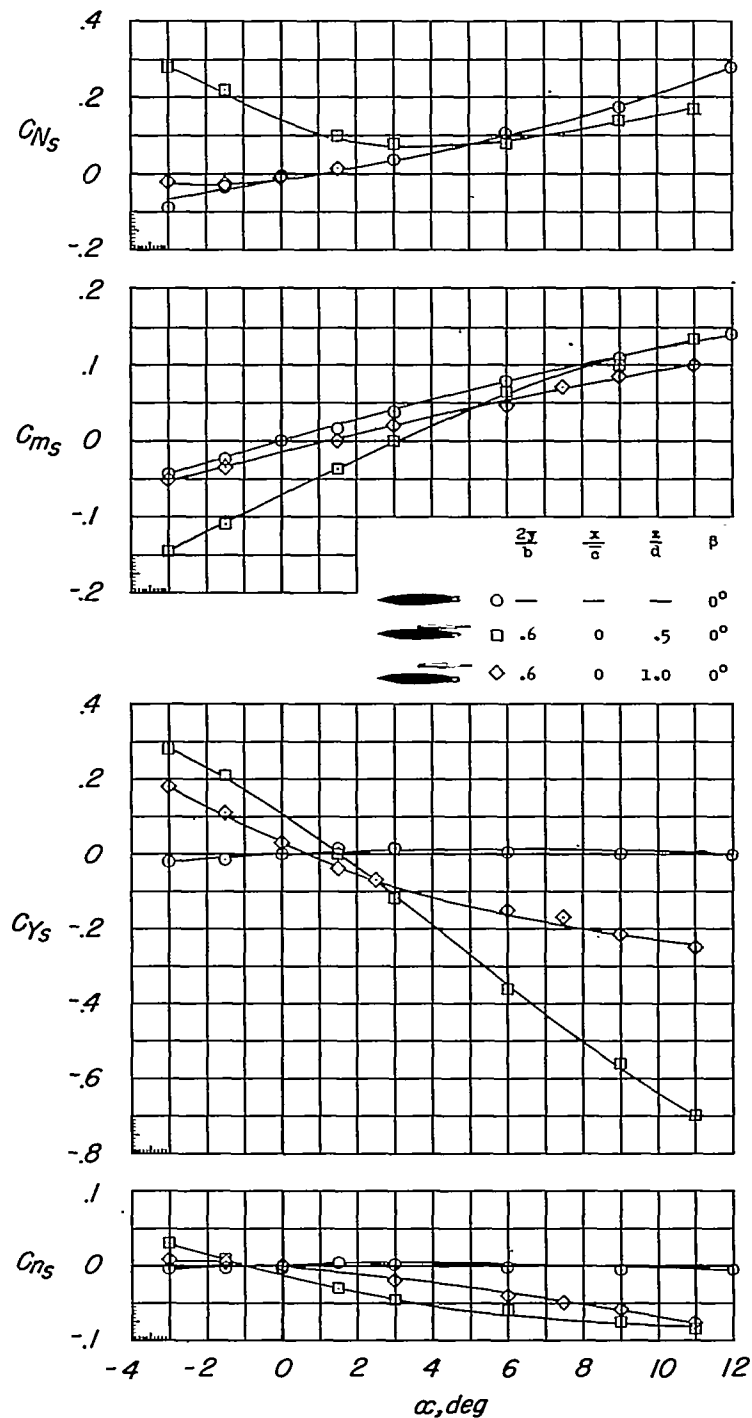
(a) M = 0.70.

Figure 14.- Aerodynamic characteristics of the DAC store at varying
vertical distances from the wing. 2y/b = 0.60; original fuselage.

(b) M = 0.80.

Figure 14.- Continued.

(c)　M = 0.90.

Figure 14.- Continued.

		$\frac{2y}{b}$	$\frac{x}{c}$	$\frac{z}{d}$	β
	○	—	—	—	0°
	□	.6	0	.5	0°
	◇	.6	0	1.0	0°
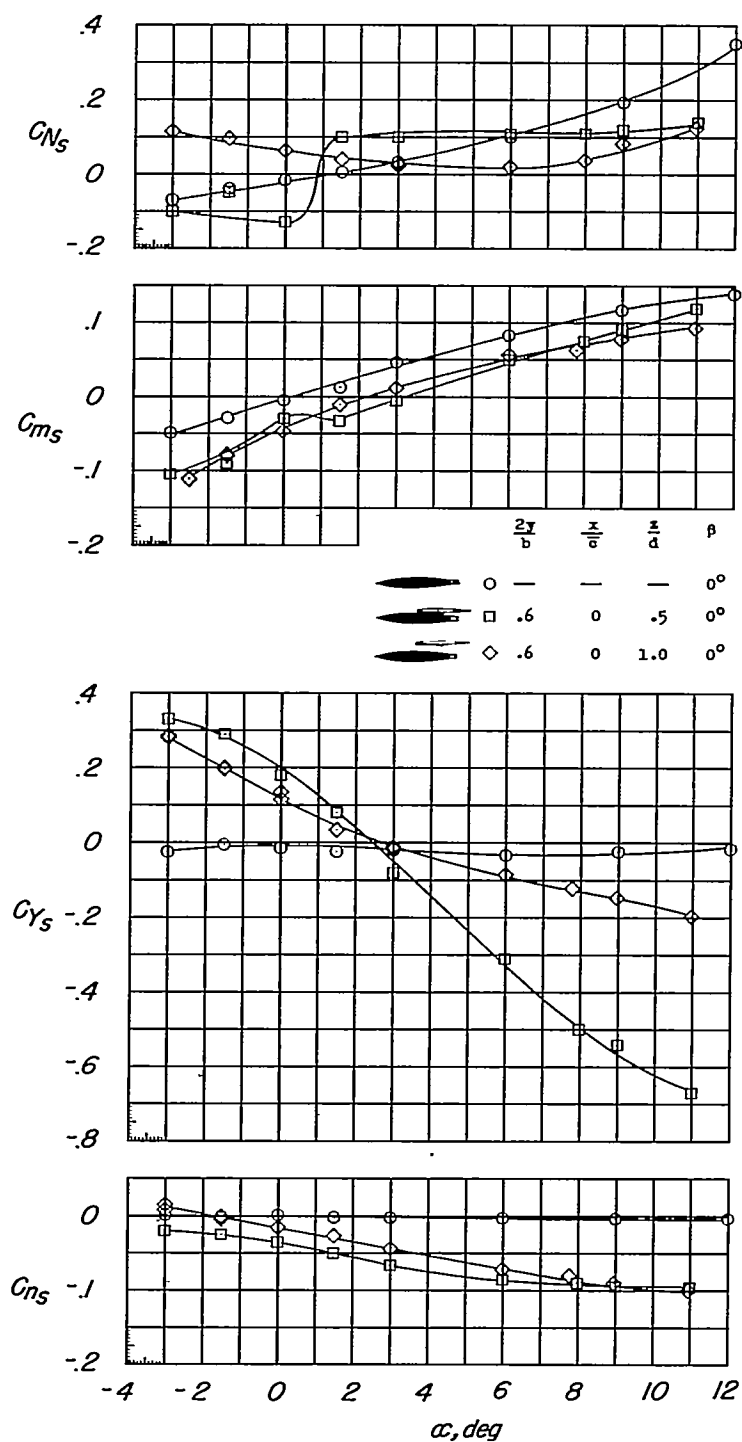
(d)   M = 0.95.

Figure 14.- Continued.
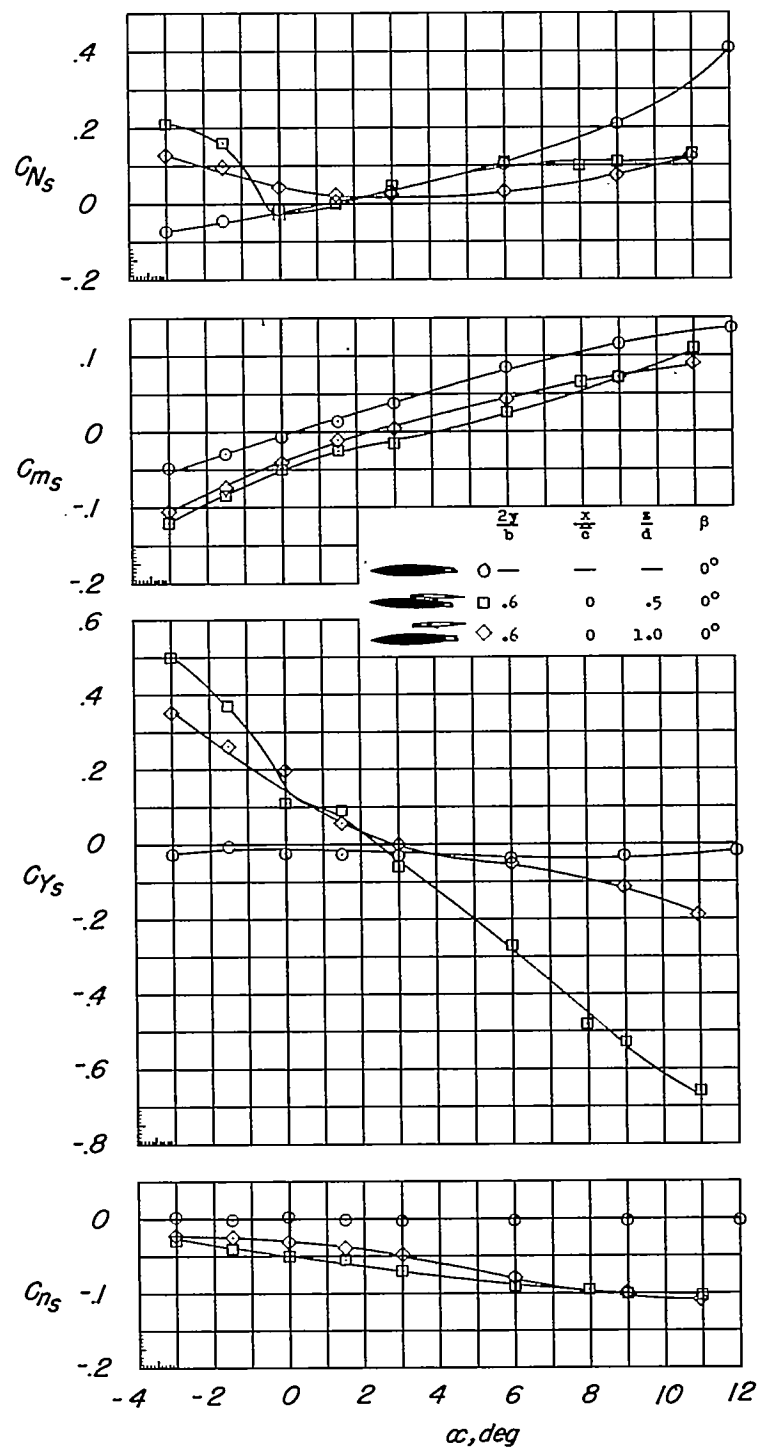
(e) M = 1.00.

Figure 14.- Continued.
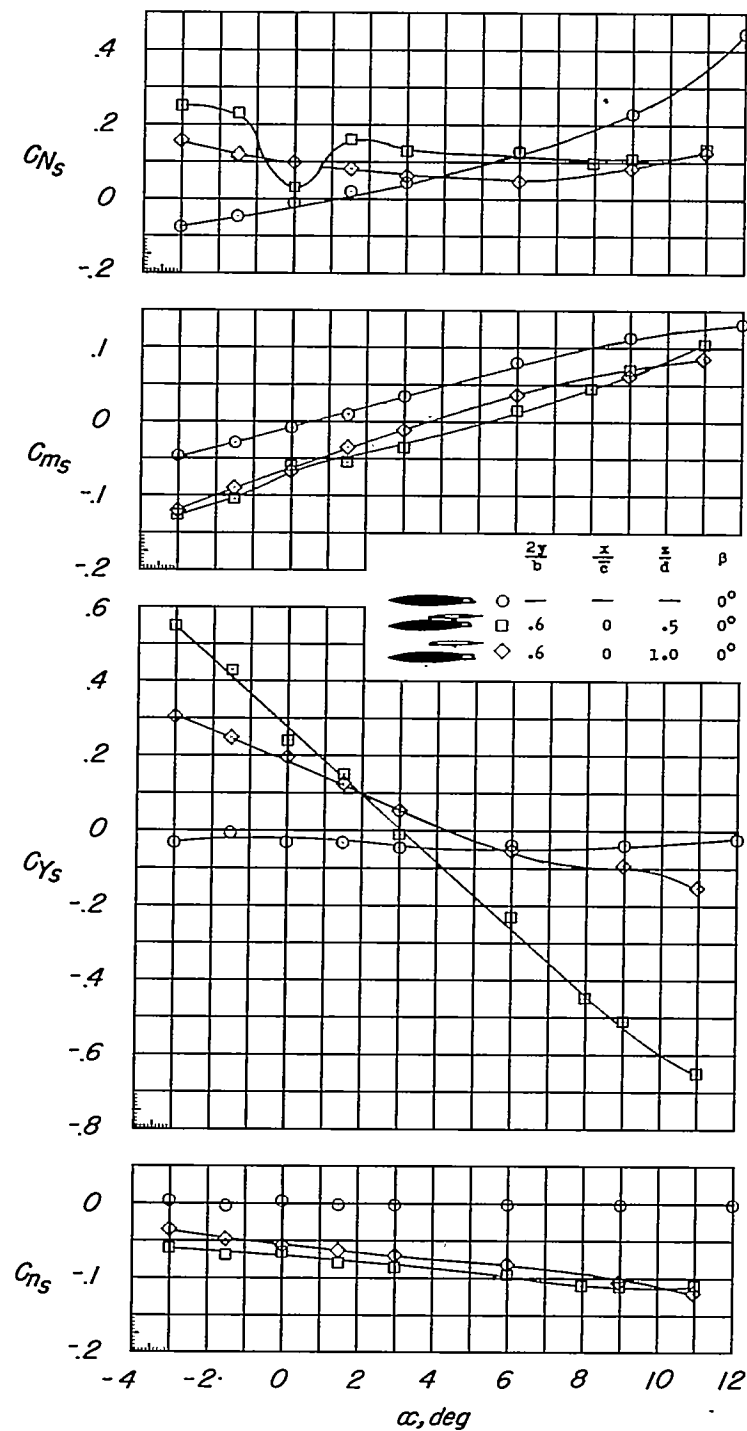
(f) M = 1.05.

Figure 14.- Continued.
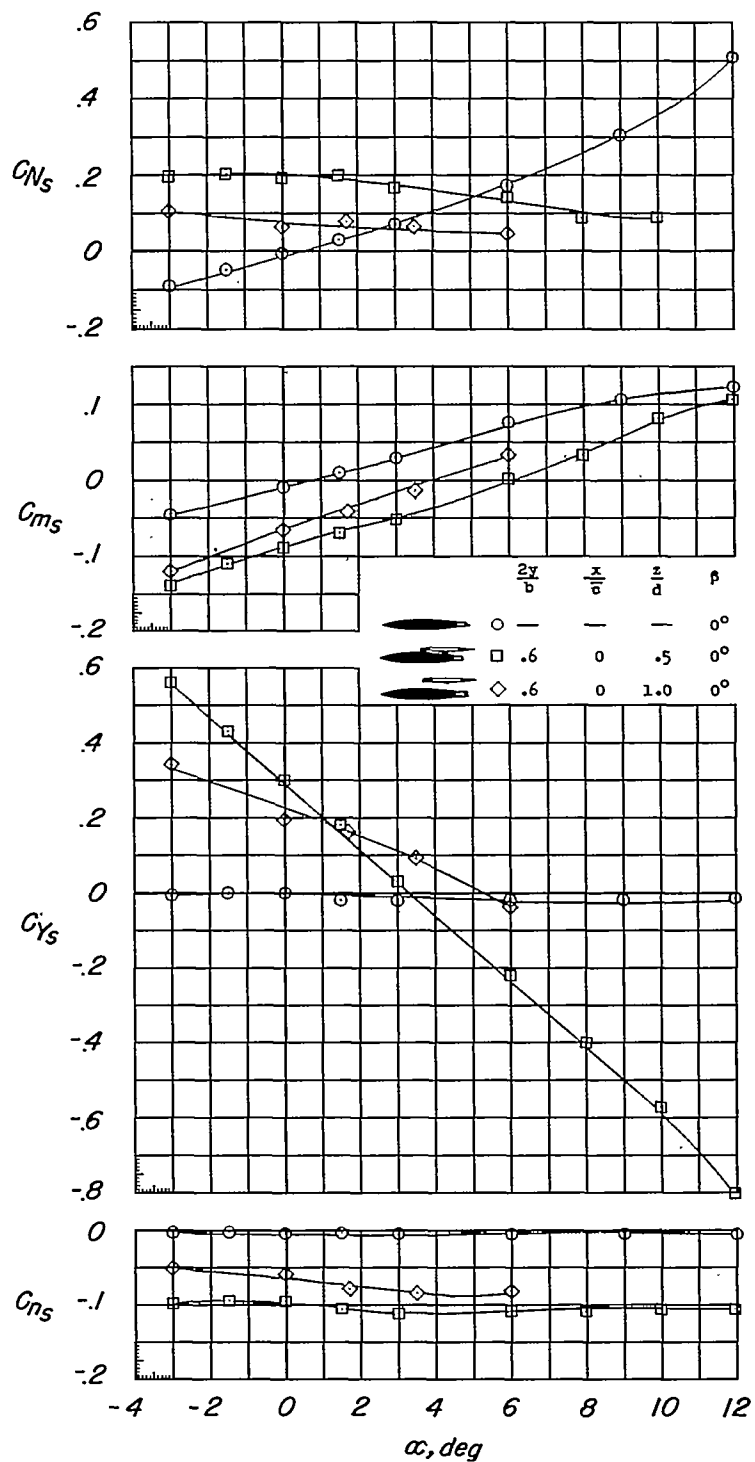
(g) M = 1.20.

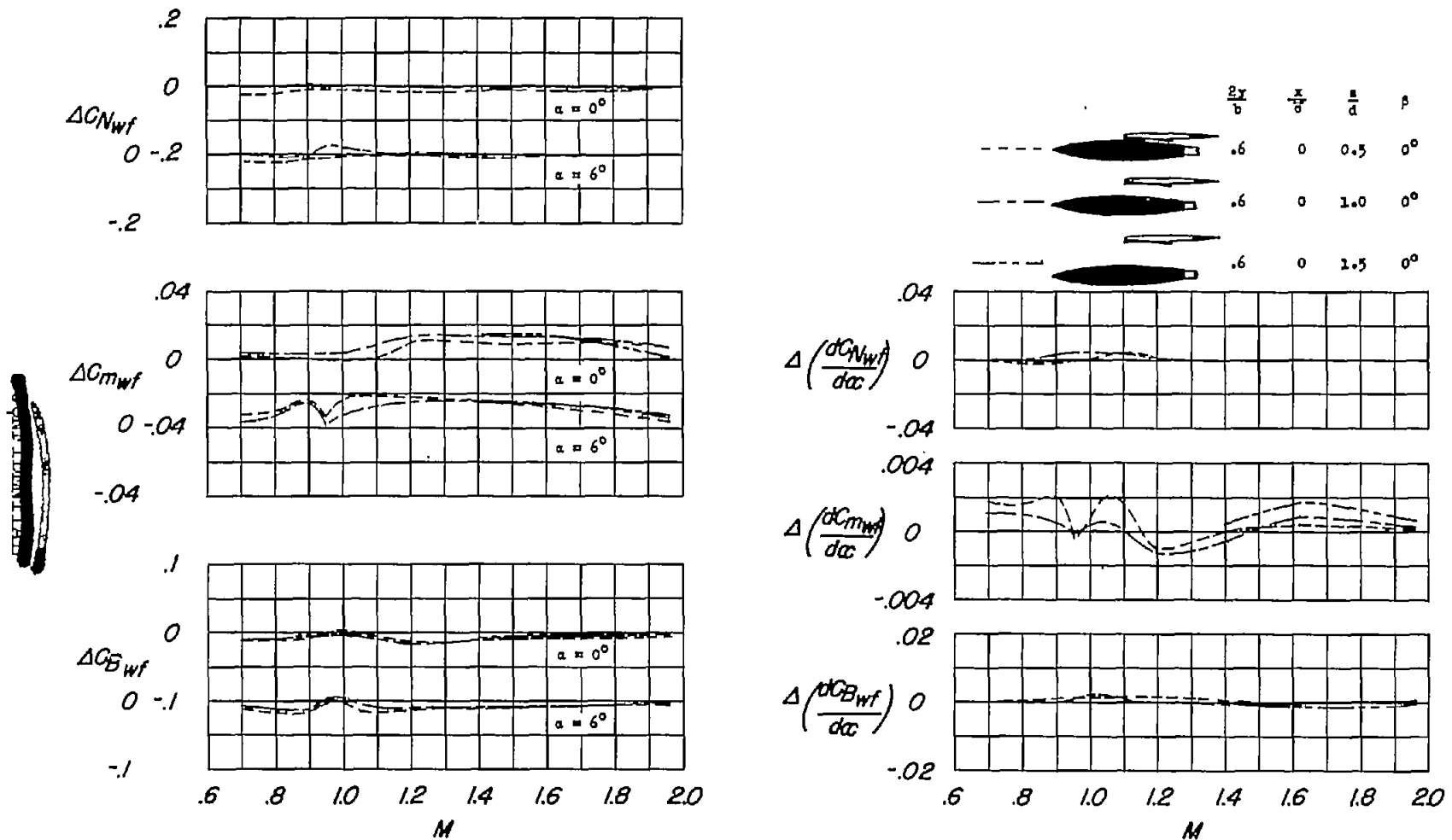Figure 14.- Continued.

(h)   M = 1.41.

Figure 14.- Continued.

	$\frac{2y}{b}$	$\frac{x}{a}$	$\frac{z}{d}$	β
○	—	—	—	0°
□	.6	0	.5	0°
◇	.6	0	1.0	0°
△	.6	0	1.5	0°

C_{N_S}

C_{m_S}

C_{Y_S}

C_{n_S}

α, deg
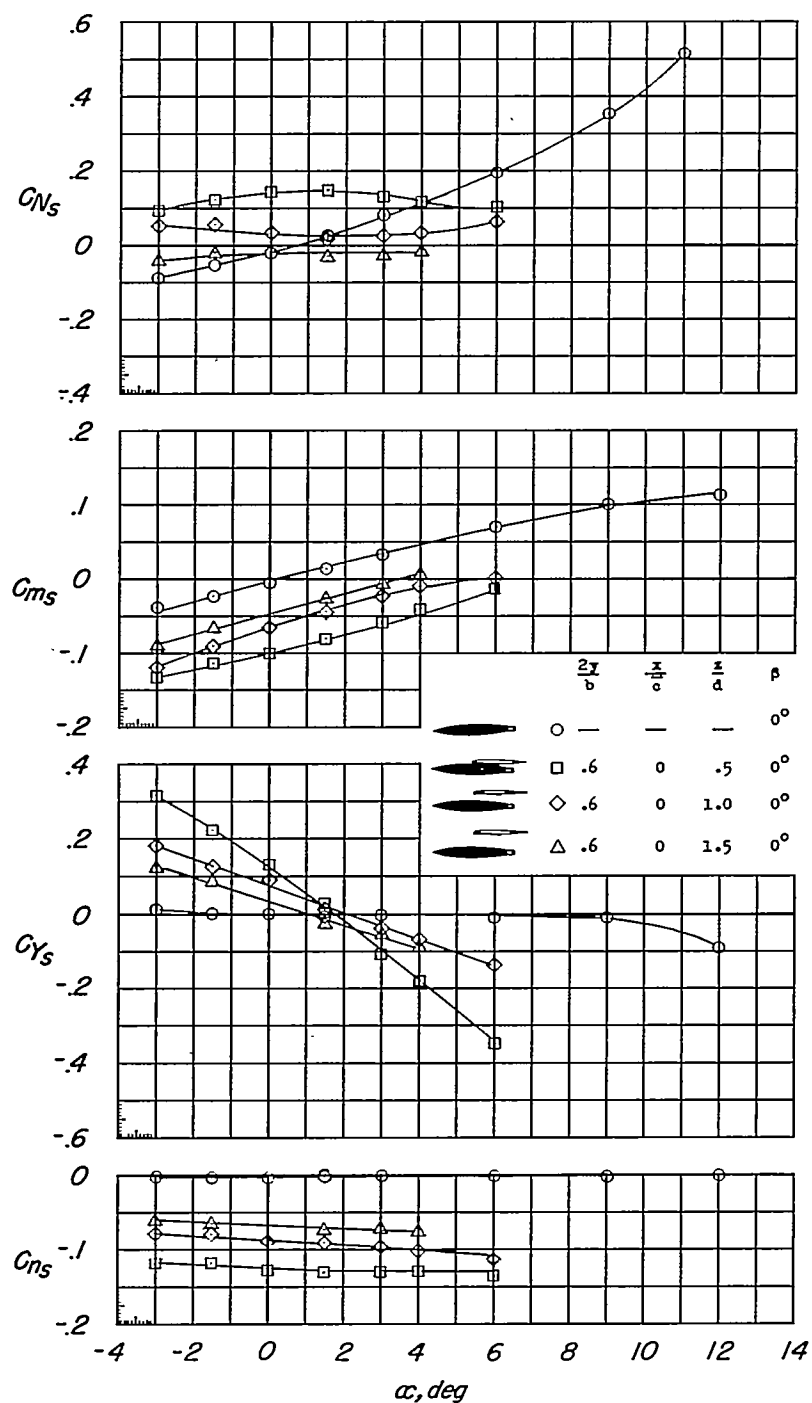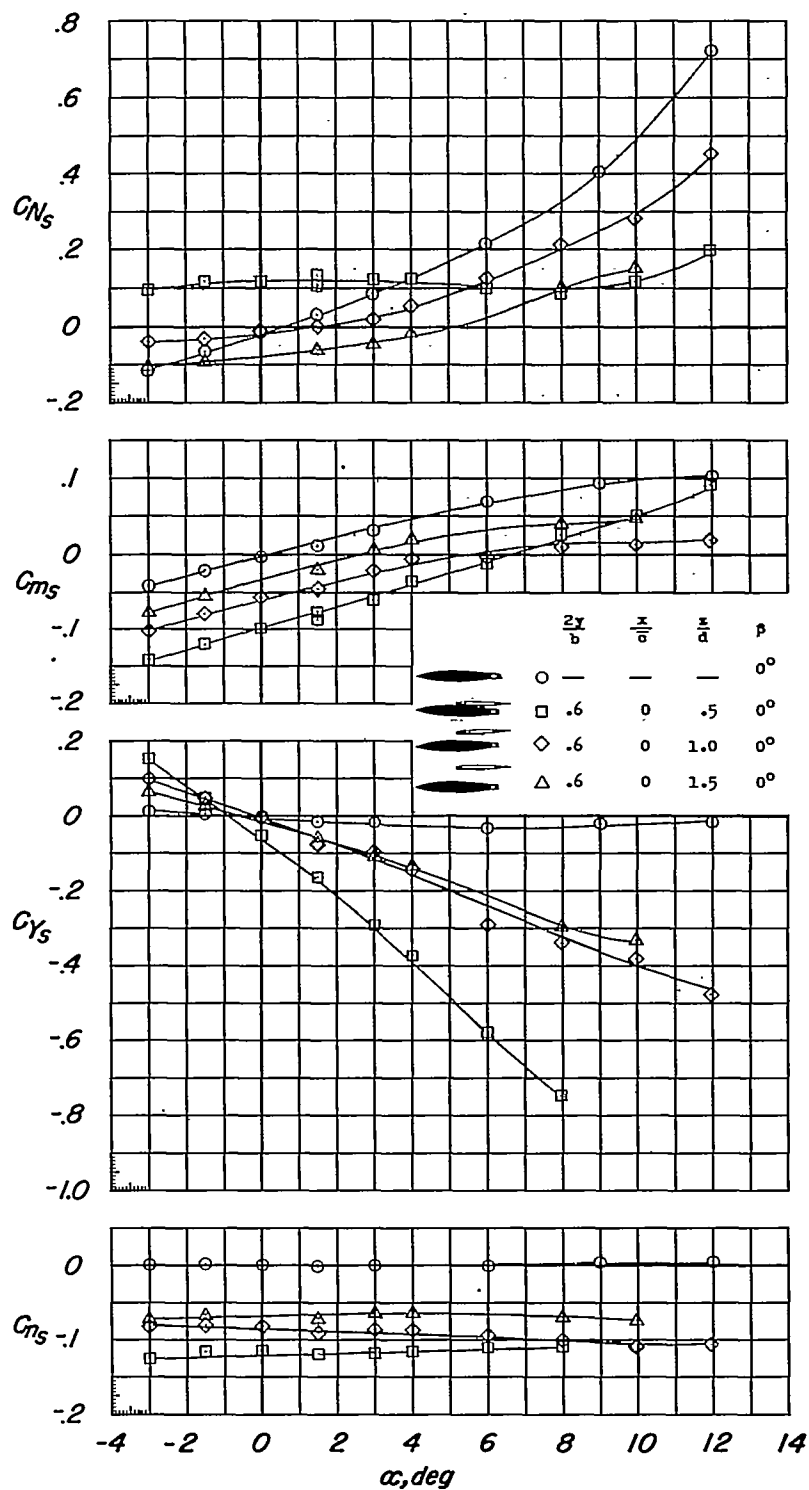
(i)　M = 1.62.

Figure 14.- Continued.

		$\frac{2y}{b}$	$\frac{x}{c}$	$\frac{z}{d}$	β
	O	—	—	—	0°
	□	.6	0	.5	0°
	◇	.6	0	1.0	0°
	△	.6	0	1.5	0°

(j)   M = 1.96.

Figure 14.- Continued.

		$\frac{2y}{b}$	$\frac{x}{c}$	$\frac{z}{d}$	β
	$\bigcirc$	—	—	—	0°
	$\square$	.6	0	.5	0°
	$\Diamond$	.6	0	1.0	0°
	$\triangle$	.6	0	1.5	0°
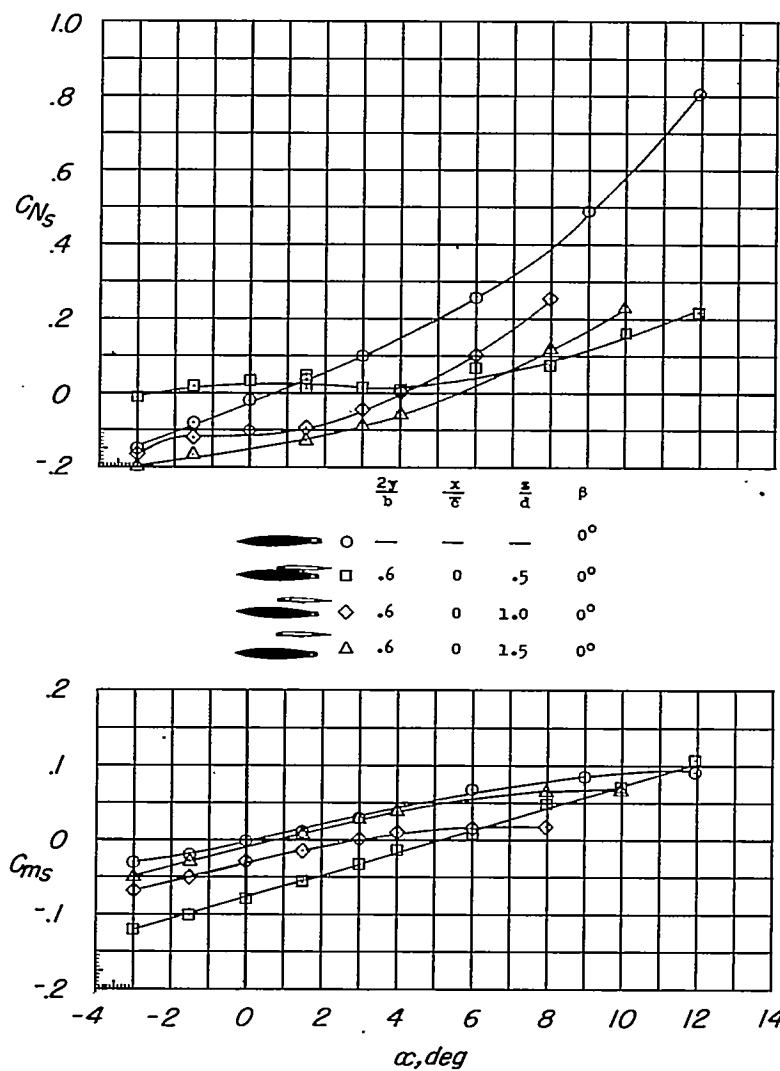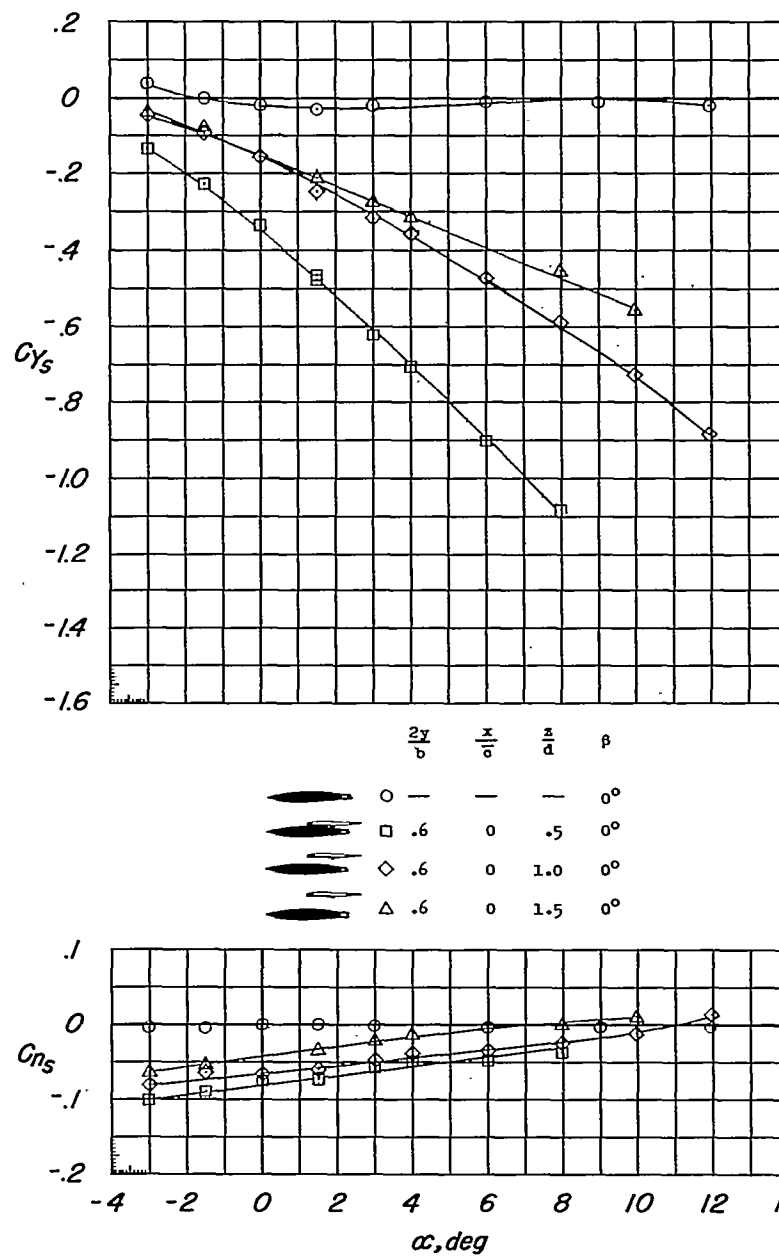
(k) M = 1.96 concluded.

Figure 14.- Concluded.
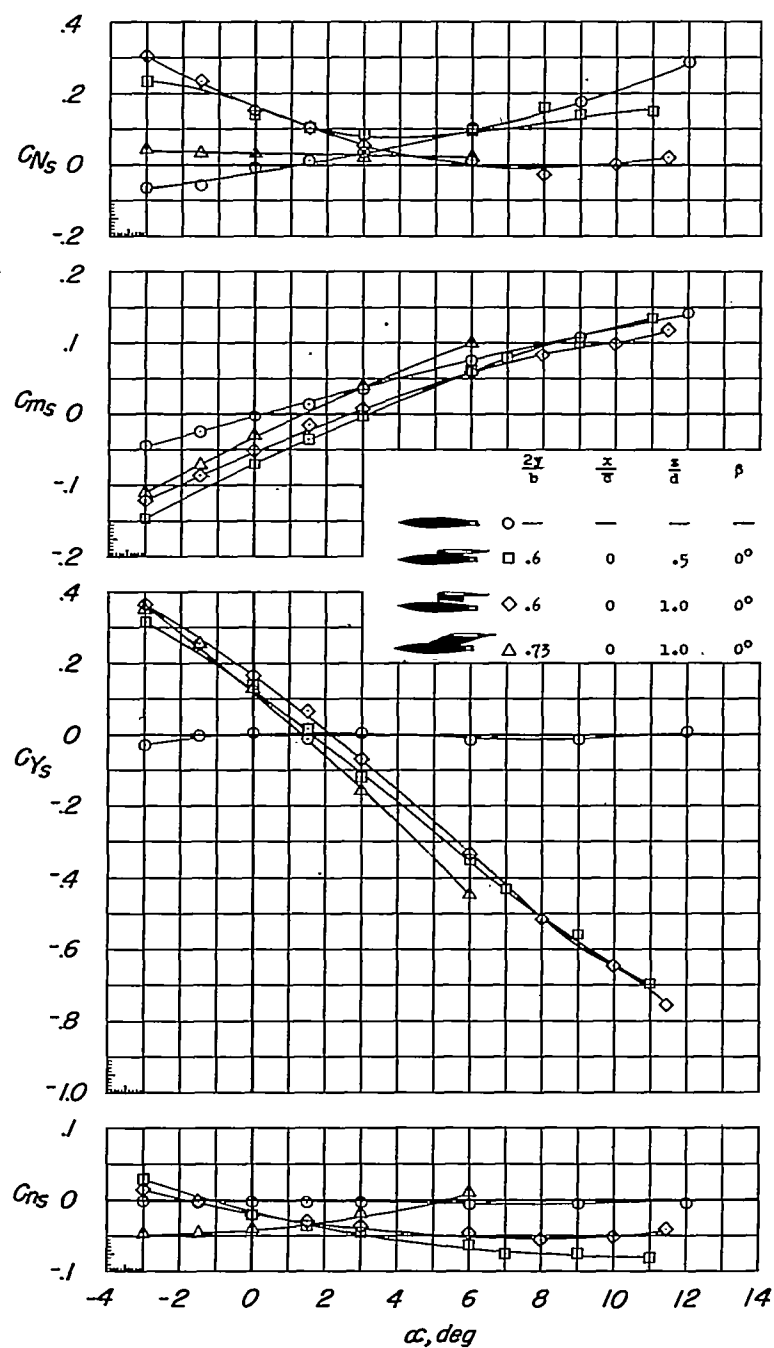
(a) M = 0.75.

Figure 15.- Aerodynamic characteristics of the DAC store in the presence
of the wing-fuselage. Original fuselage.

		$\frac{2y}{b}$	$\frac{x}{c}$	$\frac{z}{d}$	β
	o	—	—	—	—
	□	.6	0	.5	0°
	◇	.6	0	1.0	0°
	△	.73	0	1.0	0°

C_{N_S}

C_{m_S}

C_{Y_S}

C_{n_S}

α, deg

(b) M = 0.90.

Figure 15.- Continued.

(c) M = 1.05.

Figure 15.- Continued.

(d) M = 1.20.

Figure 15.- Continued.

(e)   M = 1.41.

Figure 15.- Continued.
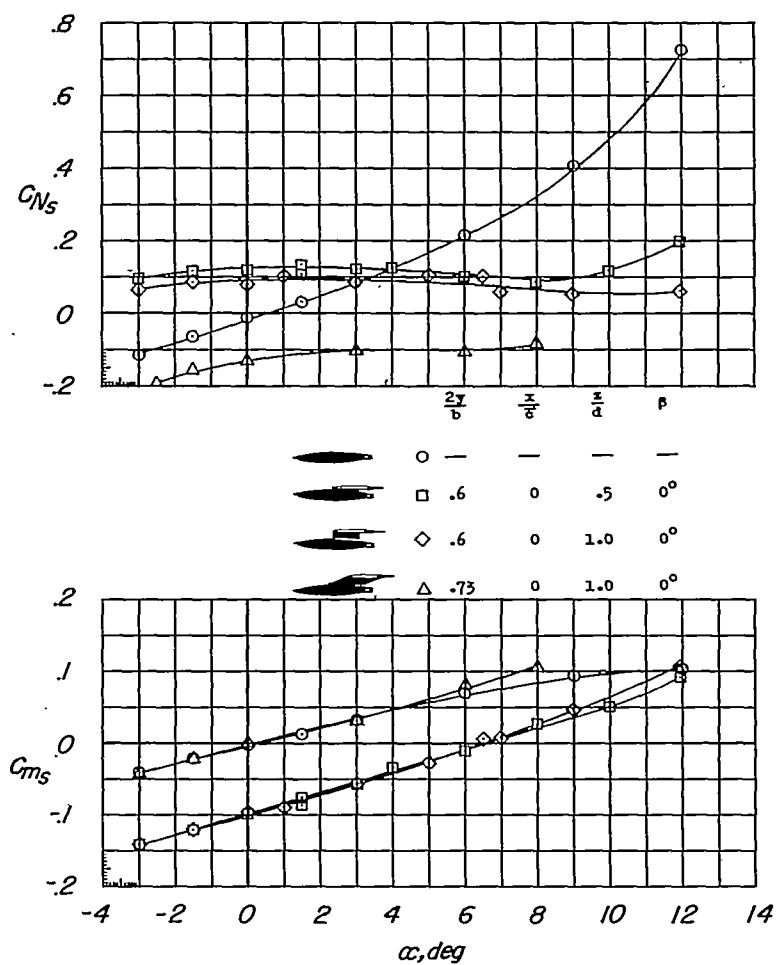
(f) M = 1.62.

Figure 15.- Continued.
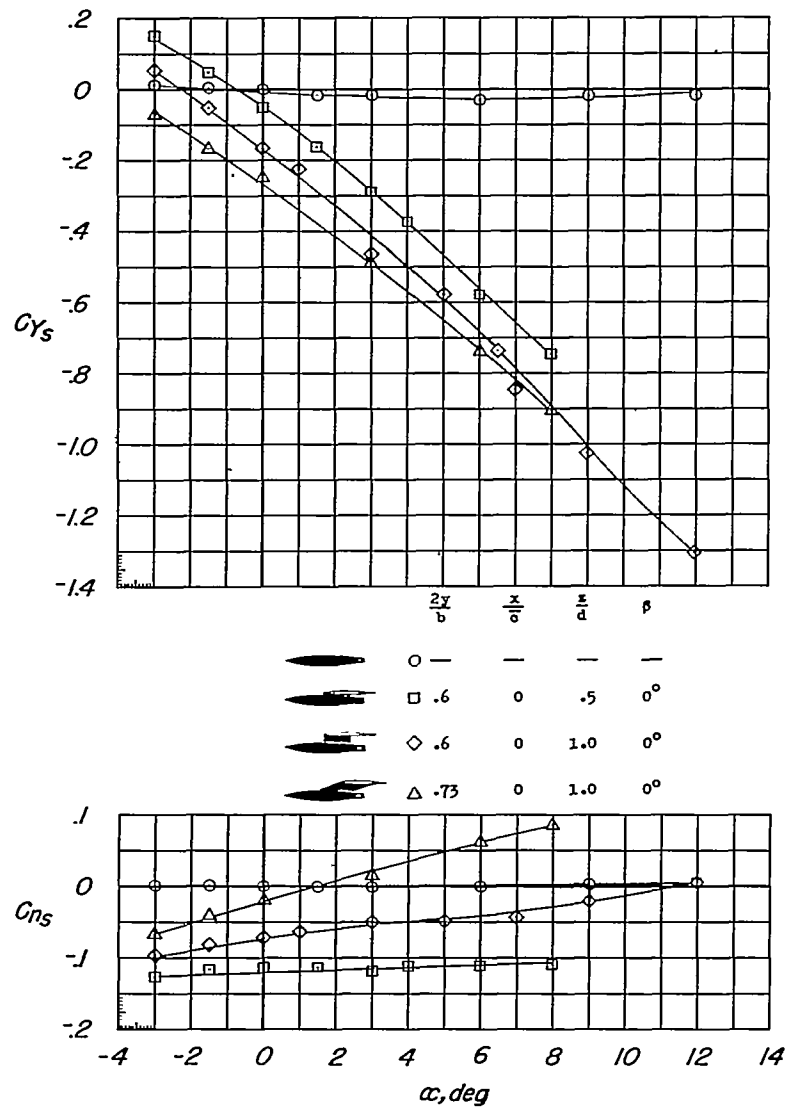
(g)   M = 1.62 concluded.

Figure 15.- Continued.
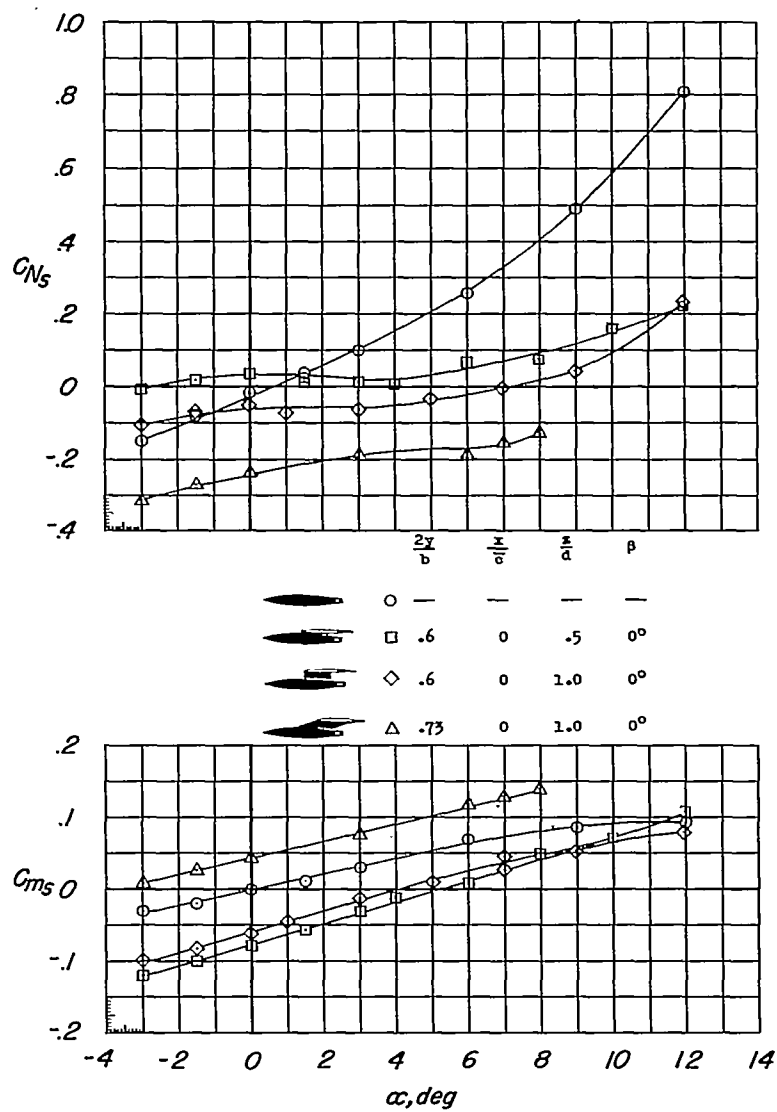
(h) M = 1.96.

Figure 15.- Continued.
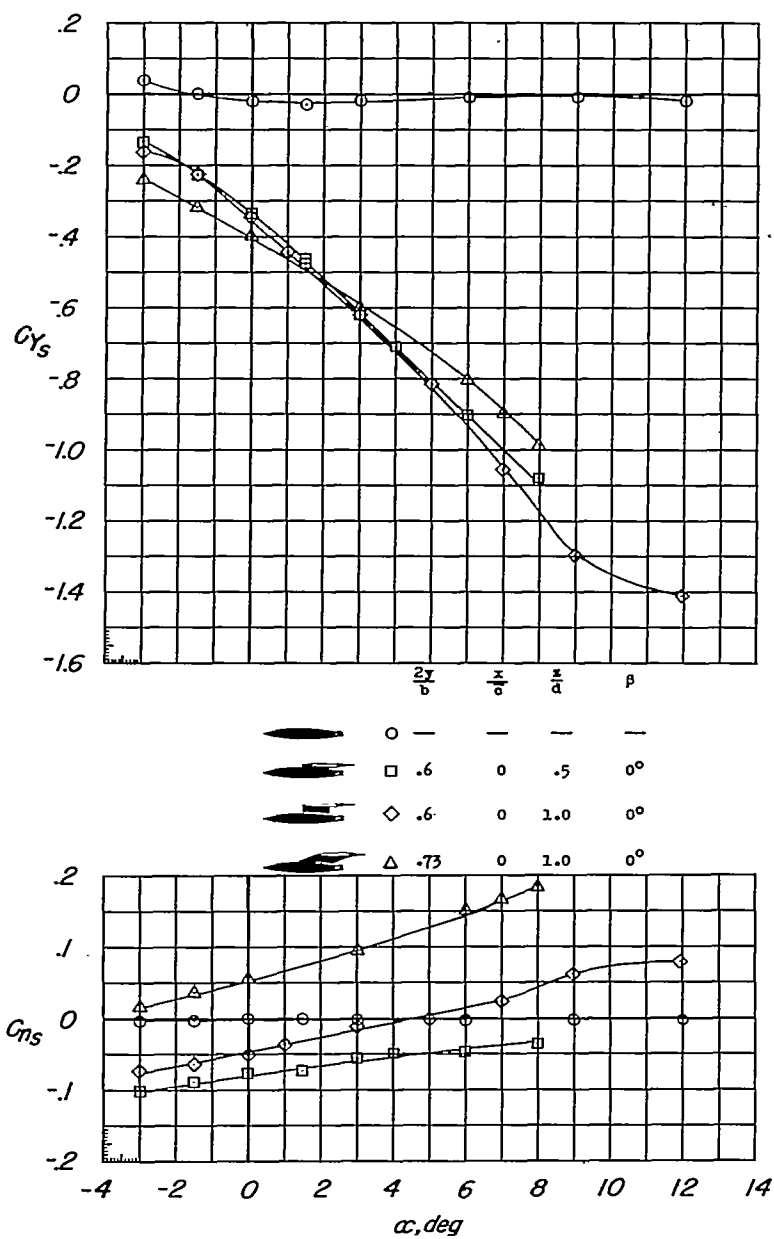
(i) M = 1.96 concluded.

Figure 15.- Concluded.
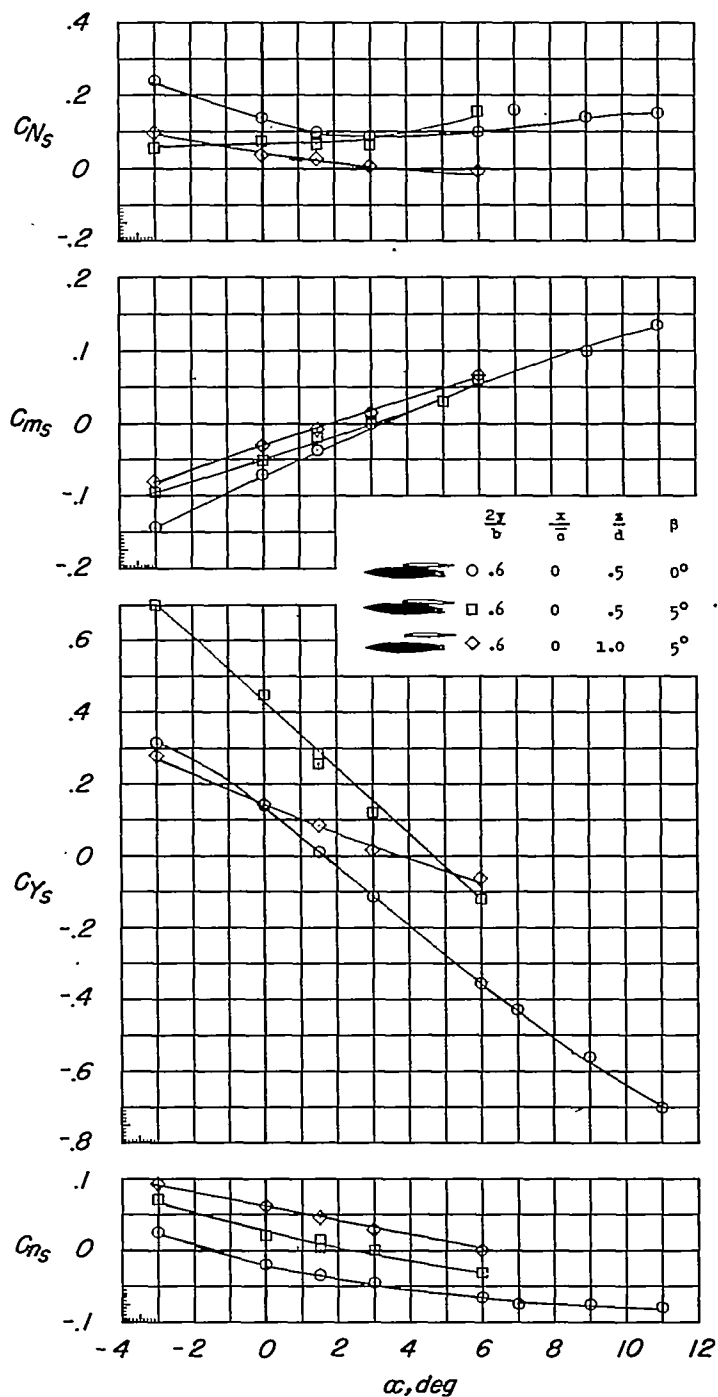
(a) M = 0.75.

Figure 16.- Aerodynamic characteristics of the DAC store at 0° and 5° skew angle for positions relative to the wing at stations 2y/b = 0.60; original fuselage.
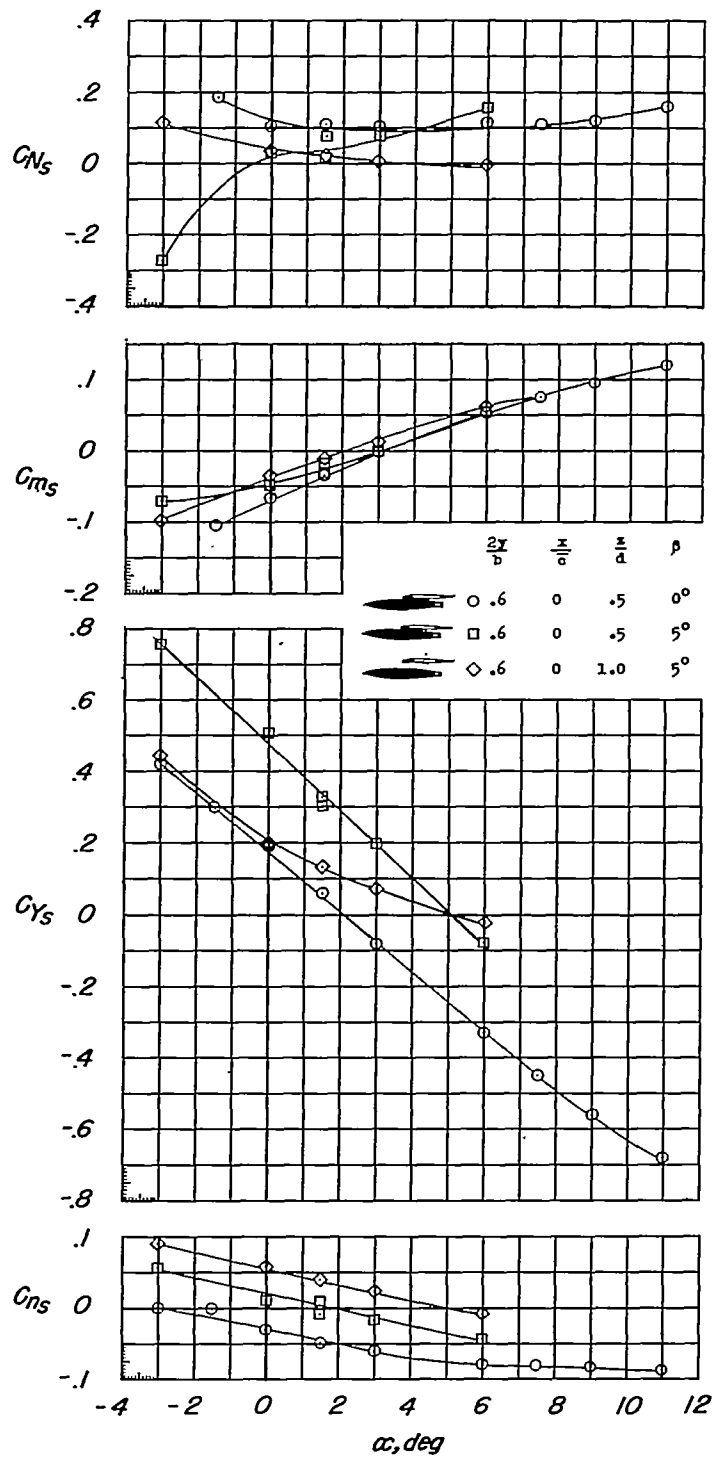
(b) M = 0.90.

Figure 16.- Continued.
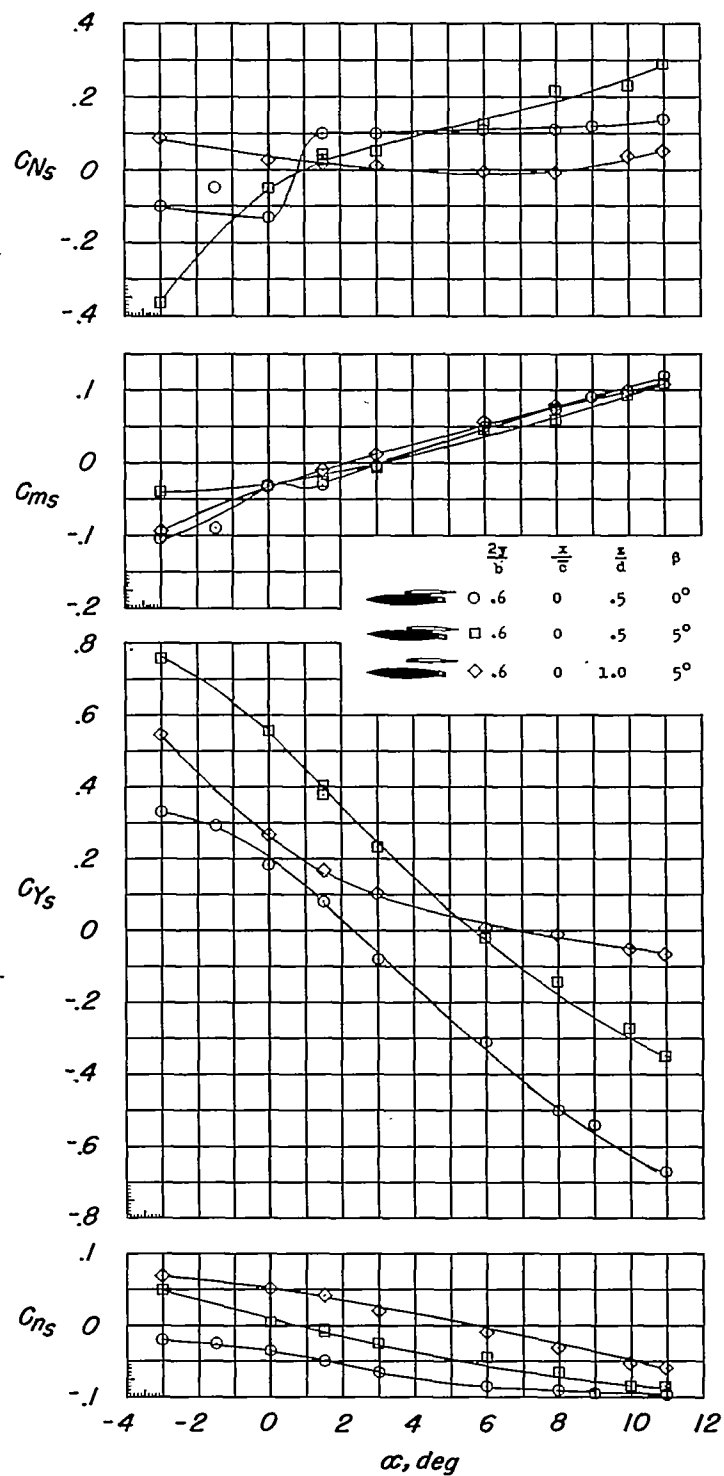
(c) M = 0.95.

Figure 16.- Continued.
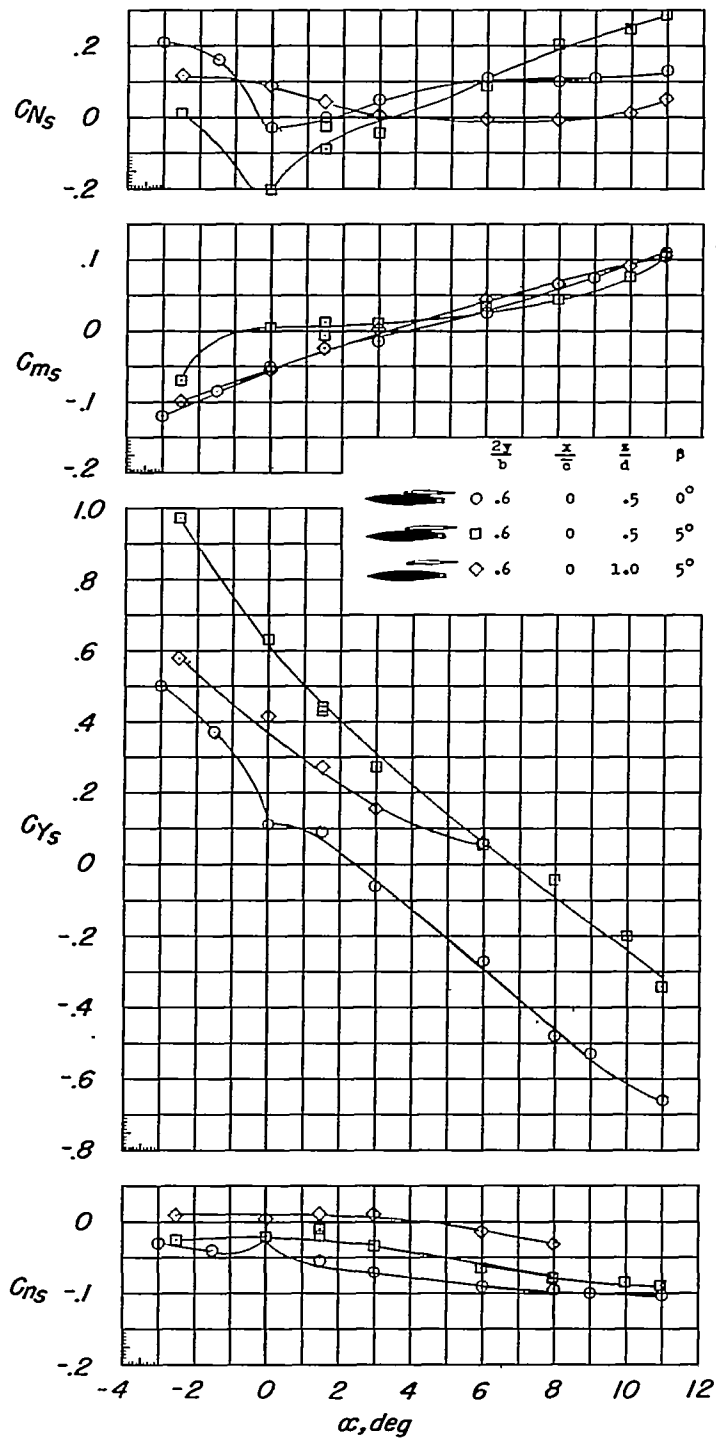
(d) M = 1.00.

Figure 16.- Continued.

	$\frac{2y}{b}$	$\frac{x}{\sigma}$	$\frac{x}{d}$	β
○	.6	0	.5	0°
□	.6	0	.5	5°
◇	.6	0	1.0	5°
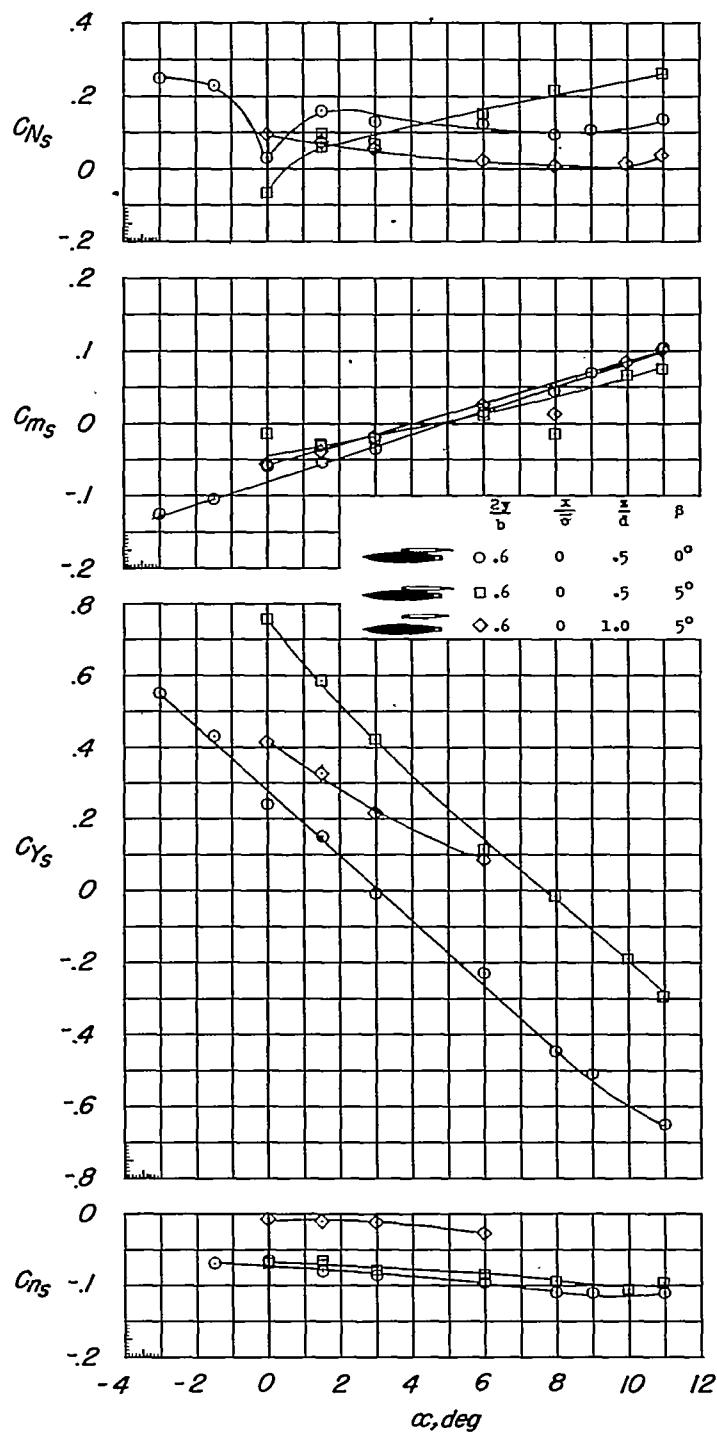
(e) M = 1.05.

Figure 16.- Continued.
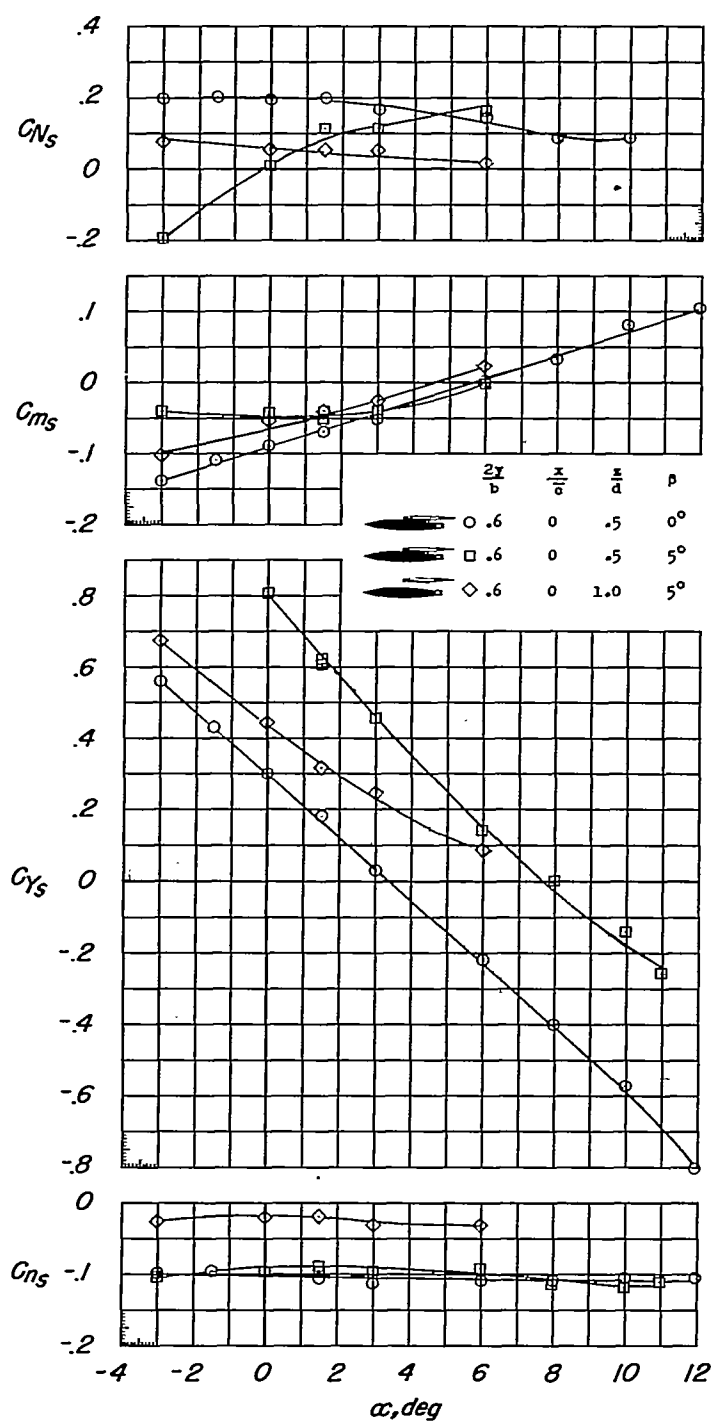
(f) M = 1.20.

Figure 16.- Continued.

(g) M = 1.41.

Figure 16.- Continued.

	$\frac{2y}{b}$	$\frac{x}{c}$	$\frac{z}{d}$	β
◁▬	○.6	0	.5	0°
◁▬	□.6	0	.5	5°
◁▬	◇.6	0	1.0	5°
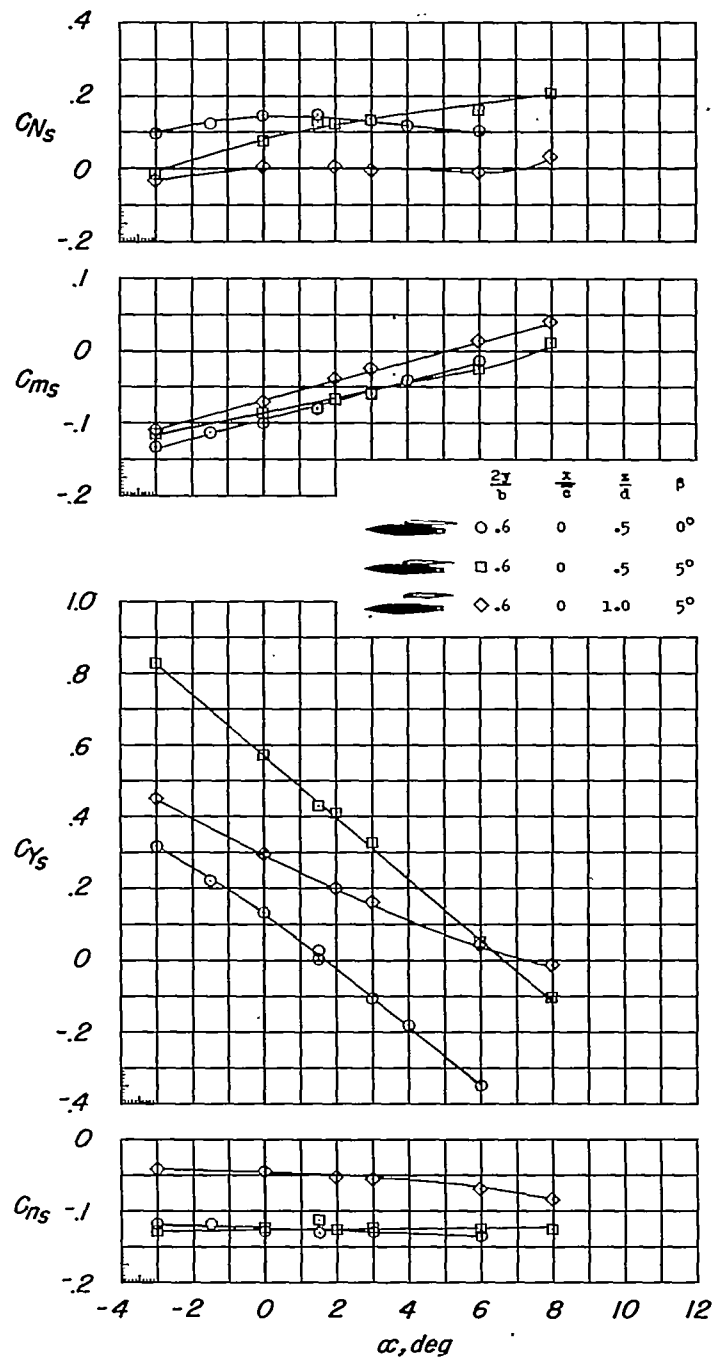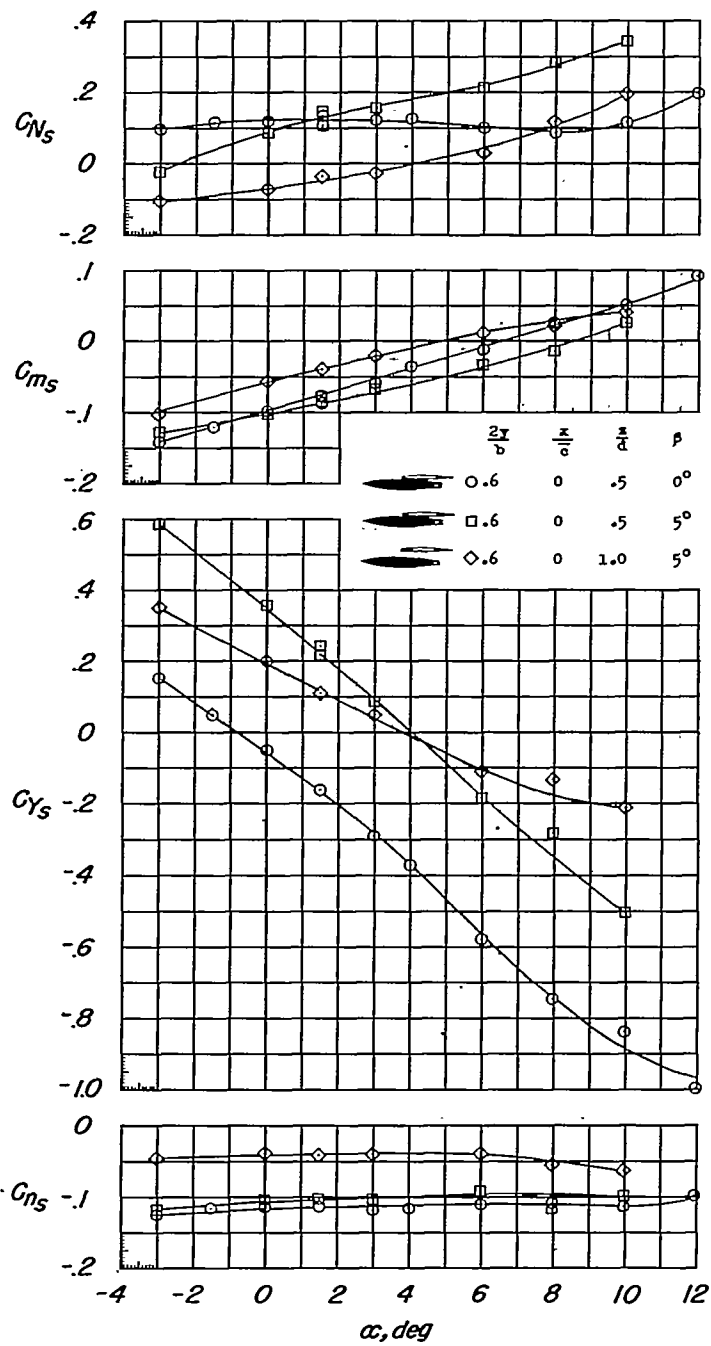
(h) M = 1.62.

Figure 16.- Continued.

	$\frac{2y}{b}$	$\frac{x}{c}$	$\frac{x}{d}$	β
○	.6	0	.5	0°
□	.6	0	.5	5°
◇	.6	0	1.0	5°
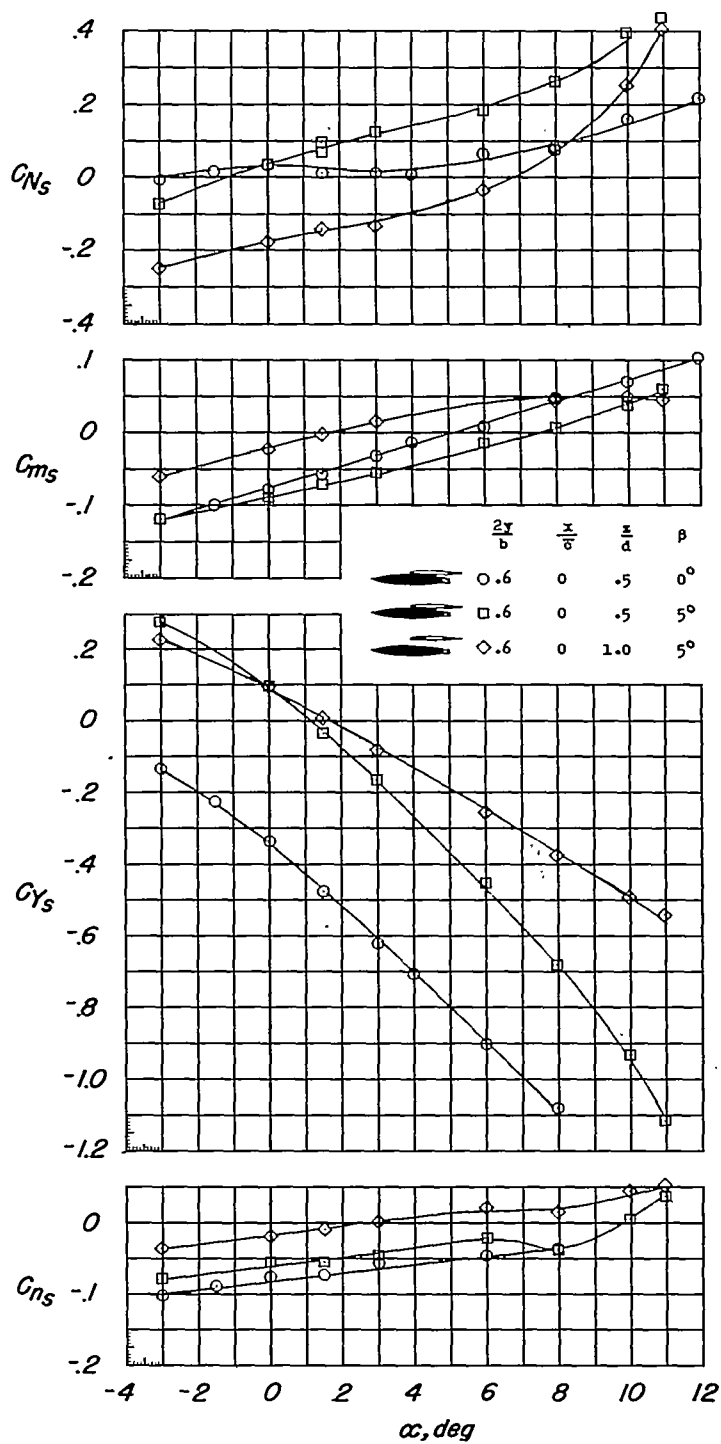
(i)   M = 1.96.

Figure 16.- Concluded.

(a) Influence of vertical store position (without pylon).

Figure 17.- Incremental wing force, moment, and incremental slope changes due to the presence of the store at various positions relative to the wing.
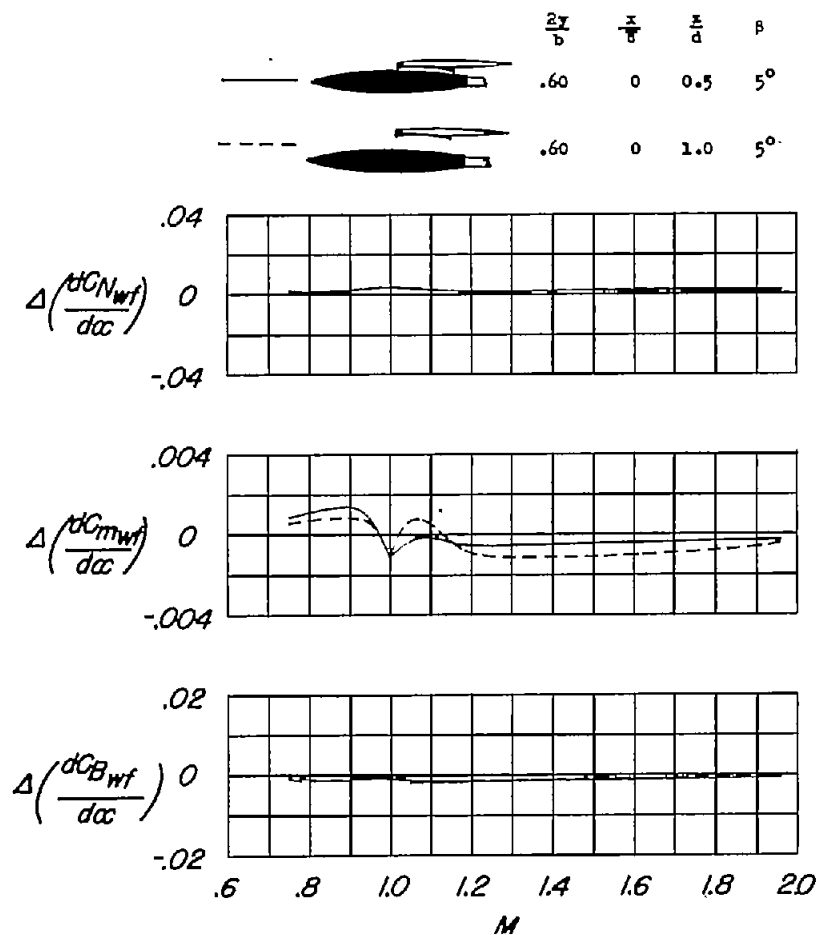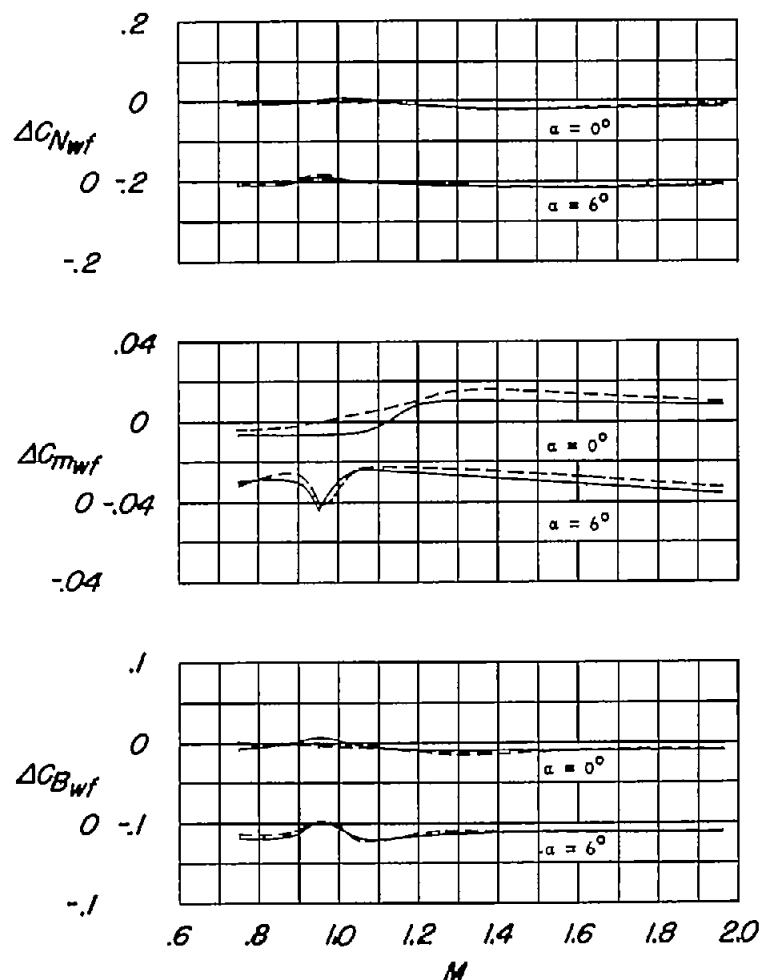
(b) Influence of vertical position of the store skewed 5° (nose inboard).

Figure 17.- Continued.
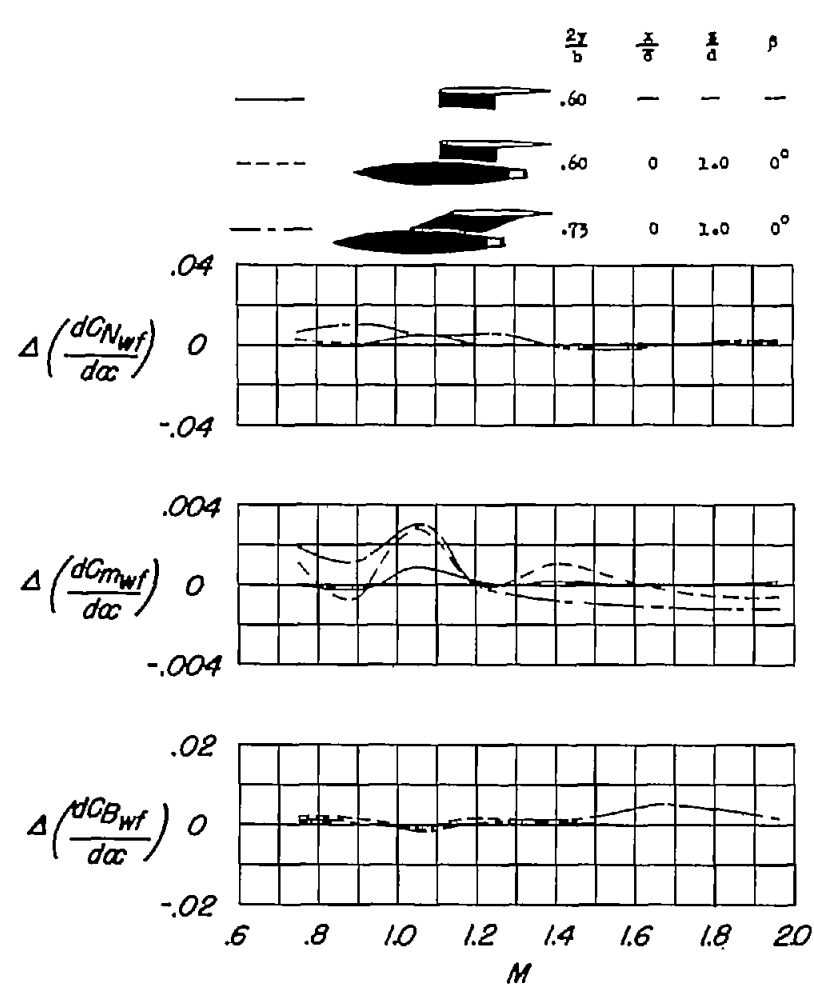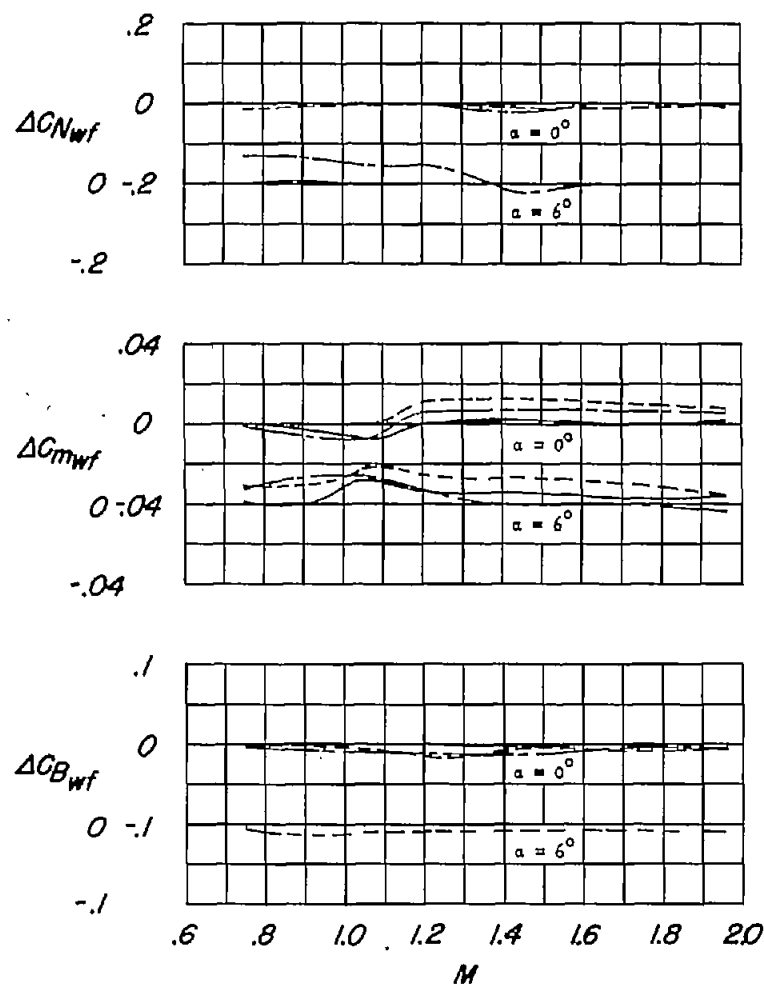
(c) Influence of spanwise store position at z/d = 1.0 (with pylon).

Figure 17.- Concluded.
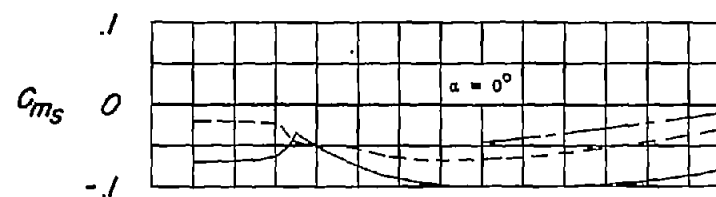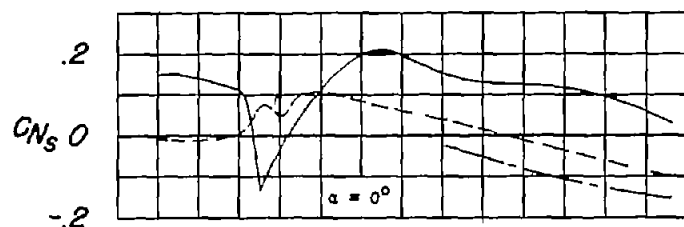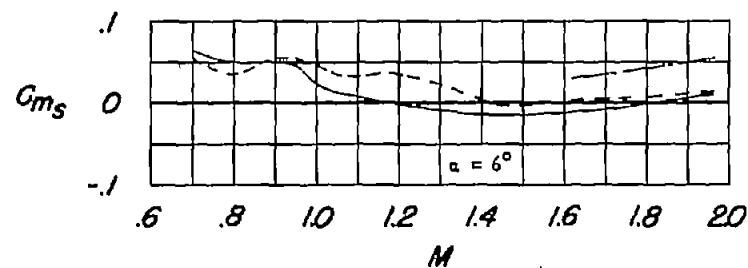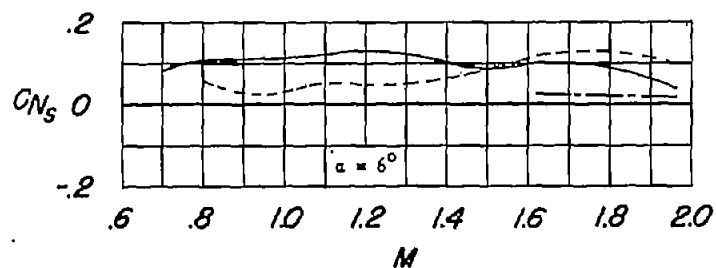
(a) Effect of vertical distance from the wing (without pylon).

Figure 18.- Variation of DAC store normal-force coefficient and pitching-moment coefficient with Mach number.
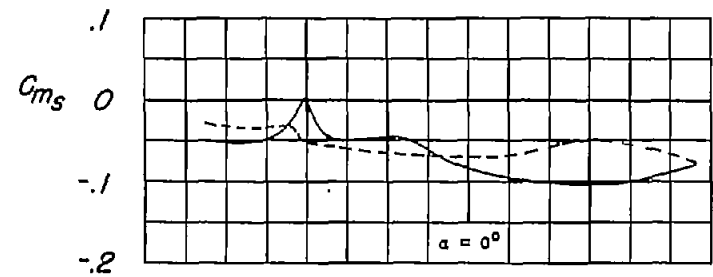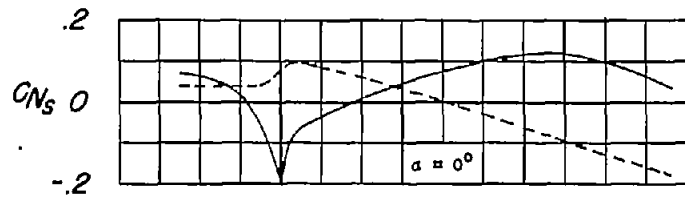
C_{N_S} .2   0   -.2

$a = 0°$

C_{m_S} .1   0   -.1   -.2

$a = 0°$

$\frac{2y}{b}$	$\frac{x}{\delta}$	$\frac{z}{d}$	β
.6	0	.5	5°
.6	0	1.0	5°

C_{N_S} .2   0   -.2

$a = 6°$

C_{m_S} .1   0   -.1

$a = 6°$

.6   .8   1.0   1.2   1.4   1.6   1.8   2.0
M

.6   .8   1.0   1.2   1.4   1.6   1.8   2.0
M
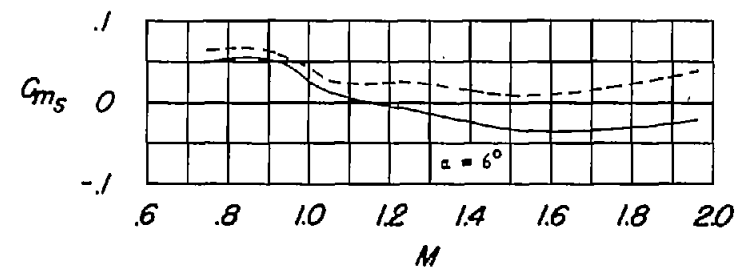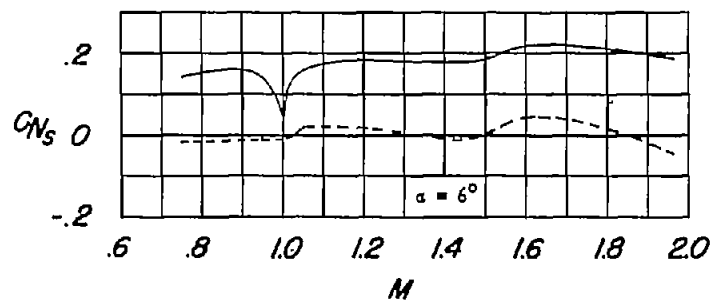
(b) Effect of vertical position on the store skewed 5° (nose inboard).

Figure 18.- Continued.
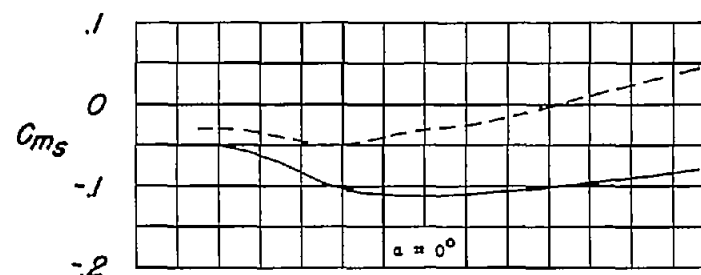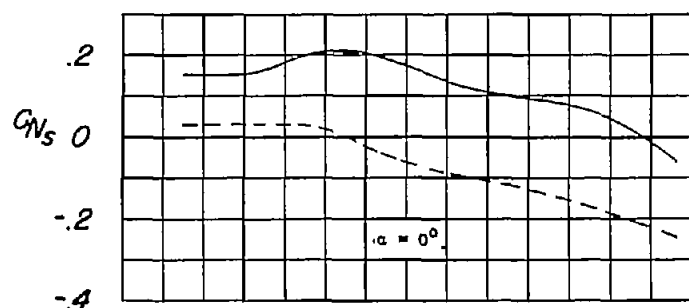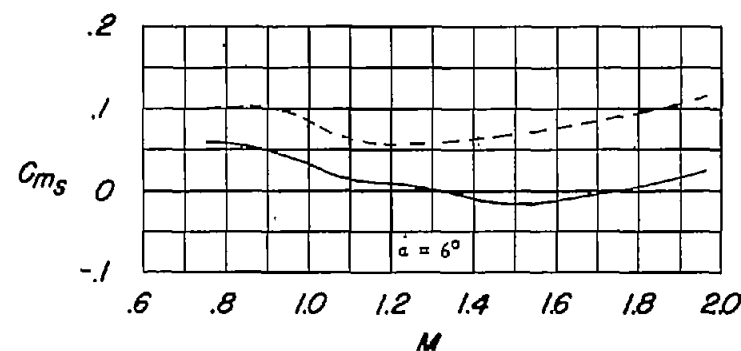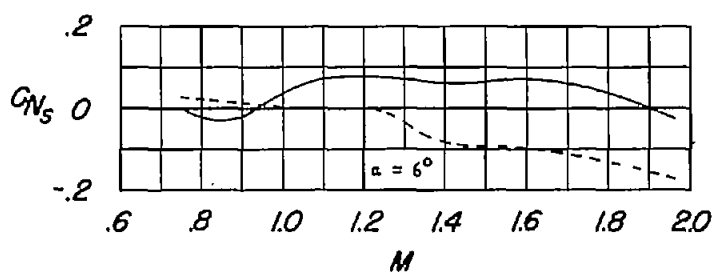
(c) Effect of spanwise store position at z/d = 1.0 (with pylon).
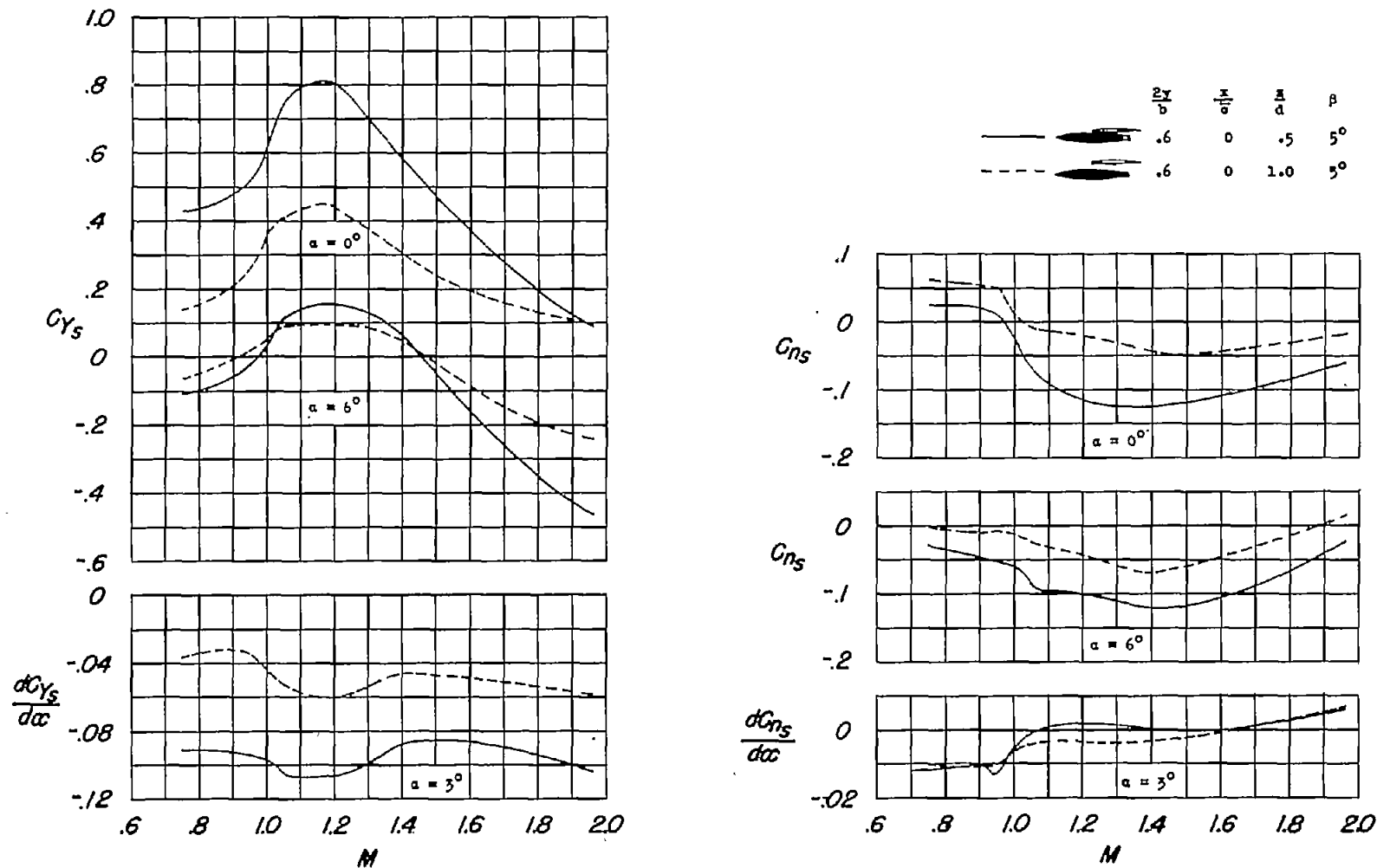
Figure 18.- Concluded.
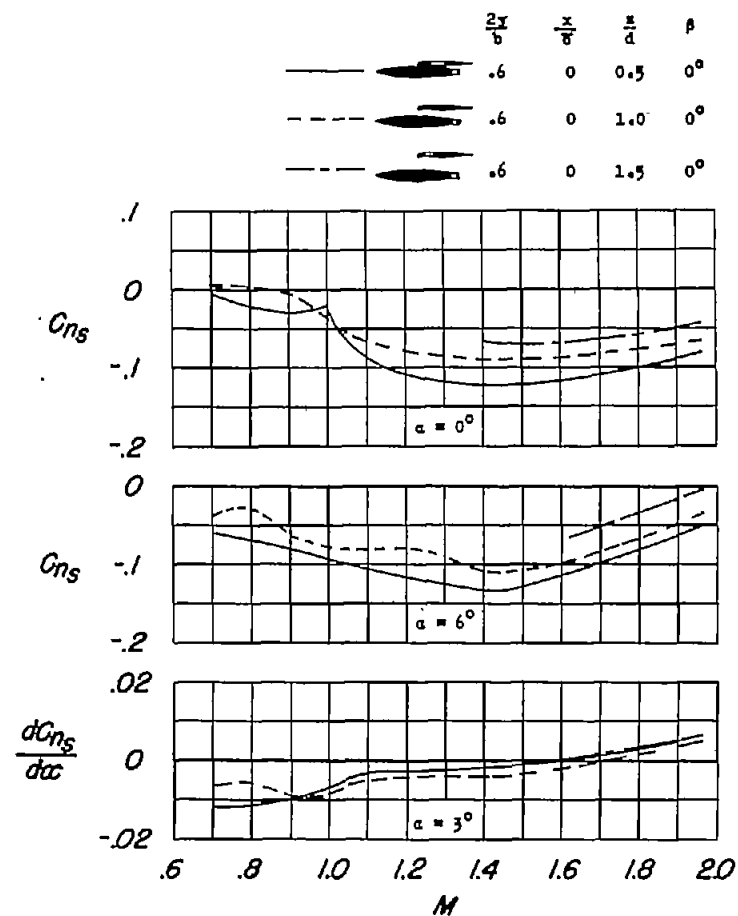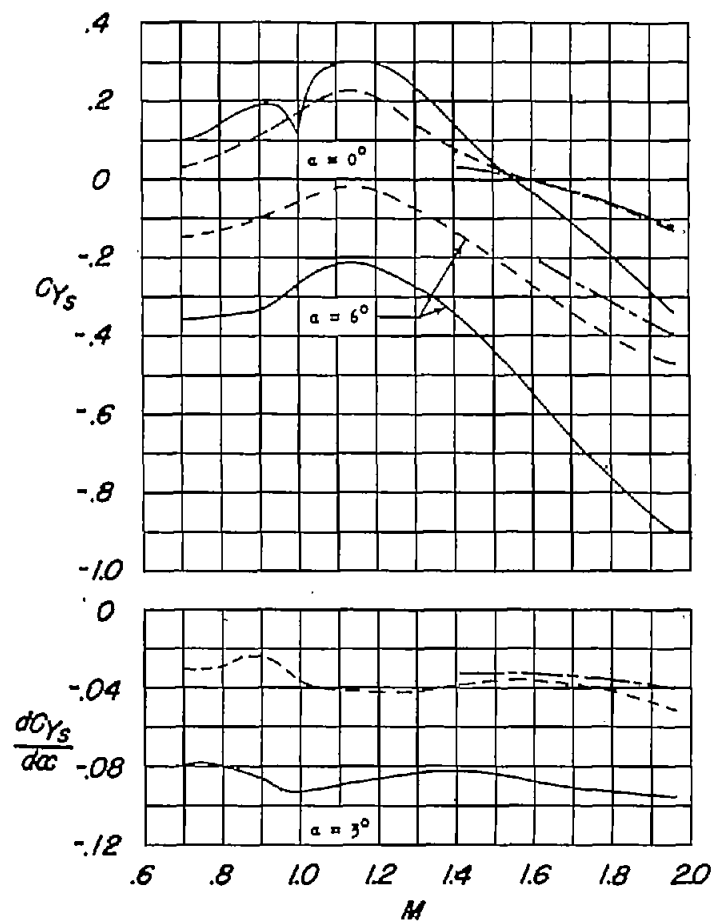
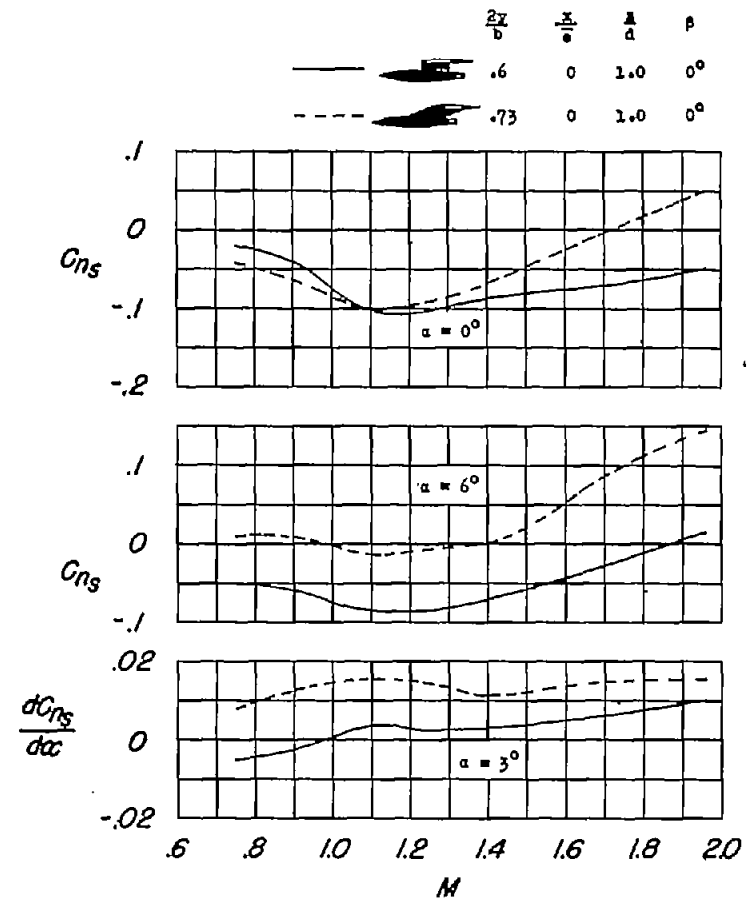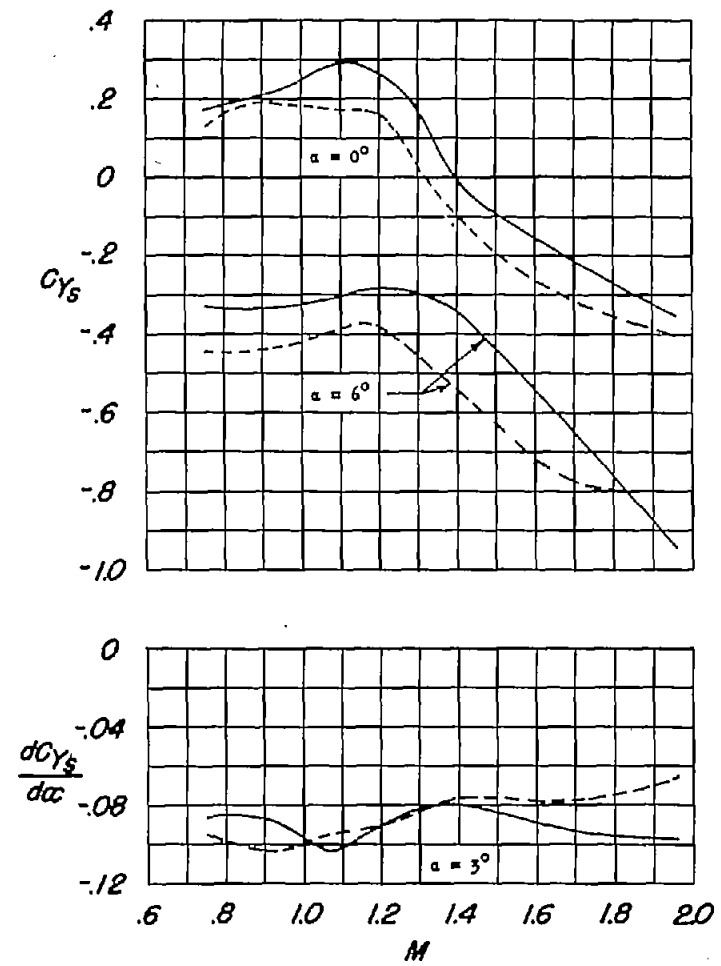(a) Effect of vertical distance from the wing (without pylon).

Figure 19.- Variation of DAC store side-force coefficient, yawing-moment coefficient, and slopes of $\dfrac{dC_{Y_s}}{d\alpha}$ and $\dfrac{dC_{n_s}}{d\alpha}$ with Mach number.

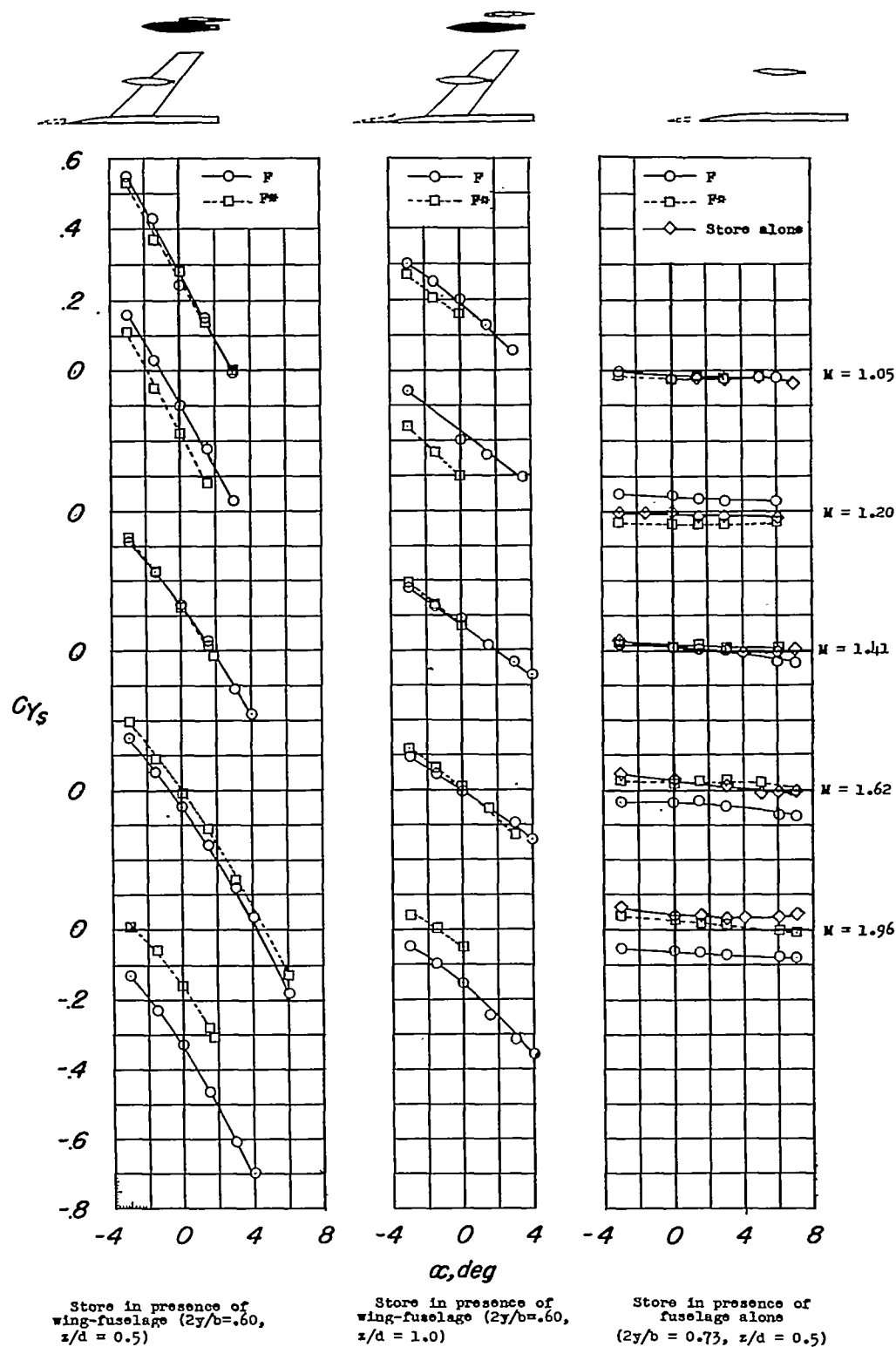(b) Effect of vertical position on the store skewed 5° (nose inboard).
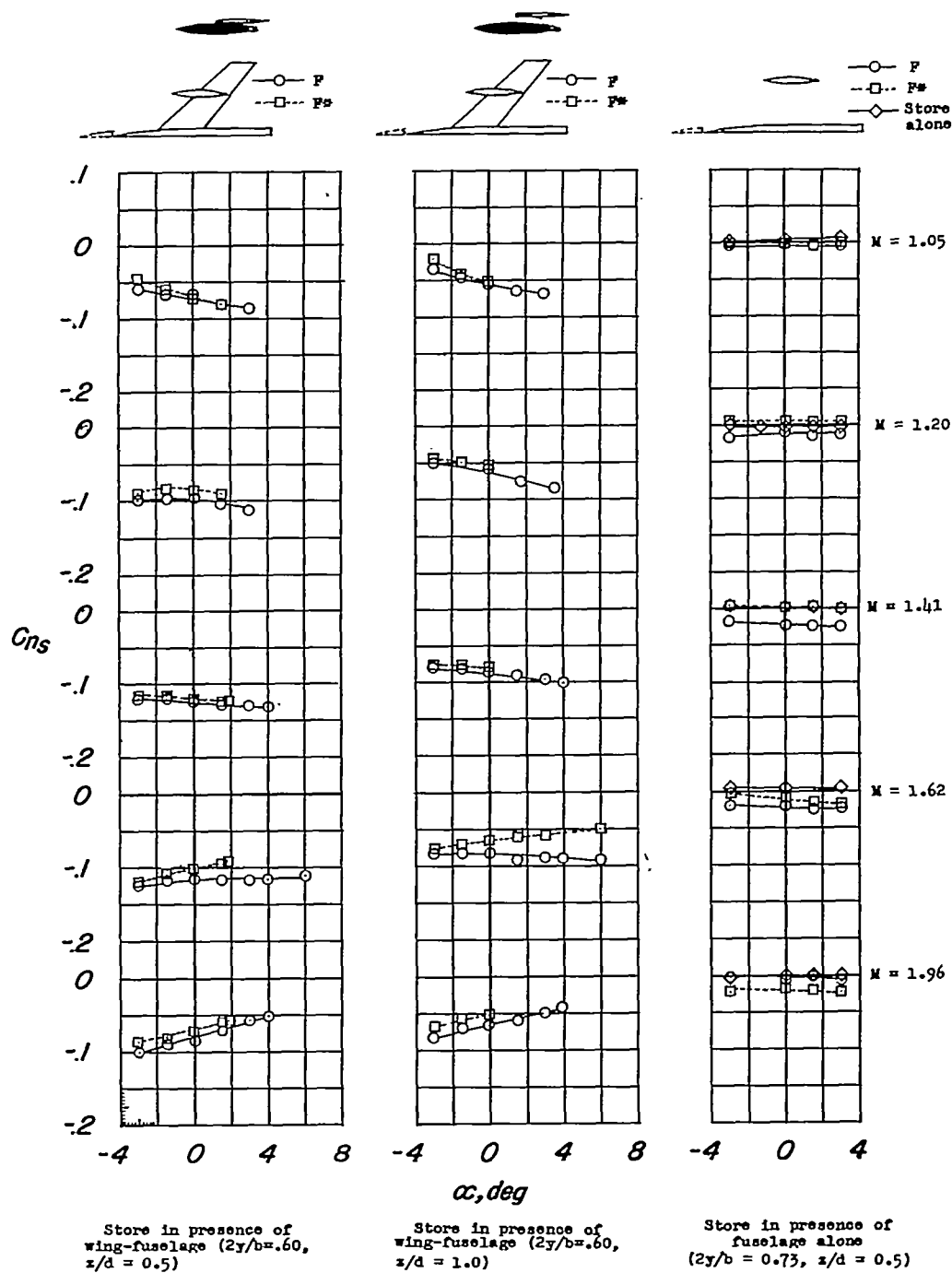
Figure 19.- Continued.

(c) Effect of spanwise store position at z/d = 1.0 (with pylon).

Figure 19.- Concluded.

(a) Side-force coefficient against angle of attack.

Figure 20.- Effect of fuselage-nose position on store side-force and yawing-moment coefficient.

(b) Yawing-moment coefficient against angle of attack.

Figure 20.- Continued.

$$\gamma = \cos^{-1}\frac{1}{1.96}$$

Store in presence of
wing-fuselage (2y/b=.60,
z/d = 0.5)

Store in presence of
wing-fuselage (2y/b=.60,
z/d = 1.0)

Store in presence of
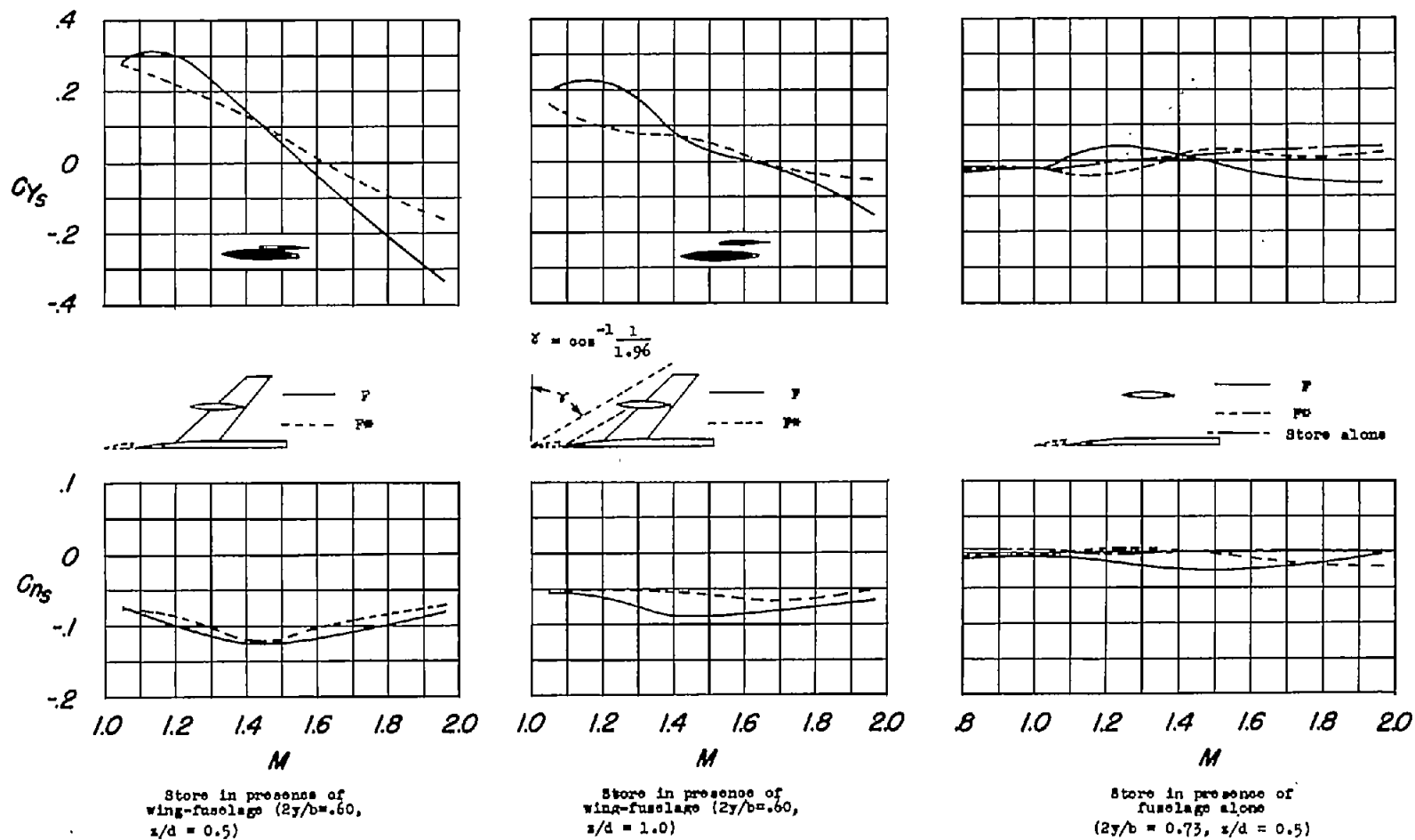fuselage alone
(2y/b = 0.73, z/d = 0.5)

(c) Variation of store side-force and yawing-moment coefficient with Mach number (α = 0°).

Figure 20.- Concluded.